University of Alberta

Analyses of *trans*-acting factors that regulate RNA interference in *Schizosaccharomyces pombe*

By

Jungsook Park

A thesis submitted to the Faculty of Graduate Studies and Research
in partial fulfillment of the requirements for the degree of

Doctor of Philosophy
Department of Cell Biology

Spring 2013

Edmonton, Alberta

ABSTRACT

RNA interference (RNAi) is a phenomenon in which small RNAs induce an efficient, sequence-specific silencing of gene expression at transcriptional (TGS) and post-transcriptional (PTGS) levels. In the fission yeast *Schizosaccharomyces pombe* (*S. pombe*), the basic roles of Argonaute protein (Ago1), Dicer (Dcr1), and RNA-dependent RNA polymerase (Rdp1) in TGS and PTGS are relatively well understood. The core RNAi effector proteins are differentially localized in this organism. Specifically, most Ago1 and Dcr1 reside in the cytoplasm, whereas the bulk of Rdp1 is found in the nucleus. However, it is not known how RNAi effector protein functions are regulated in different cellular compartments. Emerging evidence suggests that various *cis*- and *trans*-acting factors are involved in the regulation of RNAi pathways. In this thesis, I characterized *trans-acting* factors that modulate small RNA-mediated gene silencing mechanisms in *S. pombe.*

I demonstrated that the β-karyopherin Sal3 is required for the nuclear import of Rdp1 in *S. pombe*. Loss of nuclear Rdp1 was associated with substantially reduced transcriptional gene-silencing. Surprisingly, post-transcriptional gene-silencing, which occurs in the cytoplasm of other eukaryotes, was also affected. In addition to identifying Sal3 as a modulator of RNAi-dependent transcriptional gene-silencing, a potential link between nuclear import and post-transcriptional gene silencing was discovered. As well, I identified a previously unknown modulator of the Argonaute protein in *S. pombe*. In the cytoplasm, Argonaute proteins are incorporated into large, mobile puncta known

as processing bodies (PBs) that travel along microtubules. Using a candidate gene approach, I discovered that a microtubule-associated motor protein, Cut7, is important for the homeostasis of Ago1-containing PBs in the cytoplasm. The observation that Cut7 activity enhances post-transcriptional gene silencing provides direct evidence that microtubule motor proteins are part of the gene silencing machinery in the cytoplasm. Finally, preliminary data derived from the study of Ago1 mutants as well as inhibitor experiments suggest that kinases and phosphates control the localization and, by extension, the function of Argonaute proteins in fission yeast.

ACKNOWLEDGEMENTS

Throughout the course of my graduate work, whether experiencing happiness or difficulty, I have looked toward this moment—the chance to thank the many people who have encouraged and supported me.

First, I would like to express my sincere appreciation for my mentor, Dr. Tom Hobman. I still remember the first user-eye-D…. Thank you for taking me as your student and for giving me the opportunity to work on fascinating RNAi projects. Throughout my graduate studies, I have learned not only an incredible amount of scientific knowledge, but also your philosophy and enthusiasm regarding how to cooperate with peers and how to approach science, itself. Your guidance and understanding has consistently provided me with motivation and encouragement to keep on, which was especially important during the years I had to live away from my family. I know that I could not have reached this stage without your mentoring, and as I enter the next phase of my scientific life, I carry with me endless appreciation for everything you've given and done.

Thank you to all of my lab mates: Ann, Eileen, Jae, Joaquin, Justin, Matt, Shangmei, Steven, Valeria, Yang, and Zack, and to my past lab mates. During my several-year stay at the Hobman lab, your technical support, helpful discussions, daily small-talk, and truly, your friendship, has made my graduate life abroad immeasurably more enjoyable. I will miss you all.

The members of my Ph.D committee greatly contributed to my graduate research. I thank Dr. Richard Wozniack for not only giving me excellent

scientificfeedback and criticisms that matured my manuscripts, but also for support throughout my graduate studies. I also thank Dr. Andrew Simmonds for substantial help with the entire microscope and computer works that were critical for the development of my projects and for your advice on my graduate life. I would like to express my gratitude for Dr. Andrew MacMillan and Dr. Patrick Provost for taking the time to read my thesis and for serving as external examiners at the defense.

I would also like to thank Dr. Paul Young for providing me with a great deal of advice on my fission yeast experiments. Thanks to my peers in the department of Cell Biology: Chris, David, Doug, Emily, Jenny, Jing, Luc, Mike, Nathan, and Zackie. During my graduate studies, it was a great pleasure to take courses together and to engage in lots of enjoyable talks as well as scientific discussions. I would also like to thank the Cell Biology office staff for their kind help.

I would also like to express whole-hearted appreciation for my families. I would be neither where I am nor who I am today without your love. Special thanks to my companions—ACKTTZ, Eyerus, and Shawn—and to all of my friends who shared many joys and tears. Without your friendship and emotional support, I cannot imagine how much more difficult the couple of years at the end of my graduate life in Edmonton would have been. Also, spending time with you has opened my eyes to the world, helping me spend my time in a more worthwhile way.

And to Sanghyun, you will never know how much you have meant to me. You are my best friend on the journey of my life and are a great senior for my academic career, as well as a sweet husband. As I know what my thesis means to us, I could keep on—and will—based on this milestone. Thank you for your endless encouragement, understanding, and support, all of which has made me able to follow my dream.

TABLE OF CONTENTS

CHAPTER 1: Introduction 1

1.1. Overview of RNA interference (RNAi) 2

1.2. Effector complexes involved in RNAi 5
- 1.2.1. Argonaute superfamily and RNA-induced silencing complex 5
  - 1.2.1.1. Argonaute protein family: structure, characteristics, and function 5
  - 1.2.1.2. RNA-induced transcriptional silencing complex in fission yeast 9
  - 1.2.1.3. Argonaute siRNA chaperone complex 10
  - 1.2.1.4. Processing bodies 11
- 1.2.2. RNase III protein family and small RNA processing complexes 13
  - 1.2.2.1. Class 1 RNase III 14
  - 1.2.2.2. Class 2 RNase III 14
  - 1.2.2.3. Class 3 RNase III 15
- 1.2.3. RNA-dependent RNA polymerase family and RNA-dependent RNA polymerase complex 19
- 1.2.4. Chromatin modifying complex and association with RNAi complexes 21

1.3. The modes of RNAi 22
- 1.3.1. Transcriptional gene silencing 22
  - 1.3.1.1. Transcriptional gene silencing in *Schizosaccharomyces pombe* 23
    - 1.3.1.1.1. Heterochromatin structures and functions 23
    - 1.3.1.1.2. RNAi-dependent heterochromatin formation 24
  - 1.3.1.2. Non-coding RNAs and heterochromatin in epigenetic gene silencing 26
- 1.3.2. Post-transcriptional gene silencing and translational repression 29

1.4. *Trans*-acting modulators of RNAi 34
- 1.4.1. Overview of recent findings: multiple regulators of RNAi apparatus 34
- 1.4.2. Karyopherin and nuclear transport machinery 35
  - 1.4.2.1. Function and characteristic of karyopherins 35
  - 1.4.2.2. Nuclear transport of macromolecules by β-karyopherins 37
- 1.4.3. Post-translational modifications of gene silencing factors 45
  - 1.4.3.1. Post-translational modifications of Argonaute proteins 45
  - 1.4.3.2. Phosphorylation of RNase III enzymes and their associated proteins 49

1.5. Fission yeast *S. pombe*: an excellent model for studying gene silencing mechanisms 52
1.6. Rationale and Objective 52

CHAPTER 2: Materials & Methods 55

2.1. Materials 56
2.1.1. Reagents 56
2.1.2. Commonly used buffers and media 59
2.1.3. Oligonucleotides 61
2.1.4. Plasmids 63
2.1.5. Antibodies 64
2.1.6. *Schizosaccharomyces pombe* strains used 64
2.1.7. *Schizosaccharomyces pombe* online resources 66

2.2. Methods 67
2.2.1. Yeast techniques 67
2.2.1.1. Growth, maintenance, and long-term storage of *S. pombe* 67
2.2.1.1.1. Yeast cultures at permissive and restrictive temperatures 67
2.2.1.1.2. Measuring cell growth rates 67
2.2.1.1.3. Maintenance of yeast strains 68
2.2.1.1.4. Re-isolation of frozen cultures 68
2.2.1.2. Yeast transformation 68
2.2.1.2.1. Quick TRAFO method 68
2.2.1.2.2. Lithium Acetate method 69
2.2.1.2.3. Electroporation 70
2.2.1.3. Haploidizing yeast strains 70
2.2.1.4. Generating integrant strains 72
2.2.1.4.1. Illegitimate integration of plasmids 72
2.2.1.4.2. Stability test 72
2.2.1.5. Quantitation of lagging chromosomes 73
2.2.1.6. Staurosporine treatment 73
2.2.1.7. Assay with thiabendazole (TBZ) treatment 73
2.2.2. Nucleic acid purification, analysis, and modification 74
2.2.2.1. Isolation of plasmid DNA from *Eschericia coli* (*E. coli*) 74
2.2.2.2. Isolation of plasmid DNA from yeast 75
2.2.2.3. Restriction endonuclease digestion 76
2.2.2.4. Dephosphorylation of linearized vectors 76
2.2.2.5. Polymerase chain reaction (PCR) 77
2.2.2.6. Agarose gel electrophoresis 77
2.2.2.6.1. DNA agarose gel electrophoresis 77
2.2.2.6.2. RNA agarose gel electrophoresis 78
2.2.2.7. Purification of DNA fragments 78
2.2.2.8. Ligation of DNA 79
2.2.2.8.1. Low melting agarose in gel-ligation 79
2.2.2.9. Transformation of *E. coli* 80
2.2.2.9.1. Transformation of chemical-competent *E. coli* 80

2.2.2.9.2. Transformation of electro-competent *E. coli* 80
2.2.2.10. Colony PCR 81
2.2.3. Construction of recombinant plasmids 81
2.2.3.1. RFP-Rdp1 82
2.2.3.2. RFP-Rdp1-SV40-NLS 82
2.2.3.3. pAAUN-RFP 82
2.2.3.4. NT-Cut7-RFP 83
2.2.3.5. CT-Cut7-RFP 83
2.2.3.6. Cut7-GFP 83
2.2.3.7. Site-directed Mutagenesis 84
2.2.3.7.1. GFP-Ago1(Y487F) 84
2.2.3.7.2. GFP-Ago1(Y487E) 85
2.2.3.7.3. GFP-Ago1(Y513F) 85
2.2.3.7.4. GFP-Ago1(Y513E) 85
2.2.3.8. Automated DNA sequencing 85
2.2.4. Microscopy 86
2.2.4.1. Fluorescent microscopy 86
2.2.4.1.1. Aldehyde fixation 86
2.2.4.1.2. Solvent fixation 86
2.2.4.1.3. Poly-L-lysine mounting 87
2.2.4.1.4. DAPI staining of nuclei 87
2.2.4.2. Live-cell imaging 88
2.2.4.2.1. DASPMI staining of mitochondria 88
2.2.4.2.2. Immobilization of live yeast cells using agarose 89
2.2.4.3. Quantification of microscopic data 89
2.2.5. Protein gel electrophoresis and detection 89
2.2.5.1. Protein preparations 89
2.2.5.2. Sodium dodecyl-sulphate polyacrylamide gel electrophoresis (SDS-PAGE) 91
2.2.5.3. Immunoblot analyses 91
2.2.5.3.1. Protein transfer 91
2.2.5.3.2. Immunoblotting 92
2.2.6. Analysis of protein-protein interactions 93
2.2.6.1. Ball mill grinding of yeast 93
2.2.6.2. Immunoprecipitation of FLAG-Ago1 94
2.2.6.3. Immunoprecipitation of RFP-Rdp1 95
2.2.6.4. Far Western Blot 97
2.2.7. RNA techniques 98
2.2.7.1. Isolation of *S. pombe* RNA 98
2.2.7.2. Reverse transcriptase-polymerase chain reaction (RT-PCR) 99
2.2.7.3. Real-time quantitative PCR (qPCR) 99
2.2.7.4. Analysis of qPCR data 100

CHAPTER 3: The karyopherin Sal3 is required for nuclear import of the core RNA interference pathway protein Rdp1 101

3.1. Rationale and hypothesis 102

3.2. Results 103
3.2.1. Sal3 is important for the nuclear import of Rdp1 103
3.2.2. Kap111, Kap113, Kap114, and Kap123 are not required for the nuclear import of RFP-Rdp1 110
3.2.3. Rdp1 forms a complex with karyopherin Sal3 112
3.2.4. The levels of pericentromeric transcripts are increased in *sal3* mutants 114
3.2.5. *sal3* mutants are sensitive to the microtubule poison thiabendazole 118
3.2.6. *sal3* mutants exhibit chromosome segregation defects 121
3.2.7. Sal3-independent nuclear import of Rdp1 rescues RNAi defects 124
3.2.8. Chromosome segregation defects of *sal3* mutants are partially rescued by expression of Rdp1-SV40-NLS 129
3.2.9. Importin 8 function is not required for silencing centromeric transcripts in *S. pombe* 130
3.2.10. Sal3 activity is not required for localization of Ago1 and Dcr1 to P-body (PB)-like structures 133

3.3. Summary 135

CHAPTER 4: The kinesin motor protein Cut7 regulates biogenesis and function of Ago1-complexes 136

4.1. Rationale and hypothesis 137

4.2. Results 138
4.2.1. Cut7 activity is important for regulating the number and size of Ago1-containing RNPs 138
4.2.2. Cut7 forms a complex with components of the RNAi machinery 144
4.2.3. *cut7-24* mutants are not sensitive to thiabendazole at the restrictive temperature 148
4.2.4. Cut7 activity is important for post-transcriptional silencing of centromeric transcripts 150
4.2.5. Overexpression of the Ago1-binding domain of Cut7 affects the distribution of Ago1 155
4.2.6. Overexpression of the Ago1-binding region of Cut7 does not affect the targeting of Dcr1 to PBs, nor the formation of PBs 157
4.2.7. Overexpression of the Ago1-binding domain of Cut7 does not affect silencing of centromeric repeats 159

4.3. Summary 161

CHAPTER 5: Discussion 162

5.1. Overview 163

5.2. Rdp1 nuclear localization is required for TGS in *S. pombe* 164
5.2.1. RNA-dependent RNA polymerase activity: a universal feature of RNAi? 164
5.2.2. Importin 8 homolog is not involved in siRNA-mediated gene silencing, but is associated with miRNA-mediated RNAi 165
5.2.3. Existing Rdp1-independent pathway: the silencing defects associated with *Δago1* are more severe than those associated with *Δrdp1* 167
5.2.4. A revised model for Sal3 involvement in fission yeast heterochromatin formation 169

5.3. Cut7 activity is required for PTGS in *S. pombe* 172
5.3.1. Cut7 activity is required for PB homeostasis 172
5.3.2. Cut7 activity is important for enhancing PTGS 173
5.3.3. TGS is not significantly affected by decreased Cut7 activity 175
5.3.4. A proposed model for Cut7 activity in maintaining PB homeostasis and formation 175

5.4. Phosphorylation states of Ago1 may affect targeting to PBs in *S. pombe* 178
5.4.1. Kinase and phosphatase activities; critical links between RNAi and other cell signaling pathways 178
5.4.2. Cellular localization of Argonaute protein and phosphorylation 180

5.5. Future directions 182

REFERENCES 184

APPENDIX 211

LIST OF TABLES

Table 1.1.	Post-translational modification (PTM) conservation of site-specific residues on Argonautes involved in various organisms	48
Table 2.1.	Commercial sources of materials, chemicals, and reagents	56
Table 2.2.	Multi-component systems	58
Table 2.3.	DNA/RNA modifying enzymes	58
Table 2.4.	Molecular size standards	58
Table 2.5.	Detection systems	58
Table 2.6.	Buffers and Solutions	59
Table 2.7.	Yeast media	61
Table 2.8.	Oligonucleotides	61
Table 2.9.	Plasmid vectors	63
Table 2.10.	Primary antibodies	64
Table 2.11.	Secondary antibodies	64
Table 2.12	*Schizosaccharomyces pombe* strains	64
Table 2.13.	*S. pombe* online resources	66
Table 4.1.	Known motor proteins in *S. pombe*	141

LIST OF FIGURES

Figure 1.1.	Schematic of small RNA-mediated gene silencing mechanisms	4
Figure 1.2.	Structure of Argonaute protein	8
Figure 1.3.	Domain composition and structure of the members of RNase III protein family	18
Figure 1.4.	Model for RNAi-mediated heterochromatin formation in *S. pombe*	28
Figure 1.5.	Possible mechanisms of miRISC-mediated translational repression of mRNAs	33
Figure 1.6.	Overall structure of the nuclear pore complex (NPC)	41
Figure 1.7.	Nucleocytoplasmic transport	43
Figure 1.8.	Post-translational modifications of gene silencing factors involved in small RNA pathways	50
Figure 3.1.	Sal3 is required for nuclear import of Rdp1	107
Figure 3.2.	Karyopherins Kap111, Kap113, Kap114, and Kap123 are not required for nuclear import of RFP-Rdp1	111
Figure 3.3.	Rdp1 forms a complex with Sal3	113
Figure 3.4.	Sal3 is important for silencing centromeric transcripts	117
Figure 3.5.	*sal3* mutants are sensitive to the microtubule poison thiabendazole (TBZ)	120
Figure 3.6.	*sal3* mutants exhibit chromosome segregation defects	123
Figure 3.7.	Sal3-independent nuclear import of Rdp1 rescues the protein targeting to the nucleus.	126
Figure 3.8.	Sal3-independent nuclear import of Rdp1 rescues RNAi and chromosome segregation defects	127
Figure 3.9.	Loss of the importin 8 ortholog gene does not affect the localizations of RNAi core proteins or silencing of centromeric loci	131
Figure 3.10.	Localization of GFP-tagged Ago1 and Dcr1 is normal in *sal3* mutant	134

Figure 4.1.	Cut7 activity is important for regulating the number and size of Ago1-containing RNPs	142
Figure 4.2.	Cut7 forms a complex with components of the RNAi machinery	146
Figure 4.3.	*cut7-24* mutants are not sensitive to thiabendazole at the restrictive temperature	149
Figure 4.4.	Cut7 activity is important for post-transcriptional silencing of centromeric transcripts	153
Figure 4.5.	Disruption of Cut7 activity for 18 hours does not result in loss of viability or in gross disruption of the microtubule network	154
Figure 4.6.	Overexpression of the Ago1-binding domain of Cut7 affects the distribution of Ago1, but not the formation of PBs	158
Figure 4.7.	Over-expression of the Ago1-binding domain of Cut7 does not affect the silencing of centromeric repeats	160
Figure 5.1.	A revised model depicting Sal3 involvement in heterochromatin formation	171
Figure 5.2.	A proposed model depicting the role of the microtubule-associated motor protein Cut7 activity in regulating Ago1-containing PB homeostasis in *S. pombe*	177

LIST OF NOMENCLATURE AND ABBREVIATIONS

3'UTR	3'untranslated region
5-FOA	5-fluoroorotic acid
ADP	adenosine diphosphate
Ago1	Argonaute protein 1 in *Schizosaccharomyces pombe*
Arb1	Ago1-binding protein 1
Arb2	Ago1-binding protein 2
ARC	Argonaute siRNA chaperone complex
ATP	adenosine triphosphate
BSA	bovine serum albumin
cDNA	complementary deoxyribonucleic acid
CBD	cargo-binding domain
CDK	cyclin-dependent kinase
Cid12	caffeine-induced death resistant 12 protein
Chp1	chromodomain-containing protein 1
Clr4	calcitonin-like receptor 4
CLRC	chromatin modifying complex containing Clr4- Rik1-Cul4
cnt	central core region of centromere
CSM	complete synthetic media
Ct	cycle threshold
CT	carboxyl-terminal
Cul4	E3 ubiquitin ligase Cullin4
DAPI	4',6-diamidino-2-phenylindole
DASPMI	2-[4-(dimethylamino)styryl]-l-methylpyridinium iodide
°C	degree Celsius

D-elp1	*Drosophila* RNA polymerase II core elongator complex
DGCR8	DiGeorge syndrome critical region gene 8
DMSO	dimethyl sulphoxide
DNA	deoxyribonucleic acid
dsRBD	dsRNA binding domain
dsRNA	double stranded RNA
DTT	dithiothreitol
EDTA	ethylenediaminetetraacetic acid
EMM	Edinburgh minimal medium
ERK	extracellular signal-regulated kinases
GFP	green fluorescent protein
GW repeats	glycine-tryptophan repeats
H3K9me	methylated lysine 9 of histone 3
HA	hemagglutinin
hAgo2	human Argonaute 2 protein
HDAC	histone deacetylase
HMT	histone methyltransferase
HP1	heterochromatic protein 1
Hrr1	helicase required for RNAi-mediated heterochromatin assembly
HSP	heat-shock protein
HU	hydroxyurea
IgG	immunoglobulin G
imr	innermost repeats of centromere
IP	immunoprecipitation
KHC	kinesin heavy chain
kDa	kilo dalton

M	moles per litre
LMB	leptomycin B
MAPK	mitogen-activated protein kinase
ME	malt extract
miRNA	microRNA
miRISC	miRNA containing RISC complex
NES	nuclear export signal
NLS	nuclear localization signal
nmt	no message in thiamine
NP40	nonidet P-40
Nt	nucleotide
NT-CBD	amino-terminal cargo binding domain
otr	outermost repeats of centromere
PAZ	Piwi-Argonaute-Zwille
Pasha	partner of Drosha
P body (or PB)	processing body
PBS	phosphate buffered saline
PBS-T	phosphate buffered saline, tween 20
PEG	polyethylene glycol
PEV	position effect variegation
piRNA	piwi-interacting RNA
pre-rRNA	rRNA precursors
pre-miRNA	miRNA precursors
pri-miRNA	primary miRNA
PTGS	post-transcriptional gene silencing
PTM	post-translational modification

PVDF	polyvinylidene fluoride
qRT-PCR	quantitative reverse transcriptase-polymerase chain reaction
RDRC	RNA-directed RNA polymerase complex
RdRP	RNA-dependent RNA polymerase
RFP	red fluorescent protein
Rik1	RS2-interacting KH domain protein 1
RIPA	radioimmunoprecipitation buffer
RISC	RNA-induced silencing complex
RITS	RNA-induced transcriptional silencing complex
RLC	RISC loading complex
RNA	ribonucleic acid
RNAi	RNA interference
RNAPII	RNA polymerase II
RNase III	ribonuclease III
RNP	ribonucleoprotein
ROX	5-carboxy-X-rhodamine
RT-PCR	reverse transcriptase polymerase chain reaction
SDS	sodium dodecyl sulphate
SDS-PAGE	sodium dodecyl-sulphate polyacrylamide gel electrophoresis
SG	stress granule
siRNA	short interfering RNA
snRNA	small nuclear RNA
snoRNA	small nucleolar RNA
S. pombe	*Schizosaccharomyces pombe*
ssDNA	single stranded DNA
ssRNA	single stranded RNA

Stc1	siRNA to chromatin
Swi6	SWItch/sucrose nonfermentable 6
Tas3	tyrosine auxotrophy suppressor 3
TRBP	Trans-activating response RNA-binding protein
TBZ	thiabendazole
TEMED	N,N,N’,N’,-tetramethylenediamine
TGS	Transcriptional gene silencing
U	enzymatic units
V	volts
v/v	volume per volume
WB	western blot
w/v	weight per volume
YE	yeast extract
YEA	yeast extract with adenine
YEP	yeast extract with phloxin B
YES	yeast extract with supplement

CHAPTER 1:
Introduction

1.1. Overview of RNA interference (RNAi)

RNA interference (RNAi) or small RNA-mediated sequence-specific gene silencing is an evolutionarily conserved process present in the vast majority of eukaryotes. The yeast *Saccharomyces cerevisiae* (*S. cerevisiae*) is a notable exception, though RNAi is present in other budding yeast species, including *Saccharomyces castellii* and *Candida albicans* (Drinnenberg et al. 2009). RNAi modulates gene expression at both the transcriptional and post-transcriptional levels [reviewed in (Mello and Conte 2004; Hannon 2002)]. It was first discovered by Fire, Mello, and their colleagues in *Caenorhabditis elegans* (*C. elegans*) over a decade ago (Fire et al. 1998). Although the term RNAi was originally used to describe silencing mediated by exogenous double-stranded RNA (dsRNA) in *C. elegans* (Fire et al. 1998), it now broadly refers to gene silencing triggered by various small RNAs, including siRNAs, miRNA, and piRNAs [reviewed in (Ender and Meister 2010; Kim et al. 2009; Moazed 2009)]. Originally, RNAi may have evolved as a defense mechanism in lower eukaryotes to maintain genome integrity; for instance, RNAi machinery is required to protect the genome from invasion by repetitive DNA elements, such as transposons and retrotransposons (Grewal and Jia 2007; Jaronczyk et al. 2005; Mello and Conte 2004).

The canonical RNAi process can be divided into three steps (Tomari and Zamore 2005; Meister and Tuschl 2004). First, a long double-stranded RNA (dsRNA), which is expressed in the cell or introduced into the cell, can be processed into small RNA duplexes by an RNase type III ribonuclease enzyme,

called Dicer. Two main categories of these small RNAs have been defined on the basis of their precursors (Siomi and Siomi 2009). Short interfering RNAs (siRNAs) can be produced from the cleavage of long dsRNA precursors in response to viral infection or after artificial introduction, whereas microRNAs (miRNAs) are generated from the processing of genome-encoded stem-loop miRNA precursors [reviewed in (Ender and Meister 2010; Kim et al. 2009)]. Recently, several new classes of endogenous small RNA species were uncovered by using high-throughput sequencing technology (Siomi and Siomi 2009). These include PIWI-interacting RNAs (piRNAs) and endogenous siRNAs (endo-siRNAs or esiRNAs). piRNAs are present in *Drosophila melanogaster* (*D. melanogaster*), *C. elegans,* and mammals, but seem to be absent in fungi and plants (Moazed 2009). Second, these small RNAs are loaded onto an Argonaute protein of the RNA-induced silencing complex (RISC). The loaded small RNA duplex is unwound. Third, a guide strand, one strand of the duplex, targets RISC to homologous messenger RNAs (mRNAs) (Hammond et al. 2000), and then mediates several different modes of gene silencing (Figure 1.1). In *S. pombe*, the core components of the RNAi machinery, such as Argonaute (Ago1), Dicer (Dcr1), and RNA-dependent RNA polymerase (Rdp1), alters chromatin structure and silences genes at the transcriptional level (Moazed et al. 2006; Volpe et al. 2003; Volpe et al. 2002).

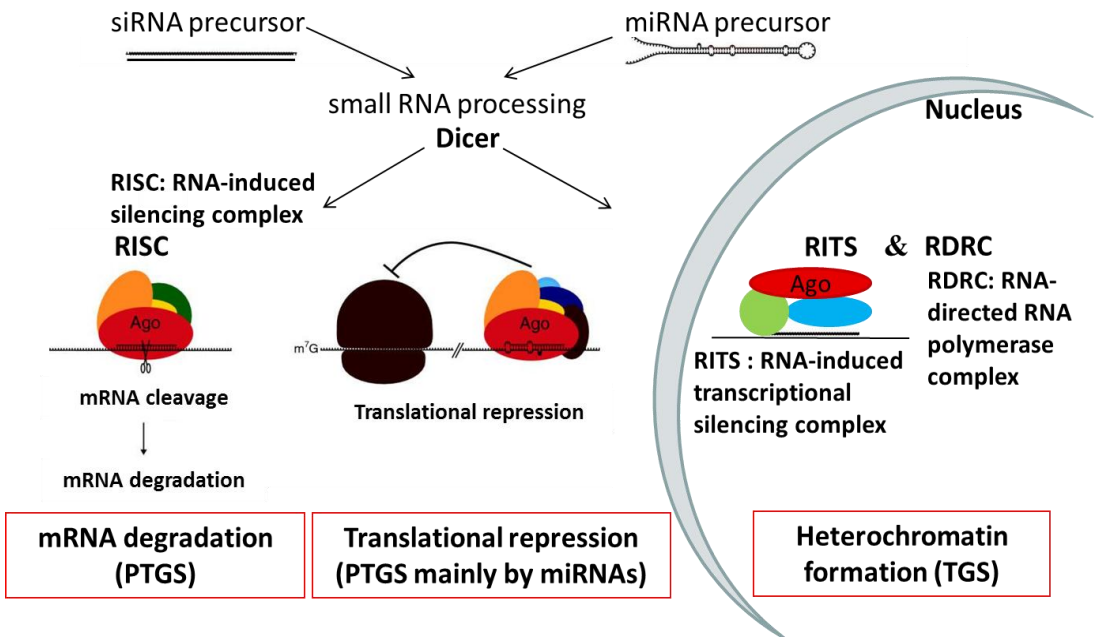

Figure 1.1. Schematic of small RNA-mediated gene silencing mechanisms. To mediate efficient gene silencing, Argonaute proteins form effector complexes by interacting with other proteins. RNAi processes can be triggered by double-stranded small interfering RNAs (siRNAs, ~22nt), which are processed from long dsRNAs by a type III RNAse enzyme called Dicer. A guide strand is incorporated into effector complexes, which are called RNA-induced silencing complexes (RISC); these direct RISC to target mRNAs. The RISC mediates several different modes of gene silencing: sequence-specific degradation of mRNAs, translational repression (effected mainly by miRNAs), and transcriptional gene silencing (TGS). In *S. pombe*, the mode of TGS is mediated by a specialized form of RISC called the RNA-induced transcriptional silencing (RITS) complex and association with RNA-directed RNA polymerase complex (RDRC). Adapted from (Moazed 2009; Hock and Meister 2008)

1.2. Effector complexes involved in RNAi

In *S. pombe*, there are several RNAi complexes involved in gene silencing: RNA-induced silencing complex (RISC), RNA-induced transcriptional silencing (RITS) complex, Argonaute siRNA chaperone complex (ARC), and RNA-directed RNA polymerase complex (RDRC). These associate with chromatin remodeling complex (CLRC). This section expounds upon these complexes.

1.2.1. Argonaute superfamily and RNA-induced silencing complex

1.2.1.1. Argonaute protein family: structure, characteristics, and function

Argonaute proteins are highly conserved from archaebacteria to humans and are considered to be key molecules in RNAi pathways (Ender and Meister 2010). Argonaute proteins were first identified in plants; members are defined by the presence of Piwi-Argonaute-Zwille (PAZ) and P-element-induced wimpy testis (PIWI) protein domains (Bohmert et al. 1998). The Argonaute protein family is divided into two sub-families: the Argonaute sub-family, which resembles *Arabidopsis thaliana* (*A. thaliana*) Ago1, and the Piwi sub-family, which is related to the *Drosophila* PIWI protein (Ender and Meister 2010; Hannon 2002; Bohmert et al. 1998). The expression of PIWI proteins is restricted to the germ line and undifferentiated cells, where they associate with a class of small RNAs known as piRNAs (Thomson and Lin 2009; Peters and Meister 2007; Cox et al. 1998). The proteins of the Argonaute sub-family, in contrast, are ubiquitously expressed and bind to siRNAs or miRNAs to mediate post-

transcriptional gene silencing (PTGS), either by destabilization of the mRNA or by translational repression (Hock and Meister 2008).

The number of Argonaute genes range from 1 in the fission yeast *S. pombe* to 27 in the nematode *C. elegans* (Yigit et al. 2006; Carmell et al. 2002). The human genome encodes four members of the Argonaute subfamily (hAgo1, hAgo2, hAgo3, and hAgo4) and four of the Piwi subfamily (HIWI, HILI, HIWI3, and HIWI2) (Peters and Meister 2007). Interestingly, of the four human Argonaute isoforms, only hAgo2 can cleave targeted mRNAs (Liu et al. 2004; Meister et al. 2004).

The molecular mass of Argonaute proteins is typically ~ 100 kDa. They contain a PAZ domain, which binds the 2-nucleotide 3' overhang of siRNAs (Lingel et al. 2004; Song et al. 2003; Cerutti et al. 2000), and a PIWI domain, which, in some isoforms, has enzymatic activity (Rivas et al. 2005; Liu et al. 2004; Cerutti et al. 2000) (Figure 1.2). More recently, structural studies of the *Thermus thermophiles* Argonaute and human Argonaute 2 revealed that the protein contains a MID domain between PAZ and PIWI, and harbors a binding pocket in the vicinity of the PIWI domain that interacts with phosphates of the 5'end of the guide siRNA (Figure 1.2) (Schirle and MacRae 2012; Jinek and Doudna 2009; Parker et al. 2005; Yuan et al. 2005; Cerutti et al. 2000).

The principle functions of Argonaute proteins in RNAi pathways have been well studied [reviewed in (Hannon 2002)]. Argonaute proteins are guided to specific target mRNAs by association with siRNAs and miRNAs, and form an effector complex called a RISC. The RISC components in human consist of Ago2,

Dicer, TRBP (Human Immunodeficiency Virus Trans-activating Response RNA-binding protein), and PACT, a multiple dsRBD-containing protein (Lee et al. 2006; Chendrimada et al. 2005; Haase et al. 2005) (Section 1.2.2.3).

In *S. pombe*, it is assumed that the RISC is formed of Ago1, Dcr1, Rdp1, and a guide strand of siRNA (Carmichael et al. 2006). The sole Ago1 protein in *S. pombe* is involved in the establishment of heterochromatin (Moazed et al. 2006; Volpe et al. 2003; Volpe et al. 2002) (Section 1.3.1.1). However, it has been shown that the Ago1 can also guide PTGS when provided with an artificial reporter plasmid (Sigova et al. 2004). Natural targets of post-transcriptional silencing in *S. pombe* have not yet been reported (Hock and Meister 2008).

(A)

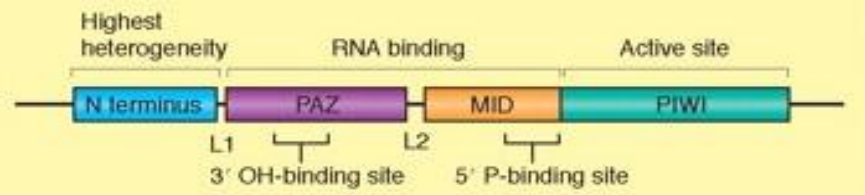

(B)

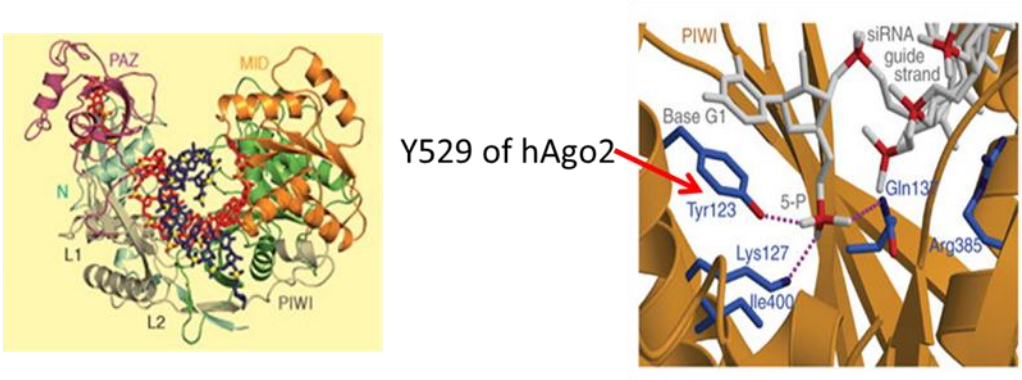

Figure 1.2. Structure of Argonaute protein. Schematic depiction showing the domain structure of a generic Argonaute protein **(A)** and the crystal structure **(B)** of *Thermus thermophiles* Argonaute. The PAZ domain for binding of small RNA 3'-end and the MID-PIWI domain lobe for binding of small RNA 5'-phosphate are depicted. *A. fulgidus* PIWI residues involved in 5'-siRNA binding pocket and the 5'-phosphate of siRNA are shown (bottom right). Structurally related residue in hAgo2 (Y529) is also shown. Adapted from (Ender and Meister 2010; Hock and Meister 2008; Till et al. 2007)

1.2.1.2. RNA-induced transcriptional silencing complex in fission yeast

In addition to their role in small RNA-mediated gene silencing at the post-transcriptional or mRNA level in the cytoplasm, Argonaute proteins also function at the transcriptional level in the nucleus (Figure 1.1). In *S. pombe*, siRNAs derived from centromeric repeats are incorporated into a specialized form of RISC called the RNA-induced transcriptional silencing (RITS) complex. The RITS complex consists of Ago1 in conjunction with single-stranded centromeric siRNA, chromodomain protein Chp1 (chromodomain-containing protein 1), and GW-homologue Tas3 (tyrosine auxotrophy suppressor 3) (Verdel et al. 2004).

The chromodomain of the Chp1 protein recognizes and binds to methylated lysine 9 of histone 3 (H3K9me), a hallmark of heterochromatin (Schalch et al. 2009; Partridge et al. 2002). Chp1 is required for heterochromatic silencing over the outer repeats of the centromere and inserted reporter genes. Deletion of the *chp1* gene causes centromere-specific decreases in Swi6 localization and H3K9me (Sadaie et al. 2004; Partridge et al. 2002). Tas3 contains glycine and tryptophan (GW) rich motifs that interact with Ago1 (Debeauchamp et al. 2008; Partridge et al. 2007; Verdel et al. 2004).

The RITS complex is required for centromeric heterochromatin formation in *S. pombe* (Verdel et al. 2004; Motamedi et al. 2004) (Section 1.3.1.1.). The association between the RITS complex and heterochromatin is dependent on the presence of Dcr1, indicating that siRNAs guide RITS to specific chromatin regions (Verdel et al. 2004). This complex also associates with an RNA-dependent RNA polymerase complex (Section 1.2.3) and a histone

methyltransferase (HMT) Clr4 containing chromatin modifying complex (Section 1.2.4). There are similarities and differences between RISC and RITS. Like RISC, RITS uses siRNAs for target recognition. However, unlike RISC, RITS associates with chromatin and initiates heterochromatin formation as opposed to mRNA inactivation (Verdel et al. 2004; Motamedi et al. 2004). To date, two models have been proposed to explain how siRNA targets specific chromosome regions. In the first, siRNA bound to Ago1 in the RITS complex forms a base-pair with an unwound DNA double helix through an undetermined mechanism. In the second, RITS-associated siRNAs are base-paired with non-coding RNA transcripts at the target locus (Motamedi et al. 2004). Both models include the association of RITS with chromatin via siRNAs.

1.2.1.3. Argonaute siRNA chaperone complex

In addition to RITS, Ago1 associates with another auxiliary complex, Argonaute siRNA Chaperone Complex (ARC), that includes the Ago1-binding proteins 1 and 2 (Arb1 and Arb2) and double-stranded siRNAs (Buker et al. 2007). While the RITS complex is associated with single-stranded siRNAs, ARC is mostly associated with double-stranded siRNAs. Buker *et al*. demonstrated that purified Arb1 inhibited the endonuclease activity of Ago1 *in vitro* and that mutant Ago1, which lacks slicer activity, was associated only with double-stranded siRNAs (Buker et al. 2007). This may indicate that Arb1 and Arb2 inhibit the release of the siRNA passenger strand from Ago1 (Buker et al. 2007).

Furthermore, both proteins are required for H3K9me, heterochromatin assembly, and siRNA generation (Buker et al. 2007).

1.2.1.4. Processing bodies

Processing bodies (P bodies or PBs) are ribonucleoprotein (RNP)-containing cytoplasmic microdomains and are known to be sites of mRNA degradation, mRNA translational control, and/or mRNA storage [reviewed in (Moser and Fritzler 2010)]. These distinct cytoplasmic foci were initially reported in 1997, when Bashkirov et al. examined the cellular localization of mXRN1p, a 5'-to-3' exonuclease that is associated with mRNA decay in mouse cells (Bashkirov et al. 1997). Five years later, it was found that these distinct RNP bodies contain the RNA binding phosphoprotein GW182 in mammalian cells (Eystathioy et al. 2002). GW182 is now a commonly used marker for P bodies.

Components of P bodies were subsequently identified in other eukaryotic cells, such as *S. cerevisiae*, *D. melanogaster*, *C. elegans*, and mammals [reviewed in (Eulalio et al. 2009; Jakymiw et al. 2007; Parker and Sheth 2007)]. To date, however, no homologue of the GW182 protein has been identified in yeast P bodies (Moser and Fritzler 2010), although GW-homologue Tas3 is associated with RITS complex in the nucleus (Verdel et al. 2004). Regardless of their origin, P bodies are enriched in enzymes that mediate mRNA decay (Sheth and Parker 2003), such as Dcp2, Dcp1, Lsm1-7, and CCR4 (Eulalio et al. 2007a; Andrei et al. 2005; Cougot et al. 2004; Sheth and Parker 2003; van Dijk et al. 2002).

These cytoplasmic foci are also known to be associated with the protein components that function in RNAi, such as hAgo2 in mammals (Leung et al. 2006; Liu et al. 2005b), and therefore have been implicated in small RNA-mediated post-transcriptional gene silencing pathways (Moser and Fritzler 2010). Evidence suggests that PBs form as a consequence of RNAi-mediated silencing (Eulalio et al. 2007b). However, other studies have shown that the RNAi process can occur in the absence of microscopically visible PBs (Eulalio et al. 2007b; Chu and Rana 2006; Rehwinkel et al. 2005). In addition, it has been observed that PBs exist in the absence of active RISC, as observed in Dicer knockout cells (Leung et al. 2006). Therefore, the function of PBs and their association with RNAi is still a matter of debate. Nevertheless, these specialized cytoplasmic RNP bodies are thought to serve an important role in increasing the efficiency of post-transcriptional regulation and in preventing the inadvertent degradation of functional mRNAs by concentrating the factors that govern these processes (Moser and Fritzler 2010). Recently, phosphorylation of hAgo2, which regulates the association of the protein with P bodies, has been reported (Johnston and Hutvagner 2011; Zeng et al. 2008; Rudel and Meister 2008) (Section 1.4.2). The functional role of phosphorylation of RNAi components, such as Argonaute proteins or GW182, may offer an intriguing area for future research.

In *S. pombe,* the RISC complex, which presumably contains Ago1, Dcr1, Rdp1, and siRNA, is thought to be associated with post-transcriptional gene silencing in cytoplasmic puncta (Carmichael et al. 2006). Interesting observations on the association of the RNAi apparatus with microtubule motor proteins led to

speculation that bidirectional movement of PBs along microtubules may be a mechanism for scanning the cytoplasmic mRNAs targeted for silencing or degradation (Stoica, Park et al. 2010). This topic will be discussed in Chapter 4.

1.2.2. RNase III protein family and small RNA processing complexes

The ribonuclease III (RNase III) family is a class of endoribonucleases that function in processing dsRNA precursors into functional RNAs that are utilized in RNAi or in regulating protein synthesis (MacRae and Doudna 2007). They are ubiquitous and have critical roles in a range of other cellular activities, such as cell division and chromosome segregation (Catala et al. 2004). An endonuclease specific for dsRNA substrates was first described in *Escherichia coli* (*E. coli*) by Zinder and colleagues in 1968 (Robertson et al. 1968). All RNase III family members contain a characteristic ribonuclease domain called the "RNase III domain" or simply "RNase III". Cleavage by RNase III enzyme produces a characteristic terminal structure of dsRNA consisting of a 5'-phosphate group and a two base overhang at the 3'end (Robertson et al. 1968). RNase III proteins vary widely in length from ~200 to ~2,000 amino acid residues. They are subdivided into three classes (Class 1, 2, and 3) based on domain composition and organization. Representative members of each class are *E. coli* RNase III, Drosha, and Dicer, respectively (MacRae and Doudna 2007; Lamontagne et al. 2001) (Figure 1.3A).

1.2.2.1. Class 1 RNase III

Class 1 RNase III enzymes are the simplest and smallest family members. They contain a single RNase III and a dsRNA binding domain (dsRBD) (Figure 1.3A) and are found in bacteria, bacteriophage, and some fungi. In *E. coli*, RNase III plays an important role in processing rRNA precursors (pre-rRNAs) (Apirion and Miczak 1993; Westphal and Crouch 1975), as well as in regulating translation by acting on target mRNAs (Aristarkhov et al. 1996; Regnier and Grunberg-Manago 1989). Activity of class 1 RNase III proteins requires the formation of a homodimer. Dimerization occurs when the two RNase III domains combine to form a single catalytic center—each domain hydrolyses one RNA strand of the duplex substrate (Zhang et al. 2004; Blaszczyk et al. 2001; Nagel and Ares 2000; Dunn 1976).

The best-characterized eukaryotic class 1 RNase III is the *S. cerevisiae* enzyme Rnt1. It participates in the regulation of specific mRNAs (Ge et al. 2005), as well as in the processing of yeast pre-rRNAs (Kufel et al. 1999), small nuclear RNAs (snRNAs), and small nucleolar RNAs (snoRNAs) (Lamontagne et al. 2001; Chanfreau et al. 1998b; Chanfreau et al. 1998a).

1.2.2.2. Class 2 RNase III

Class 2 proteins, also known as members of the Drosha family, contain a single dsRBD and two RNase III domains (RNase IIIa and IIIb) (Figure 1.3A). These enzymes function as monomers in which the nuclease center is formed by two RNase III domains (Han et al. 2004). They localize predominantly to the

nucleus (Wu et al. 2000). It has been shown that Drosha activity is required upstream of Dicer in miRNA biogenesis, processing the several kilo-base-long primary miRNAs (pri-miRNAs) into short hairpin-shaped intermediates known as miRNA precursors (pre-miRNAs), which are approximately 70 nucleotides in length (Lee et al. 2003). After they are processed by Drosha, pre-miRNAs are exported from the nucleus to the cytoplasm by the karyopherin Exportin 5 (Bohnsack et al., 2004; Lund et al., 2004; Yi et al., 2003). Then, they are cleaved by Dicer to generate mature miRNAs (Hutvagner et al. 2001; Ketting et al. 2001).

Drosha does not function in isolation *in vivo,* rather, the specificity of substrate recognition requires a Drosha-associated protein called DiGeorge syndrome critical region gene 8 (DGCR8) in humans (Han et al. 2006). Pasha (partner of Drosha), an ortholog of DGCR8 in *C. elegans* and in *D. melanogaster,* forms a complex with Drosha termed the Microprocessor (Kim et al. 2009) (Figure 1.3B). This complex functions in the processing of pri-miRNAs (Denli et al. 2004; Gregory et al. 2004). Although Drosha is absent in plants, the general features of the miRNA pathway are conserved in plants and animals, but not in fungi and protozoa (Moazed 2009).

1.2.2.3. Class 3 RNase III

Class 3 RNase III enzymes, also known as the Dicer family, are the largest family members. They have bidentate ribonuclease activity that generates 22-nt siRNAs from long dsRNA precursors (Bernstein et al. 2001). These modular 200 kDa enzymes function downstream of Drosha to produce mature miRNAs which,

like siRNAs, are incorporated into Argonaute proteins to form miRNA RISC (miRISC) (Kawamata and Tomari 2010; Kim et al. 2009; Hutvagner et al. 2001; Ketting et al. 2001; Bernstein et al. 2001). Once loaded onto an Argonaute protein, the miRNA duplex is unwound. A guide strand remains associated with an Argonaute protein as a part of the mature RISC (Kawamata and Tomari 2010).

Biochemical experiments have shown that Dicer interacts with the PIWI domain of hAgo2 through its RNase IIIa domain (Sasaki and Shimizu 2007; Tahbaz et al. 2004). Interestingly, Dicer also associates with other dsRNA-binding proteins. For example, in *D. melanogaster*, Dicer1 requires Loquacious (also known as R3D1), which contains three dsRBDs for pre-miRNA processing (Forstemann et al. 2005; Jiang et al. 2005; Saito et al. 2005). In humans, Dicer interacts with two closely related dsRBD-containing proteins, TRBP and PACT (Kim et al. 2009; Lee et al. 2006; Chendrimada et al. 2005; Haase et al. 2005). Although neither TRBP nor PACT is required for miRNA processing *per se*, they are both involved in RISC formation (Lee et al. 2006; Chendrimada et al. 2005; Haase et al. 2005). Dicer, TRBP, and/or PACT contribute to RISC assembly by loading the miRNA onto hAgo2 by forming a RISC loading complex (RLC) (MacRae et al. 2008; Chendrimada et al. 2005; Maniataki and Mourelatos 2005). Evidence suggests that after being released from Dicer, the thermodynamically stable end of the miRNA duplex is bound to TRBP in the RLC, while the other end interacts with hAgo2 (Preall and Sontheimer 2005; Tomari et al. 2004b). Consequently, the strand containing the 5′end with lower thermodynamic stability of base pairing (the guide strand) is incorporated into mature RISC and the other

strand (the passenger strand) is destroyed (Tolia and Joshua-Tor 2007). In *D. melanogaster*, R2D2, a protein with two dsRBDs, also senses the thermodynamic inequalities of RNA duplexes. R2D2 forms a stable heterodimeric complex with Dicer2 and binds to the more stable end of the RNA duplex. AGO2 is oriented toward the other end of the RNA duplex (Tomari et al. 2004a; Tomari et al. 2004b; Liu et al. 2003).

The discovery that RNase III enzymes function in generating miRNAs and siRNAs for RNAi has fueled interest in their structures and mechanisms (MacRae and Doudna 2007). Still, many unanswered questions remain. For instance, the roles of accessory domains of RNase III family members are not yet fully understood.

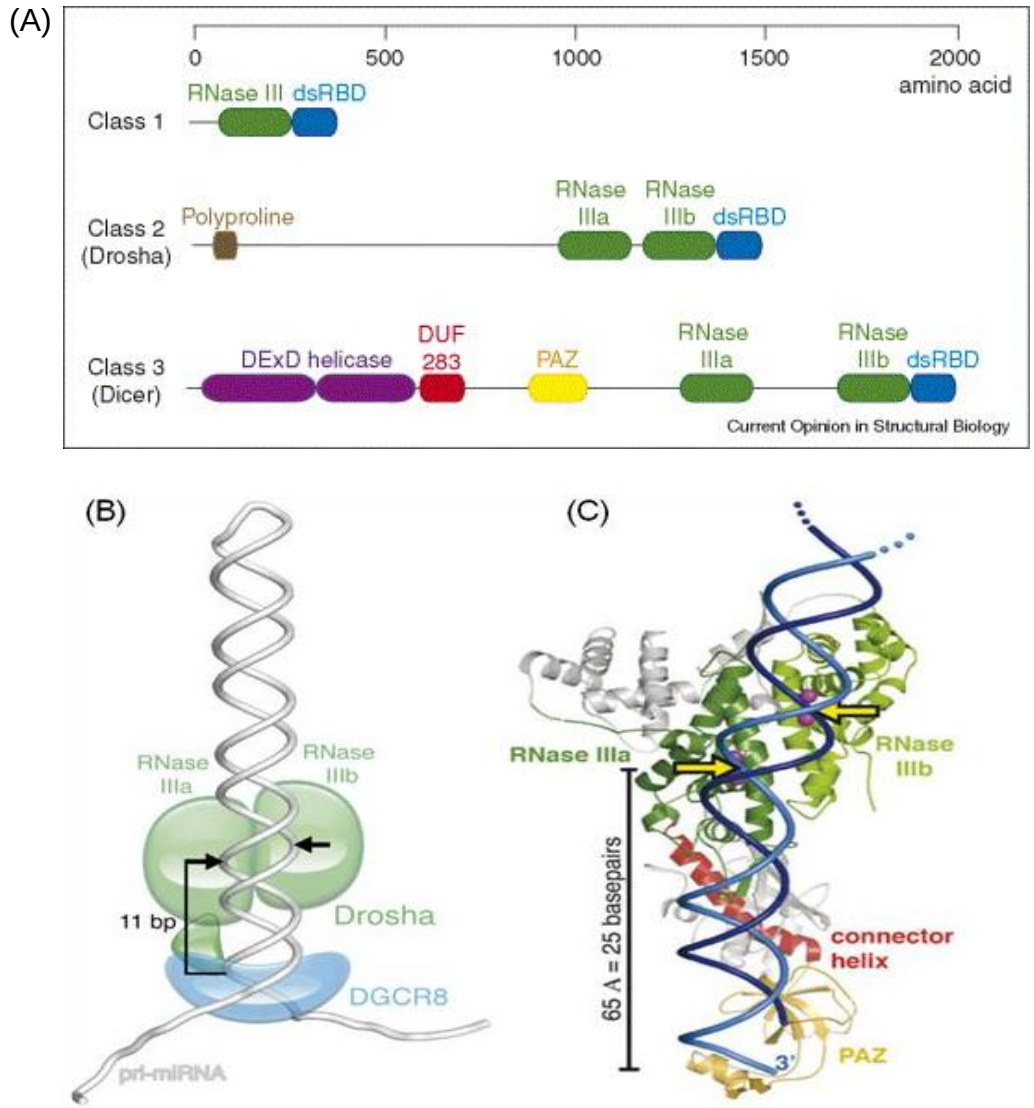

Figure 1.3. Domain composition and structure of the members of RNase III protein family. (A) Schematic of the RNase III enzyme classes. The top bar indicates scale in units of amino acid residues. Functional domains are color-coded as follows: ribonuclease domain (RNase III), green; dsRBD, blue; proline-rich region, brown; DExD helicase domain, purple; DUF283, red; PAZ domain, yellow. **(B)** Schematic of the Microprocessor complex bound to a pri-miRNA. Drosha and DGCR8 subunits are green and blue, respectively. Black arrows indicate the cleavage sites in the pri-miRNA. **(C)** The two RNase III domains of *Giardia* Dicer are arranged to form an intramolecular dimer with a single processing center. The region of the RNase III domains is linked to the PAZ-containing handle region by a connector helix. Modeling dsRNA onto the structure of Dicer demonstrates that the distance from the PAZ domain to the ribonuclease domains determines the length of the RNA produced by Dicer. Yellow arrows indicate sites of RNA cleavage. Adopted from (MacRae and Doudna 2007)

1.2.3. RNA-dependent RNA polymerase family and RNA-dependent RNA polymerase complex

In lower eukaryotes, such as plants (Schiebel et al. 1993; Dalmay et al. 2000), worms (Sijen et al. 2001; Smardon et al. 2000), fungi (Martens et al. 2002; Cogoni and Macino 1999), and fission yeast (Volpe et al. 2002), RNA-dependent RNA polymerase (RdRP) is an essential component of RNA silencing pathways (Lipardi and Paterson 2010). The primary role of RdRP in these pathways is the generation of dsRNAs. This can occur either by *de novo* second-strand synthesis or siRNA-primed transcription from single-stranded transcripts. Through its role in RNAi, RdRP function is critical for many cellular processes (Sugiyama et al. 2005). For example, in *Arabidopsis*, SDE1/SGS2/RDR6 has anti-viral activity and RDR2 has a role in production of siRNAs from endogenous transcripts (Xie et al. 2004; Mourrain et al. 2000). RRF-1 and EGO-1 in *C. elegans* are required for production of secondary siRNAs from RNAi-targeted transcripts in somatic cells and germ-line development, respectively (Sijen et al. 2001; Smardon et al. 2000). Also, *N. crassa* Sad1 is essential for silencing unpaired DNA during meiosis (Shiu et al. 2001).

Because there are no obvious RdRP homologs in *Drosophila* or mammals, it was assumed that RNAi in these organisms did not require RdRP activity. The Paterson group recently showed that the largest subunit of the *Drosophila* RNA polymerase II (RNAPII) core elongator complex, D-elp1, has RdRP activity (Lipardi and Paterson 2009), suggesting that this polymerase activity may be common to RNAi in all organisms. The study showed that D-elp1 was involved in

RNAi, transposon suppression, and endo-siRNA production, but not miRNA targeting (Lipardi and Paterson 2009). However, this report was recently retracted due to the misinterpretation of the nearest neighbor analysis [(Lipardi and Paterson 2011), also refer to Section 5.2.1].

Motamedi *et al*. identified the second major RNAi complex required for heterochromatin assembly in fission yeast *S. pombe*, the RNA-directed RNA polymerase complex (RDRC) composed of Rdp1, Hrr1 (helicase required for RNAi-mediated heterochromatin assembly), and Cid12 (caffeine-induced death resistant 12) (Motamedi et al. 2004). Together with Ago1 and Dcr1, Rdp1 is the third major protein in the RNAi machinery of *S. pomb*e. It is the core component of the RDRC which amplifies RNAi signals in this organism (Volpe et al. 2002). Hrr1 is a member of the DEAD box RNA helicase family (Tomari et al. 2004a; Tabara et al. 2002)—it mediates interaction with Ago1. Cid12 is a member of the Trf4/Trf5 family of poly (A)-polymerases, which contains a nucleotidyl-transferase domain (Lee et al. 2009; Chen et al. 2005). Importantly, the RITS complex recruits the RDRC and these two major complexes physically interact together in a Clr4-dependent manner (Motamedi et al. 2004). RDRC is recruited to specific heterochromatin regions where ongoing transcription allows this complex to use the nascent RNAs as templates for generating dsRNAs and subsequently siRNAs by Dcr1 (Colmenares et al. 2007).

1.2.4. Chromatin modifying complex and association with RNAi complexes

The main characteristic of heterochromatin, di- or trimethylation of H3K9, is conserved in fungi, plants, and animals. This modification is catalyzed by the HMT Clr4 (calcitonin-like receptor 4), the yeast counterpart of *D. melanogaster* SU(VAR)3-9, and human SU39h (Grewal and Jia 2007; Peters et al. 2001). Clr4 forms a chromatin modifying complex, CLRC (Clr4- Rik1-Cul4 complex), with the heterochromatin remodeling components Rik1 (RS2-interacting KH domain protein 1) and Cul4 (E3 ubiquitin ligase Cullin4) (Grewal and Jia 2007; Hong et al. 2005; Peters et al. 2001).

The H3K9me marks serve as docking sites for HP1 (Heterochromatin Protein 1) family chromodomain proteins (Jenuwein 2001; Jenuwein and Allis 2001). In fission yeast, Chp1, Chp2, and Swi6/HP1 bind to sites enriched in H3K9me. In addition, the siRNAs, which are associated with RITS, facilitate the recruitment of Clr4 to heterochromatin in this organism (Grewal 2010; Grewal and Jia 2007), resulting in H3K9me. This enzyme binds to H3K9me through its own chromodomain (Zhang et al. 2008). H3K9me thus not only recruits chromodomain proteins, but also generates a feedback loop by stabilizing the association of chromatin with RITS and CLRC through the chromodomain of Chp1 and Clr4, respectively (Grewal 2010; Verdel et al. 2009; Zhang et al. 2008; Verdel et al. 2004).

1.3. The modes of RNAi

RNAi pathways can be broadly classified into different modes based on their mechanism of action, subcellular location, and the origin of the small RNA molecules that they use (Moazed 2009). siRNAs act in both the nucleus and the cytoplasm and are involved in TGS and PTGS (Buhler and Moazed 2007). The vast majority of miRNAs act exclusively in the cytoplasm, where they mediate mRNA degradation or translational repression (Filipowicz et al. 2005). However, some plant miRNAs may act directly in promoting DNA methylation in the nucleus (Bao et al. 2004).

1.3.1. Transcriptional gene silencing

Transcriptional gene silencing (TGS) was first discovered in plants, where small RNAs, derived from transgenes and viral RNAs, were found to guide DNA methylation of homologous DNA sequences (Matzke et al. 1989). DNA methylation and histone modifications are common mechanisms used for silencing chromatin in many eukaryotes (Li 2002). In contrast to plants, small RNAs in *S. pombe* can only induce histone methylation: *S. pombe* appears to lack any detectable DNA methylation. Thus, gene silencing in fission yeast is mediated primarily by histone modifications (Moazed 2009). In mammals, siRNAs that are complementary to transcription start sites or to more upstream regions of gene promoters can trigger inhibition of gene transcription (Janowski et al. 2006). It has also been reported that human Argonaute-1 homolog (AGO1) plays a role in directing TGS at the promoter sites. AGO1 associates with RNAPII

and is required for H3K9me and TGS (Kim et al. 2006). Furthermore, promoter-directed human miRNAs, such as miRNA-230, can facilitate TGS (Benhamed et al. 2012; Kim et al. 2008). It also has been reported that hAgo2 localizes to the nucleus (Weinmann et al. 2009), providing evidence to support the hypothesis that small RNA-mediated gene silencing occurs in the nuclei of mammalian cells. However, the details of small RNA-mediated gene silencing mechanisms and Argonaute protein function on mammalian chromatin in the nucleus remain unclear.

1.3.1.1. Transcriptional gene silencing in *Schizosaccharomyces pombe*

RNAi-dependent TGS has been extensively studied in *S. pombe* (Halic and Moazed 2010; Moazed 2009; Moazed et al. 2006; Volpe et al. 2002). The mode of TGS in *S. pombe* is mediated by association of RITS with RDRC (Verdel et al. 2004; Motamedi et al. 2004). These complexes facilitate siRNA-mediated TGS through heterochromatin formation.

1.3.1.1.1. Heterochromatin structures and functions

In most eukaryotes, centromeres, telomeres, and mating-type loci are heterochromatic regions that share a common feature of repetitive DNA elements, referred to as *dg* and *dh* repeats (Grewal and Jia 2007). The heterochromatic centromeres of fission yeast are similar to those of humans in their structure and epigenetic modifications (Grewal and Jia 2007; Pidoux et al. 2004; Pidoux and Allshire 2004). Each fission yeast centromere contains a unique central core

region (*cnt*), where a kinetochore binds. This core region is flanked by two types of DNA repeat sequences: the innermost (*imr*) and outermost (*otr*) repeats. The *otr* region is further composed of *dh* and *dg* repeats (Figure 1.4), which are coated with H3K9me (Moazed et al. 2006; Yamada et al. 2005; Pidoux and Allshire 2004; Volpe et al. 2002).

Heterochromatin is required to maintain genome integrity (Chang et al. 2012) and proper chromosome segregation during cell division (Djupedal and Ekwall 2009). It is also crucial for cell fate determination and the silencing of repetitive DNA elements (Grewal 2010). De-repression of heterochromatin is often detrimental to higher organisms and causes diseases, such as cancer or embryonic lethal conditions (Djupedal and Ekwall 2009).

1.3.1.1.2. RNAi-dependent heterochromatin formation

The formation of centromeric heterochromatin in *S. pombe* requires the sequential action of various proteins that modify chromatin and promote the binding of other factors (Figure 1.4). A direct link between heterochromatin formation and the RNAi pathway was first established when Volpe *et al*. showed that RNAi components of *S. pombe* are required for heterochromatin formation in the centromeric regions (Volpe et al. 2003; Volpe et al. 2002).

Long dsRNA transcripts are synthesized by RNAPII activity on the centromeric *otr*, which are then processed by Dcr1 into siRNAs. Evidence indicates that dsRNA synthesis and generation of siRNAs takes place at sites where transcription of noncoding centromeric RNAs occurs. First, Rdp1 can be

cross-linked to centromeric DNA repeats (Sugiyama et al. 2005; Volpe et al. 2002) and to the forward and reverse RNA transcripts that originate from centromeric repeat regions (Motamedi et al. 2004). Second, production of heterochromatic siRNAs requires Clr4, Swi6, and histone deacetylase (HDAC) Sir2 (Buhler et al. 2006; Hong et al. 2005). Third, association of the two major complexes, RDRC and RITS, requires the chromatin component Clr4, suggesting that it occurs on the chromatin (Motamedi et al. 2004).

Following the generation of heterochromatic siRNAs by Dcr1, the siRNAs guide RITS to homologous nascent transcripts via a base-pairing mechanism. RDRC associates with the RITS complex and generates more dsRNAs, ultimately increasing the pool of heterochromatic siRNAs. Chromatin modifying complex (CLRC) is also tethered to the sites, where transcription of noncoding centromeric RNAs occurs, via interaction with RITS. This is mediated through a LIM-domain protein, Stc1 (siRNA to chromatin), which bridges the two complexes (Bayne et al. 2010). The association of centromeric siRNAs with Clr4 leads to H3K9me (Grewal 2010; Moazed 2009; Motamedi et al. 2004). This is followed by Swi6/HP1 binding and spreading of H3K9me, thereby assembling the heterochromatin platform on the *otr* repeats. Here, more RNAi and heterochomatin factors dock to efficiently establish heterochromatin structures. Once bound to H3K9me sites, Swi6/HP1 negatively regulates transcription of centromeric RNAs, maintaining the transcriptionally silent status of the heterochromatin (Lejeune and Allshire 2011; Lejeune et al. 2010; Ebert et al. 2006; Volpe et al. 2002). This may suggest that tethering RITS to a nascent

transcript mediates chromatin modifications and initiates RNAi-dependent heterochromatic gene silencing (Buhler et al. 2006). It is evident that formation of heterochromatin in *S. pombe* is facilitated by extensive interdependency between the generation of H3K9me and the RNAi machinery.

1.3.1.2. Non-coding RNAs and heterochromatin in epigenetic gene silencing

Studies of *S. pombe* revealed an additional important feature of heterochromatin: its mode of inheritance (Moazed 2009). Once assembled, heterochromatin can be inherited by progeny after many cell divisions. That is, the progeny can retain the old modified histones during DNA replication. These long-term, inheritable changes are independent of the underlying DNA sequence, a phenomenon referred to as epigenetic inheritance (Djupedal and Ekwall 2009; Ringrose and Paro 2004). Their retention serves as a signal for the recruitment of new chromatin modifying factors that are required for the re-establishment of old modification patterns (Moazed 2009).

To ensure epigenetic inheritance, RDRC-dependent siRNA amplification and an RNAi-mediated positive feedback loop are required because the affinity of existing, modified histones for new, specific binding proteins may be too low to allow for the re-establishment of chromatin states (Grewal and Jia 2007; Zaratiegui et al. 2007; Ringrose and Paro 2004). Evidence suggests that the core RNAi machinery, RITS, RDRC, and Dcr1, in association with CLRC, localizes to the nuclear center where they govern epigenetic inheritance as well as heterochromatin assembly in *S. pombe* (Grewal 2010; Moazed 2009; Verdel et al.

2009). In contrast, *N. crassa* and higher eukaryotes employ a different mechanism for their epigenetic control in that they rely on DNA methylation (Moazed 2009; Li 2002).

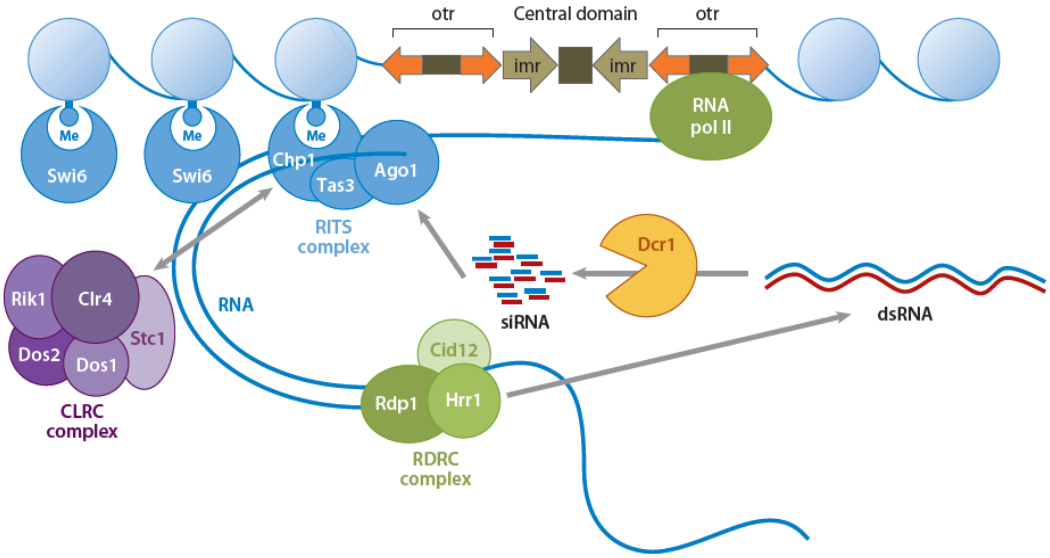

Figure 1.4. Model for RNAi-mediated heterochromatin formation in *S. pombe*. The siRNA-guided RITS complex targets the nascent centromeric transcript synthesized by RNA Pol II during the S phase of the cell cycle. RITS associates with the RDRC complex, where the RdRP activity of the RDRC complex generates more dsRNA. Dcr1 processes the dsRNA into siRNA, contributing to the loop. The CLRC complex associates with the RITS complex, which comes in close proximity with chromatin. Clr4 methylates H3K9 and allows Swi6 (HP1 homolog) to dock at the modified chromatin, thereby forming heterochromatin.

Abbreviations: Ago1, Argonaute 1; Chp1, chromodomain-containing protein 1; Cid12, caffeine-induced death resistant 12; Clr4, calcitonin-like receptor 4; CLRC, Clr4- Rik1-Cul4 complex; Dcr1, Dicer 1; Dos1/2, delocalization of Swi6 1/2; Hrr1, helicase required for RNAi-mediated heterochromatin assembly; *imr*, innermost repeat; *otr*, outermost repeat; Rdp1, RNA-dependent RNA polymerase 1; RDRC, RNA-dependent RNA polymerase complex; Rik1, RS2-interacting KH domain protein 1; RITS, RNA-induced transcriptional silencing; Stc1, siRNA to chromatin; Swi6, SWItch/sucrose nonfermentable 6; Tas3, tyrosine auxotrophy suppressor 3. Adapted from (Chang et al. 2012)

1.3.2. Post-transcriptional gene silencing and translational repression

Argonaute proteins bind siRNAs and miRNAs in order to mediate repression of specific target mRNAs, either by mRNA degradation or by inhibiting translation of mRNAs (Hock and Meister 2008). Key determinants of the regulatory mechanism of these modes are dependent on two factors. First, small RNA duplex must bind to an Argonaute component of RISC, which possesses an endonucleolytic function. The second factor is the degree of complementarity between the small RNAs and the target mRNAs (Ender and Meister 2010; Paddison et al. 2002; Elbashir et al. 2001).

In humans, perfect complementarity between miRNAs or siRNAs and mRNAs promotes endonucleolytic cleavage of the target mRNAs by hAgo2 (Hammond et al. 2000; Martinez and Tuschl 2004; Martinez et al. 2002; Hutvagner and Zamore 2002), whereas mismatches in the central region of the miRNA and target mRNAs leads hAgo2 to repress gene expression at the level of translation or mRNA stabilization (Paddison et al. 2002; Elbashir et al. 2001). The 3’ untranslated region (3’UTR) of many mRNAs contain conserved sequence elements that retain a high level of complementarity to seed regions, sites of nucleotides 2–8 of the guide miRNA sequences, which can be target sites for most miRNAs (Lewis et al. 2003). In plants, miRNAs often exhibit nearly perfect complementarity to target sequences positioned either in ORFs or in 3’UTRs of mRNAs (Pillai et al. 2007). Most miRNAs in animals, however, show imperfect matches on 3’UTR sites with poor conservation outside of the seed region (usually positions 10 and 11, counting from the 5’end). Because Argonaute

proteins in RISCs require extensive base-pairing at positions 10–12 of the guide miRNA for their slicer activity (Wang et al. 2009; Wang et al. 2008; Tolia and Joshua-Tor 2007), the lack of complementarity in miRNAs precludes the endonucleolytic cleavage of the target mRNAs. Instead, it represses translation in animals (Pillai et al. 2007; Tolia and Joshua-Tor 2007; Pillai et al. 2005).

The proposed mechanisms underlying translational repression are still controversial. There is evidence indicating that miRNA-mediated repression occurs during the translation initiation step. As well, other studies concluded that miRNA-mediated repression occurs after initiation [reviewed in (Huntzinger and Izaurralde 2011)]. Controversy aside, translational repression has been proposed to occur in four distinct ways in animals: inhibition of translation initiation (Mathonnet et al. 2007; Thermann and Hentze 2007; Wakiyama et al. 2007; Pillai et al. 2005), inhibition of translation elongation (Nottrott et al. 2006; Maroney et al. 2006; Petersen et al. 2006; Kim et al. 2004), co-translational nascent polypeptide degradation (Carthew and Sontheimer 2009; Nottrott et al. 2006), and premature termination of translation and ribosome dissociation (Petersen et al. 2006) (Figure 1.5).

In addition to their capacity to mediate translational inhibition, miRNAs also contribute to degradation of target mRNAs that contain imperfect complementarity (Behm-Ansmant et al. 2006; Giraldez et al. 2006; Wu et al. 2006; Bagga et al. 2005; Wu and Belasco 2005). In such cases, miRNAs direct their targets to the 5'-to-3' mRNA decay pathway, where mRNAs are first deadenylated. In animals, the target mRNAs are deadenylated by the CAF1−

CCR4–NOT deadenylase complex, which is required for the removal of the poly(A) tail of mRNAs (Eulalio et al. 2009; Fabian et al. 2009; Eulalio et al. 2008; Wakiyama et al. 2007; Behm-Ansmant et al. 2006). Target mRNAs are then decapped by the decapping enzyme DCP2. Decapped mRNAs are ultimately degraded by the major cytoplasmic 5'-to-3' exonuclease XRN1 (Eulalio et al. 2009; Eulalio et al. 2007; Behm-Ansmant et al. 2006; Giraldez et al. 2006; Wu et al. 2006; Rehwinkel et al. 2005).

The mechanism of miRNA-mediated mRNA decay requires association of Argonaute proteins with GW182, a 182 kDa protein that contains multiple glycine-tryptophan repeats (GW repeats) (Eulalio et al. 2009; Eulalio et al. 2008; Jakymiw et al. 2007; Behm-Ansmant et al. 2006; Liu et al. 2005a; Meister et al. 2005). These repeats act as Argonaute-binding platforms and, accordingly, are termed "Argonaute hooks" (Eulalio et al. 2009; Eulalio et al. 2008; El-Shami et al. 2007; Till et al. 2007). There are three paralogs of GW182 in vertebrates: TNRC6A (also known as GW182), TNRC6B, and TNRC6C, as well as a single ortholog found in *D. melanogaster* and two (AIN-1 and AIN-2) in *C. elegans*. Fungi and plants appear to lack GW182 orthologs (Behm-Ansmant et al. 2006).

During miRNA-mediated mRNA destabilization, GW182 also interacts with poly(A)-binding protein (PABP). PABP associates with mRNA poly(A) tails and eukaryotic translation initiation factor 4G subunit (eIF4G) of the cap-binding complex (Beilharz et al. 2009; Zekri et al. 2009; Fabian et al. 2009). Because mRNA circularization requires binding between eIF4G and PABP, the interaction of GW182 with PABP may block circularization in which case initiation of

translation is less efficient and consequently, protein expression is reduced (Huntzinger et al. 2010; Beilharz et al. 2009; Fabian et al. 2009; Zekri et al. 2009). At present, it is not clear why some target mRNAs are degraded while others are not. It has been suggested that the number, type, and position of mismatches in the miRNA and mRNA duplex play important roles in triggering degradation or translational arrest by miRNAs (Aleman et al. 2007).

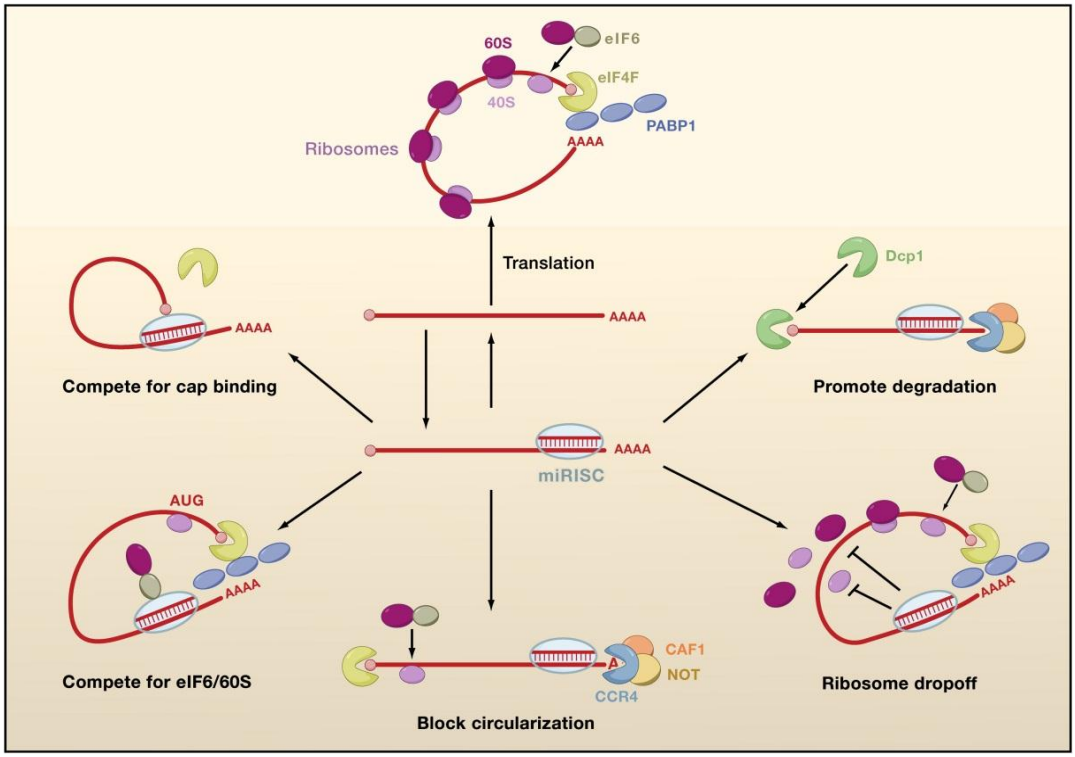

Figure 1.5. Possible mechanisms of miRISC-mediated translational repression of mRNAs. Nonrepressed mRNAs recruit initiation factors and ribosomal subunits and form circularized structures that enhance translation (top). When miRISCs bind to mRNAs, they can repress initiation at the cap recognition stage (upper left) or the 60S recruitment stage (lower left). Alternatively, they can induce deadenylation of the mRNA and thereby inhibit circularization of the mRNA (bottom). They can also repress a post-initiation stage of translation by inducing ribosomes to drop off prematurely (lower right). Finally, they can promote mRNA degradation by inducing deadenylation followed by decapping (upper right). Copyright permission acquired (License Number: 3020431473913). Adapted from (Carthew and Sontheimer 2009)

1.4. *Trans*-acting modulators of RNAi

1.4.1. Overview of recent findings: multiple regulators of RNAi apparatus

Evidence has shown that various accessory proteins are involved in regulation of RNAi machinery (Rudel et al. 2011; Stoica, Park et al. 2010; Weinmann et al. 2009; Loschi et al. 2009; Pare et al. 2009; Zeng et al. 2008). For example, inhibition of Hsp90 ATPase activity impairs the association of hAgo2 with Dicer (Tahbaz et al. 2001). A recent study from our lab has also shown that, in mammalian cells, targeting of hAgo2 to stress granules (SGs) and PBs is dependent upon Hsp90 (Pare et al. 2009). These findings suggest that the function of hAgo2 in small RNA-mediated gene silencing pathways may be regulated by the activity of Hsp90 chaperone complex.

In addition, the conserved translin–TRAX (translin-associated protein X) complex, also known as C3PO, promotes RNAi by facilitating RISC activation in *Drosophila* and human cells (Ye et al. 2011; Liu et al. 2009). C3PO was demonstrated to be a Mg^{2+}-dependent RNA-specific endonuclease which promotes RISC activation by removing the passenger strand of the siRNA duplex (Li et al. 2012; Liu et al. 2009). Recently, Weinmann *et al*. reported that the karyopherin importin 8 is required for nuclear import of mammalian Argonaute proteins and, surprisingly, for the miRNA-dependent targeting of Argonautes to mRNAs in the cytoplasm (Weinmann et al. 2009). This indicates that transport factors are also involved in regulation of RNAi pathways, mediating protein localization.

Microtubule–associated motor proteins have recently been implicated in PB and SG dynamics (Loschi et al. 2009). In mammalian cells, knockdown of dynein heavy chain 1 (DHC1) inhibits PB and SG formation. In addition, impairment of kinesin-1 heavy chain (KIF5B) or kinesin light chain 1 (KLC1) delays SG disassembly. Moreover, evidence shows that movement of PBs is dependent on ATP and an intact microtubule network in *S. pombe* and mammalian cells. Disruption of the microtubule network causes a significant reduction in PB mobility together with an induction of PB assembly and enlargement of existing PBs (Aizer et al. 2008; Sweet et al. 2007; Carmichael et al. 2006).

1.4.2. Karyopherin and nuclear transport machinery

1.4.2.1. Function and characteristic of karyopherins

Karyopherins (kaps) are soluble transport factors that bind to nuclear localization signals (NLSs) or nuclear export signals (NESs) on cargo being transported across the nuclear envelope (NE), an impermeable double membrane that encapsulates the contents of the nucleus in eukaryotic cells (Terry et al. 2007; Mosammaparast and Pemberton 2004; Lusk et al. 2004). Karyopherins are known as importins or exportions, based on the direction of transport they mediate. Two kaps (yeast Msn5 and mammalian importin 13) are able to function in both directions (Mosammaparast and Pemberton 2004).

The largest group of transport receptors is comprised of structurally related members of the β-karyopherin (or β-kap) protein family (Terry et al. 2007).

There are fourteen members of the β-kap family in *S. cerevisiae,* and nineteen in *Homo sapiens* (O'Reilly et al. 2011; Cook et al. 2007; Tran et al. 2007). Relatively, a small family of α-kaps (or importin α) is found; which serves as adaptors between β-kaps and cargo proteins (Mason et al. 2009; Goldfarb et al. 2004). However, it is thought that a large portion of nucleocytoplasmic transport is independent of α-kaps. Rather, it is mediated by recognizing the signals by one or more β-kap family members. Most β-kaps bind cargo directly, although Kapβ1, a member of the β-kap family, commonly uses adaptors to recognize the cargo [reviewed in (O'Reilly et al., 2011; Terry et al., 2007; Lusk et al., 2004)].

The sequence identity of all functionally defined β-kaps is considerably low at 15% ~ 20%; however, they share a similar architecture and similar molecular weight of 90 kDa ~ 150 kDa [reviewd in (Chook & Suel, 2011)]. β-kap proteins are composed of consecutive ~20 HEAT repeats, an ~40 amino acid motif (Andrade et al. 2001) that was first identified in Huntingtin, elongation factor 3, PR65/A subunit of protein phosphatase 2A, and yeast PI3-kinase TOR1. The sequence similarity is strongest in the N-terminal half of HEAT, where RanGTP binds, reflecting the functional similarity of the β-kap members [reviewed in (Hoelz et al. 2011; Kappel et al. 2010)]. Each HEAT motif folds into a pair (A and B) of antiparallel α-helices (Chook and Blobel 1999; Cingolani et al. 1999; Groves et al. 1999), and consecutive HEAT motifs stack together in a parallel fashion, usually with a slight clockwise twist. It produces molecules with an overall superhelical architecture, and thus provides the β-kaps with extreme intrinsic flexibility.

The structural studies (Chook and Blobel 1999; Cingolani et al. 1999; Lee et al. 2003; Cingolani et al. 2002) have revealed that the intrinsic flexibility is important for facilitating the appropriate conformational changes associated with cargo binding and release, thus one Kap can recognize diverse cargo proteins [reviewd in (Chook and Suel 2011; Terry et al. 2007; Conti et al. 2006; Mosammaparast and Pemberton 2004)]. Consistent with this scenario, our recent findings have shown that Sal3, a member of the β-kap family, mediates at least two protein imports, Rdp1 and Cdc25, in fission yeast (Park et al. 2012; Chua et al. 2002).

It should also be mentioned that an individual NLS (or NES) can be recognized by more than one β-kap (Mosammaparast and Pemberton 2004; Lusk et al. 2004). For example, both β-kaps, Kap121P and Kap123p, are required for import of ribosomal protein (RPL25) in budding yeast (Lusk et al. 2004; Rout et al. 1997). Kap114p, Kap121p, and Kap123p are needed for the import of core histones in yeast (Mosammaparast et al. 2001; Muhlhausser et al. 2001; Mosammaparast et al. 2002). These observations may suggest that many proteins, particularly those with essential nuclear functions, utilize several pathways to enter the nucleus.

1.4.2.2. Nuclear transport of macromolecules by β-karyopherins

Nuclear pore complex (NPC): The cellular compartmentalization by the NE, a hallmark of eukaryotes, demands thousands of macromolecules' transport into the nucleus in order to regulate DNA replication, transcriptional machinery,

chromatin organization, etc. These transport events are controlled by nuclear pore complexes (NPCs), an eight-fold symmetric structure that is embedded in the NE and acts as the gatekeeper (Hoelz et al. 2011; Cronshaw et al. 2002; Reichelt et al. 1990). The 100 nm diameter NPC has a core structure consisting of a hollow cylinder with spoke-ring complexes (Rout and Aitchison 2001). It consists of several major domains: the selective central channel (or central transporter region), the core scaffold that supports the central channel, the transmembrane regions, the nuclear basket, and the cytoplasmic filaments (Alber et al. 2007) (Fig. 1.6A, B). In vertebrate, the NPC mass is estimated at 60–100 million Daltons, whereas the yeast NPC is estimated at ~50 million Daltons (Reichelt et al. 1990). Using electron microscopy, it has been shown that this overall structure is broadly conserved throughout all eukaryotes (Wente and Rout 2010).

The NPC is composed of approximately 30 different proteins, collectively termed nucleoporins (or nups), that are evolutionarily conserved in distant eukaryotes ranging from yeast to human (DeGrasse et al. 2009; Mosammaparast and Pemberton 2004; Rout et al. 2000; Cronshaw et al. 2002; Davis and Blobel 1986). Based on their approximate localization within the NPC, the nups can be classified into six categories: integral membrane proteins of the pore membrane domain of the nuclear envelope (POMs), membrane-apposed coat nups, adaptor nups, channel nups, nuclear basket nups, and cytoplasmic filament nups [reviewed in (Hoelz et al. 2011; Hsia et al. 2007)] (Figure 1.6C). Most of the nucleoporins in the channel, nuclear basket, and cytoplasmic filaments, contain repeated peptide motifs with phenylalanine and glycine, termed FG-repeats, and

aptly named FG-nups [reviewed in (Hoelz et al. 2011; Wente and Rout 2010)]. The FG-repeat regions of the FG-nups in yeast form the permeability barrier and serve as docking sites for β-kap-cargo complexes. However, because of the intrinsically unstructured nature of the FG-repeats, the exact nature of the permeability barrier remains elusive.

Nucleocytoplasmic transport: Most macromolecules, such as mRNAs, tRNAs, ribosomal proteins, ribosomal subunits, and many soluble proteins, are selectively transported via active mechanisms that are mediated by the β-kap family of nuclear transport receptors and the small guanosine triphosphatase (GTPase) Ran [reviewed in (Chook and Suel 2011; Lusk et al. 2004; Fried and Kutay 2003; Weis 2003)]. The GTPase Ran forms a nuclear/cytoplasmic gradient, which regulates kap-cargo interaction, and thus is critical for vectorial transport. In the nucleus, there is approximately a 100-fold greater concentration of RanGTP than in the cytoplasm, due to the presence of a regulator of chromosome condensation 1, or RCC1. This is also known as Ran Guanine nucleotide Exchange Factor (RanGEF) (Bischoff and Ponstingl 1991). In contrast, the majority of Ran in the cytoplasm is in the GDP-bound form due to the cytoplasmic localization of its GTPase Activating Protein, RanGAP [reviewd in (Chook and Suel 2011; Terry et al. 2007; Lusk et al. 2004)] (Figure 1.7B).

For the NLS-containing cargos, an import cycle starts with the formation of the β-kap-cargo complex in the cytoplasm, and then proceeds with translocation through the NPC. It is terminated by disassembly of the complex in the nucleus through a binding of RanGTP to the β-kap (Figure 1.7A). RanGTP

not only disassembles import complexes upon entrance into the nucleus, but also promotes the assembly of export complexes inside the nucleus (Figure 1.7B). To achieve continuous efflux of the β-kaps, Ran guanosine diphosphate (RanGDP) has to be re-imported into the nucleus, and the nuclear import of RanGDP has to be mediated by a dedicated RanGDP import factor, NTF2 (also known as p10) (Ribbeck et al. 1998) (Figure 1.7B). Interestingly, this macromolecular protein does not utilize the β-kap–dependent transport mechanism. Instead, it is associated with FG-nups for nuclear transport. The binding of β-kaps to the FG-repeats enables the proteins to overcome the entropic barrier, to access the channel, and to diffuse through the NPC (Rout et al. 2000; Rout et al. 2003).

In contrast to the macromolecules that utilize the active transport mechanism, small molecules or other metabolites are passively diffused across the NPC (Cronshaw et al. 2002; Reichelt et al. 1990). It is generally accepted that cargos smaller than ~40 kDa can diffuse into the nucleus (Wozniak et al. 1998). However, some of the smallest proteins, such as Rev protein, an RNA-binding protein of human immunodeficiency virus type 1 (HIV-1 Rev) (Arnold et al. 2006), parathyroid hormone-related protein (PTHrP) (Cingolani et al., 2002), or histone H1 (Jakel et al., 1999), utilize kap-mediated and signal-dependent import pathways. This may suggest that nuclear import is determined by the rate at which cargos enter the nucleus, and not by molecular size (Nardozzi et al. 2010).

Figure 1.6. Overall structure of the nuclear pore complex (NPC). (A) Structural domains of the nuclear pore complex. **(B)** Cryo-electron tomographic reconstruction of the Dictyostelium discoideum NPC [Electron Microscopy Data Bank (EMDB) code 1097, (Beck et al., 2004)]. The cytoplasmic filaments, the symmetric core, and the nuclear basket are colored in cyan, orange, and purple, respectively. **(C)** A schematic model of the NPC and Nups. The four concentric cylinders are composed of integral pore membrane proteins (POMs), coat nucleoporins, adaptor nucleoporins, and channel nucleoporins. Natively unfolded phenylalanine-glycine (FG) repeats of a number of nucleoporins make up the transport barrier in the central channel and are indicated by a transparent plug. Adapted from (Hoelz et al., 2011; Rout & Aitchison, 2001)

(A)

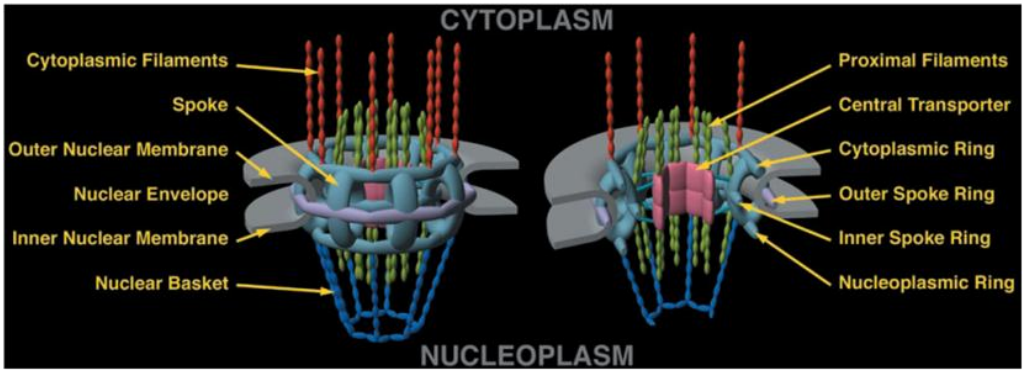
CYTOPLASM
Cytoplasmic Filaments
Spoke
Outer Nuclear Membrane
Nuclear Envelope
Inner Nuclear Membrane
Nuclear Basket
Proximal Filaments
Central Transporter
Cytoplasmic Ring
Outer Spoke Ring
Inner Spoke Ring
Nucleoplasmic Ring
NUCLEOPLASM

(B)

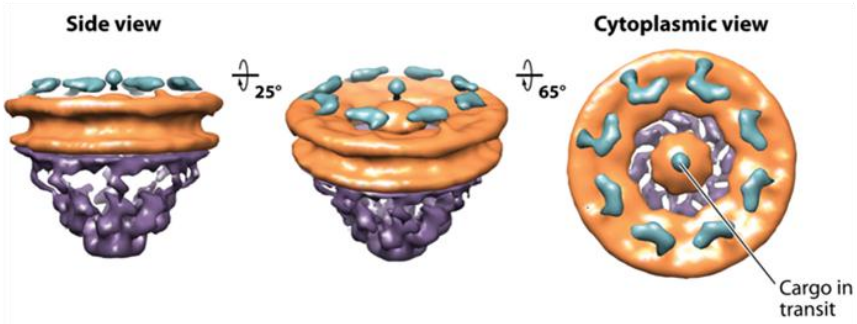
Side view
Cytoplasmic view
25°
65°
Cargo in transit

(C)

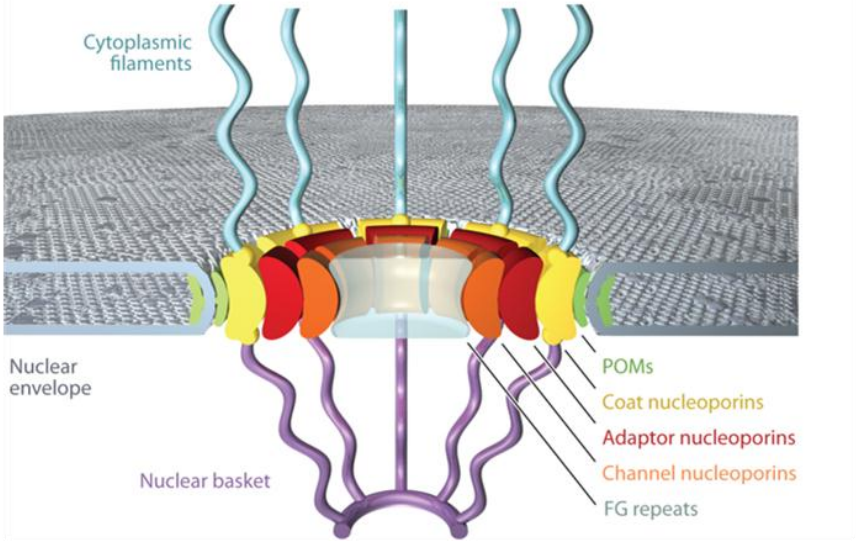
Cytoplasmic filaments
Nuclear envelope
Nuclear basket
POMs
Coat nucleoporins
Adaptor nucleoporins
Channel nucleoporins
FG repeats

Figure 1.7. Nucleocytoplasmic transport. (A) Schematic drawing of nuclear import and export processes mediated by β-karyopherins (also known as β-like importins and exportins). The two nuclear pore complexes (NPCs) show the characteristic nuclear basket and cytoplasmic fibrils. **Import**: An importin binds a cargo in the cytoplasm (bottom left), then proceeds via translocation through the NPC, and then releases it upon binding RanGTP in the nucleus (upper left). **Export:** An exportin binds both cargo and RanGTP in the nucleus (upper right) and releases the cargo upon conversion of RanGTP into RanGDP (bottom right).
(B) Schematic drawing of the Ran cycle. The high concentration of RanGDP in the cytosol is maintained by a GTPase-activating protein (RanGAP), which is bound to the cytoplasmic fibrils of the NPC. In contrast, the high concentration of RanGTP in the nucleus is maintained by a regulator of chromosome condensation 1 (RCC1), a chromatin-bound guanine exchange factor (RanGEF) which acts on the RanGDP that is transported into the nucleus by its dedicated import factor, nuclear transport factor 2 (NTF2). Adapted from (Cook et al., 2007)

(A)

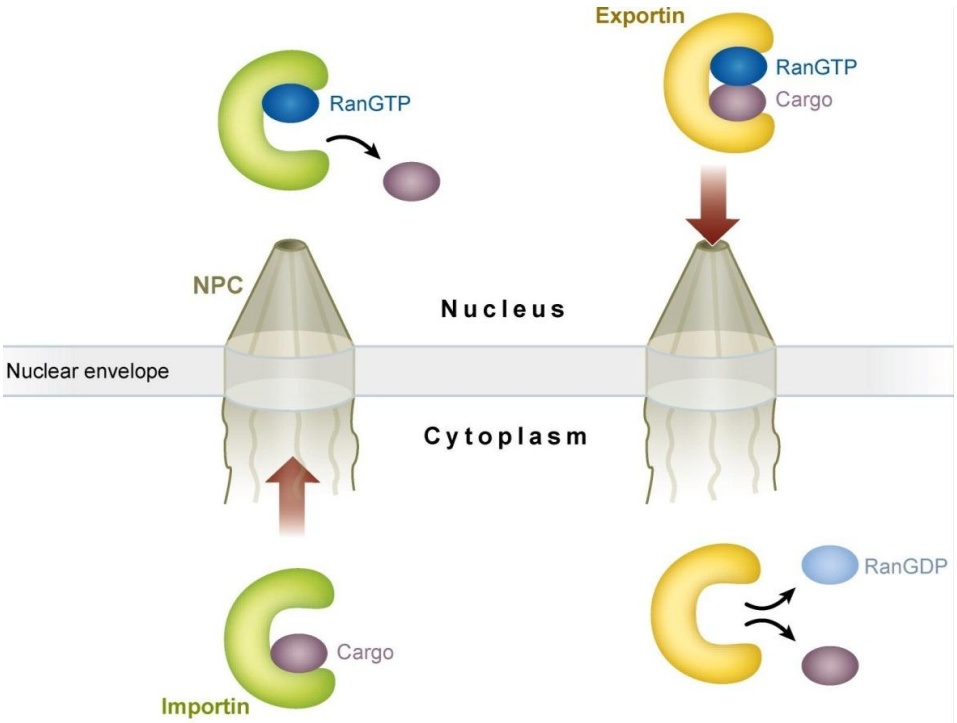
Exportin
RanGTP
Cargo
RanGTP
NPC
Nucleus
Nuclear envelope
Cytoplasm
RanGDP
Cargo
Importin

(B)

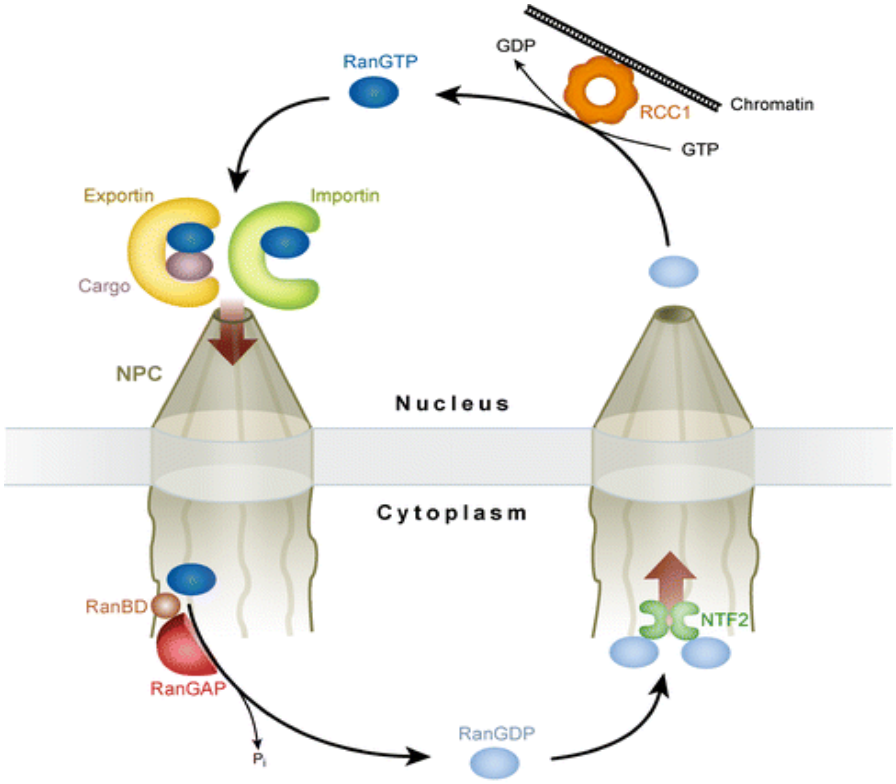
RanGTP
GDP
RCC1
Chromatin
GTP
Exportin
Importin
Cargo
NPC
Nucleus
Cytoplasm
RanBD
RanGAP
NTF2
RanGDP
Pi

1.4.3. Post-translational modifications of gene silencing factors

Proteins can be post-translationally modified in order to fulfill their biological functions in a cell. One major post-translational modification is protein phosphorylation, which is catalyzed by kinases (Bimbo et al. 2005). Increasing evidence shows that RNAi pathways may be subjected to this type of regulation.

1.4.3.1. Post-translational modifications of Argonaute proteins

Recent studies from several groups have revealed that Argonaute proteins are subject to multiple post-translational modifications (Figure 1.6 and Table 1.1). Zeng *et al*. first demonstrated that hAgo2 is phosphorylated at serine 387 (S387); this modification facilitates the localization of hAgo2 to PBs (Zeng et al. 2008). Mutating S387 to alanine (S387A) led to a reduced localization of hAgo2 to cytoplasmic PBs. Zeng *et al*. further showed that hAgo2 phosphorylation at S387 is mediated by a member of the MAPK (mitogen-activated protein kinase) signaling pathway (Zeng et al. 2008). However, it is not known if phosphorylation of S387 affects the RNAi activity of hAgo2.

Rudel *et al*. demonstrated that hAgo2 is also phosphorylated at tyrosine 529 (Y529), which is a highly conserved tyrosine located within the 5'-phosphate binding pocket in the MID domain of Argonaute proteins (Rudel et al. 2011). Importantly, it inhibits RNAi activity by blocking interaction of hAgo2 with small RNAs (Rudel et al. 2011). Substitution of a glutamate for tyrosine at position 529 severely impairs PB localization of hAgo2. This indicates that the presence of a negative charge in the 5'-phosphate binding pocket prevents binding of the

negatively charged 5'-phosphate of small RNAs. Recently, our lab reported that hAgo2 with a Y529F mutation also diminishes targeting of hAgo2 to PBs (Pare et al. 2011). This may suggest that phosphorylation and dephosphorylation of Y529 is a critical part of the hAgo2 small RNA loading cycle (Pare et al. 2011). Altogether, there are at least seven amino acid residues within hAgo2 that are phosphorylated (Rudel et al. 2011). However, only the role of phosphorylation of Y529 in RNAi has been characterized in extensive detail. The roles of the other residues remain to be determined.

Argonaute proteins are also modified by hydroxylation in mammalian cells (Qi et al. 2008). Qi *et al*. reported that hAgo2 interacts with type I collagen prolyl-4-hydroxylase and that this enzyme mediates the hydroxylation of hAgo2 at proline 700. Hydroxylation stabilizes hAgo2 and enhances its localization to PBs. It has also been demonstrated that murine mLin41 protein, which is an E3 ubiquitin ligase, co-localizes and interacts with Ago2. The mLin41 polyubiquitinates Ago2 and targets it for degradation in mouse ES cells (embryonic stem cells) (Rybak et al. 2009).

Argonaute proteins of the PIWI subgroup are also subject to post-translational modifications. For example, Aubergine, a member of the PIWI family in *D. melanogaster*, is methylated at arginine residues within conserved sDMA motifs (typically Gly-Arg-Gly) (Kirino et al. 2010). Methylation of Mili and Miwi, which are members of the murine PIWI protein family, has also been observed. These modifications appear to be important in stabilizing PIWI proteins (Reuter et al. 2009; Vagin et al. 2009).

Table 1.1 describes the conserved site-specific residues on Argonaute proteins that are subjected to post-translational modifications. The most recent discoveries of these post-translational modifications of Argonautes and other gene silencing factors in several organisms are shown in Figure 1.8.

Table 1.1. Post-translational modification (PTM) conservation of site-specific residues on Argonautes involved in various organisms.

PTM	Modified residue, based on hAgo2	Function	Domain	hAgo2	*A. thaliana* Ago1	*C. elegans* Alg1	*D. melanogaster* Ago1	*S. pombe* Ago1
phosphorylation	pS253	unknown	PAZ	√	**X**	**X**	√	**X**
phosphorylation	pT303	unknown	PAZ	√	**X**	√	√	**X**
phosphorylation	pT307	unknown	PAZ	√	T to S substitution	√	√	T to S substitution
phosphorylation	pS387	P-body localization	N/A	√	**X**	**X**	**X**	**X**
phosphorylation	pY393	unknown	N/A	√	√	√	√	√
phosphorylation	pY529	Small RNA binding	MID	√	√	√	√	√
phosphorylation	pS798	unknown	PIWI	√	√	√	√	√
Prolyl-4-hydroxylation	P700	Argonautes stability	PIWI	√	Not tested	Not tested	Not tested	Not tested
Poly ADP-Ribose	Unknown	Regulates miRNA activity upon stress	Unknown	√	Not tested	Not tested	Not tested	Not tested
Ubiquitination	Unknown	Argonautes stability	Unknown	√	Not tested	Not tested	Not tested	Not tested

The tick (√) represents residues that are fully conserved and predicted to be modified. The cross (x) represents residues that are not conserved and therefore will not be modified. For post-translational modifications, where site-specific residues have yet to be determined: "Not tested" represents that there is insufficient evidence to suggest whether post-translational modification is present, whereas the tick (√) indicates that the Argonaute has been experimentally shown to be modified. Adapted from (Johnston and Hutvagner 2011)

1.4.3.2. Phosphorylation of RNase III enzymes and their associated proteins

Together with Argonautes, Dicer proteins are also important for miRNA-mediated gene silencing pathways in mammalian cells. As mentioned, human Dicer interacts with TRBP and PACT, which contain dsRBDs (Kim et al. 2009; Lee et al. 2006; Chendrimada et al. 2005) (refer to Section 1.2.2). A recent study by Paroo *et al*. showed that MAPK pathway-dependent phosphorylation of TRBP enhances the stability of the miRNA generating complex (Paroo et al. 2009).

Drosha, a Class 2 RNAse III enzyme that is required for pri-miRNA processing (Lee et al. 2003), is also subject to post-translational modification (Tang et al. 2010). The segment between amino acids 270 and 390 of Drosha harbors a nuclear localization signal (NLS) that is required for targeting this enzyme to the nucleus. Tang et al. further identified that the two phospho-amino acid residues (S300) and (S302) are important to locate Drosha in the nucleus for pri-miRNA processing (Tang et al. 2010). Together, these studies suggest that post-translational modifications play vital roles in the localization and protein stability of gene silencing factors.

Figure 1.8. Post-translational modifications of gene silencing factors involved in small RNA pathways. (A) Phosphorylation, hydroxylation, and ubiquitination of gene silencing factors. Human Drosha is phosphorylated at two serine residues, S300/S302, by an unknown kinase(s). Phosphorylation of Drosha triggers protein nuclear localization, where the pri-miRNA processing occurs. MAP kinases Erk1/2 phosphorylate human TRBP at S142, S152, S283, and S286, which increases the protein stability of TRBP and Dicer. Ago2 is regulated by multiple modifications. A prolyl hydroxylase C-P4H(I) hydroxylates P700 in hAgo2, enhancing the stability of hAgo2 and increasing PB localization. Phosphorylation of hAgo2 at S387 by MAPKAPK2, induced by the p38 pathway, also promotes PB localization of the protein. In mice, a stem cell-specific E3 ligase, mLin41, ubiquitinates Ago2 and targets it for proteosome-dependent degradation. **(B) Methylation of the Piwi proteins in mice.** Piwi proteins are methylated at conserved arginine residues in the N-termini by protein methyltransferase PRMT5 and its cofactor WDR77: (Top) Arginines 74, 95, 100, 146, and 163 are methylated in Mili. Miwi2 has a putative methylation site at the N-terminus. (Bottom) Miwi is methylated at arginine 14 and 49. **(C) Methylation of Piwi proteins in *Drosophila*.** *Drosophila* Piwi proteins are methylated at conserved arginine residues in the N-termini by dPRMT5 and its cofactor valois (*Drosophila* homolog of WDR77). Red dots represent methylation sites. Adapted from (Kim et al. 2010; Heo and Kim 2009)

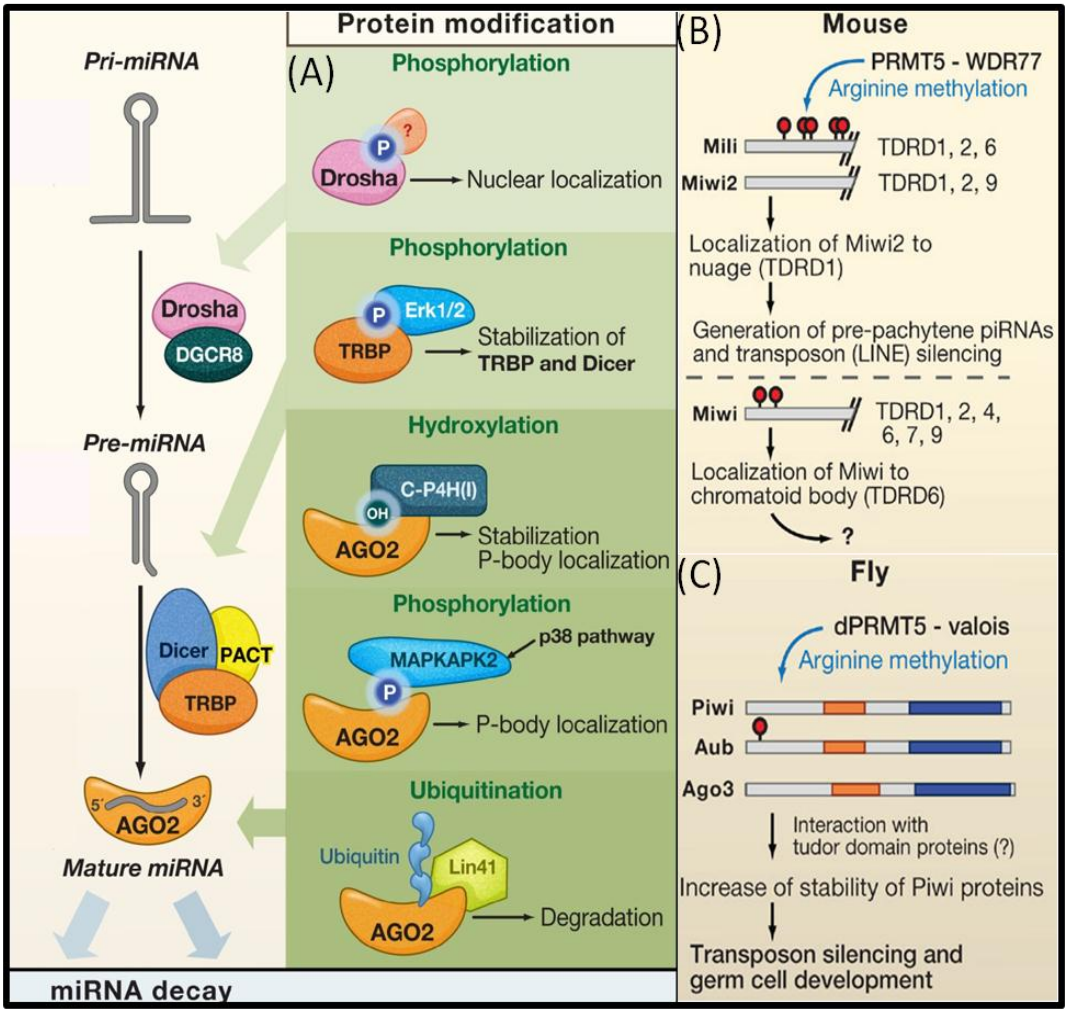
Protein modification
Pri-miRNA
(A)
Phosphorylation
Drosha
Nuclear localization
Phosphorylation
Drosha
DGCR8
Erk1/2
TRBP
Stabilization of
TRBP and Dicer
Hydroxylation
Pre-miRNA
C-P4H(I)
OH
AGO2
Stabilization
P-body localization
Phosphorylation
Dicer
PACT
TRBP
p38 pathway
MAPKAPK2
AGO2
P-body localization
Ubiquitination
5'
3'
AGO2
Mature miRNA
Ubiquitin
Lin41
AGO2
Degradation
miRNA decay
(B)
Mouse
PRMT5 - WDR77
Arginine methylation
Mili
TDRD1, 2, 6
Miwi2
TDRD1, 2, 9
Localization of Miwi2 to
nuage (TDRD1)
Generation of pre-pachytene piRNAs
and transposon (LINE) silencing
Miwi
TDRD1, 2, 4,
6, 7, 9
Localization of Miwi to
chromatoid body (TDRD6)
?
(C)
Fly
dPRMT5 - valois
Arginine methylation
Piwi
Aub
Ago3
Interaction with
tudor domain proteins (?)
Increase of stability of Piwi proteins
Transposon silencing and
germ cell development

1.5. Fission yeast *S. pombe*: an excellent model for studying gene silencing mechanisms

The fission yeast *S. pombe* has served as an important model system for RNAi research because studying gene silencing mechanisms in multi-cellular organisms is complicated by the presence of multiple isoforms of Argonaute, Dicer, and RdRP (Carmichael et al. 2006). Since *S. pombe* encodes only one Argonaute protein, Ago1 (Tolia and Joshua-Tor 2007; Carmell et al. 2002), as well as one Dicer and one RdRP enzyme (Volpe et al. 2002), functional redundancy is not an issue. In addition, because this organism contains relatively large domains of constitutive, well-conserved, but simple heterochromatin at the pericentromeric regions, it has proven to be a powerful biological system to study nuclear siRNA-dependent heterochromatin assembly and heterochromatic gene silencing (Shimada et al. 2009; Carmichael et al. 2006; Grewal and Moazed 2003). Additionally, many *S. pombe* proteins have homologs in mammalian cells making it possible to translate findings to potentially analogous function in mammalian cells.

1.6. Rationale and Objective

The discovery of RNAi has broad implications, as this small RNA-mediated regulation of the gene expression system is estimated to modulate over one-half of all human genes (Friedman et al. 2009). It is involved in diverse biological processes, including cell proliferation, differentiation, developmental timing, cell death, metabolic control, transposon silencing, and antiviral defence

(Esteller 2011; Carthew and Sontheimer 2009; Friedman et al. 2009; Ghildiyal and Zamore 2009; Kim et al. 2009). In addition, Argonaute proteins are implicated in a variety of diseases, including Fragile X syndrome, autoimmune diseases, and cancers (Li et al. 2008; Taubert et al. 2007; Jakymiw et al. 2006). Currently, RNAi is widely used to study eukaryotic gene functions and will play a key role in the delivery of new molecular therapeutic strategies for the treatment of cancers and infectious diseases (de Fougerolles et al. 2007; Mello and Conte 2004; Fuchs et al. 2004). However, several complications and limitations in using RNAi for therapeutic purposes have been reported (Saetrom et al. 2007). For example, immunostimulatory effects, such as interferon response, may be triggered by shRNAs and siRNAs (Sledz et al. 2003). MicroRNAs may also cause the down-regulation of genes other than the intended target, a phenomenon known as off-target effects. In addition, most small RNAs use the same cellular factors, so they compete for and saturate important enzymes and effector complexes needed for biogenesis and targeting (Birmingham et al. 2006; Fedorov et al. 2006; Jackson et al. 2006; Lin et al. 2005; Marques and Williams 2005; Bridge et al. 2003; Sledz et al. 2003). These issues suggest that more research into RNAi pathways is needed to understand the consequences of therapeutic interventions using small RNA molecules.

Fission yeast *S. pombe* may prove helpful in understanding these regulatory mechanisms, as the basic roles of Ago1, Dcr1, and Rdp1 in TGS and PTGS are relatively well understood. The core RNAi effector proteins are differentially localized in yeast (Carmichael et al. 2006; Motamedi et al. 2004).

Our laboratory has also shown that Ago1 is involved in cell cycle regulation in *S. pombe* (Stoica et al. 2006). Emerging data, including my own, indicate that various accessory proteins and factors are involved in regulation of the activities and localization of the RNAi apparatus (Johnston and Hutvagner 2011; Stoica, Park et al. 2010; Weinmann et al. 2009; Loschi et al. 2009; Rudel et al. 2011; Pare et al. 2009; Liu et al. 2009; Rybak et al. 2009; Qi et al. 2008; Zeng et al. 2008). However, it is not known how RNAi protein functions are regulated in the different cellular compartments. The RNAi apparatus—because of its various functions, including its central role in governing gene expression—is subject to extensive regulation through interaction with other proteins and/or by post-translational modifications. Therefore, I hypothesized that there are multiple *trans*-acting factors that modulate localization and/or activity of RNAi proteins. Based on this hypothesis, the objective of my thesis research was to identify and characterize the factors involved in the regulation of RNAi protein localization and/or function in *S. pombe*.

CHAPTER 2:
Materials & Methods

2.1. Materials

2.1.1. Reagents

Reagents and supplies were purchased from the indicated suppliers and used according to the manufacturers' recommendations unless otherwise stated.

Table 2.1. Commercial sources of materials, chemicals, and reagents

Reagents	Source
40% Acrylamide/Bis-acrylamide solution (29:1)	Bio-Rad
Agar	Difco
Acid washed glass beads (425-600 micron)	Sigma-Aldrich
Acetone (Certified ACS)	Fisher Scientific
Adenine hemisulfate salt	Sigma-Aldrich
Agarose A (Electrophoresis grade)	Invitrogen
Agarose (UltraPure™ Low Melting Point)	Invitrogen
Ammonium sulfate (enzyme grade)	Fisher
Ammonium persulphate	Sigma-Aldrich
Ampicillin	Sigma-Aldrich
ANTI-FLAG M2 Magnetic Beads	Sigma-Aldrich
Bacto-tryptone	Difco
Bacto-yeast extract	Difco
Bovine serum albumin (BSA)	Sigma-Aldrich
Bromophenol blue	Sigma-Aldrich
Chloroform	Thermo Fisher Scientific
Complete™ EDTA-free protease inhibitors	Roche
Coomassie Brilliant Blue	Invitrogen
Chromotek-GFP-Trap®	Chromotek
Chromotek-RFP-Trap®	Chromotek
4',6-diamidino-2-phenylindole (DAPI)	Sigma-Aldrich
2-[4-(dimethylamino)styryl]-l-methylpyridinium iodide (DASPMI)	Sigma-Aldrich
Diatomaceous earth	Sigma-Aldrich
Dimethyl sulphoxide (DMSO)	Sigma-Aldrich
Dithiothreitol (DTT)	Sigma-Aldrich
Edinburgh minimal medium (EMM)	Sunrise Science Products
Ethanol	Commercial Alcohols
Ethylenediaminetetraacetic acid (EDTA)	Sigma-Aldrich
Formaldehyde, 37% (v/v)	Sigma-Aldrich
5-FOA (5-fluoroorotic acid)	Sigma-Aldrich
G418	Sigma-Aldrich
Glycerol	Thermo Fisher Scientific
Glycine	EM Science
Guanidine hydrochloride	Fisher Scientific
Glacial acetic acid	Fisher
Halt™ Phosphatase Inhibitor Cocktail, EDTA-Free	Thermo Scientific
4-(2-hydroxyethyl)-1-piperazineethanesulphonic acid (HEPES)	Fisher Scientific

Table 2.1. (Continued)

Reagents	Source
L-Histidine	Sigma-Aldrich
Hydrochloric acid	Fisher
Hydroxyurea (HU)	Sigma-Aldrich
Isopropanol	Sigma-Aldrich
Kanamycin	Sigma-Aldrich
L-Lysine hydrochloride	Sigma-Aldrich
Lauria broth base	Invitrogen
LB agar	Invitrogen
Leptomycin B	Sigma, LC Laboratories
L-Leucine	Sigma-Aldrich
Lambda protein phosphatase	New England BioLabs
Malt extract	Difco
Methanol	Thermo Fisher Scientific
N,N,N',N',-tetramethylenediamine (TEMED)	Sigma-Aldrich
Nonidet P-40 (NP40)/IGEPAL CA-630	Sigma-Aldrich
Paraformaldehyde	Fisher
Phenol, buffer saturated	Invitrogen
Phloxin B	Sigma-Aldrich
Polyethylene glycol (PEG) 3350	Sigma-Aldrich
Polyethylene glycol (PEG) 4000	EMD
Poly-L-lysine	Sigma-Aldrich
ProLong Gold with DAPI	Invitrogen
Protein-A sepharose	Amersham Biosciences
Restore™ Western Blot Stripping Buffer	Pierce
RNase/DNase free water	Invitrogen
Skim milk powder	Carnation
Sodium azide	Sigma-Aldrich
Sodium chloride (NaCl)	Sigma-Aldrich
Sodium dodecyl sulphate (SDS)	Bio-Rad
Sodium Fluoride (NaF)	Sigma-Aldrich
Sodium hydroxide (NaOH)	Sigma-Aldrich
Sodium Orthovandate (Na_3VO_4)	Sigma-Aldrich
Sodium salicytate	EM Science
Sorbitol	Sigma-Aldrich
Staurosporine	Sigma-Aldrich
Sucrose	EMD Chemicals
Trichloroacetic acid (TCA)	Fisher Scientific
Thiabendazole (TBZ)	Sigma-Aldrich
TRI Reagent or TRIzol	Invitrogen
Tris (Biotechnology Grade)	AMRESCO
Triton X-100	VWR International
Tween 20 (polyoxyethylenesorbitan monolaureate)	Thermo Fisher Scientific
UltraPure distilled water	Invitrogen
Uracil	Sigma-Aldrich
Yeast extract	Difco
Y-PER	Thermo Scientific
Zymicase I enzyme	InterSpex Products, Inc.

Table 2.2. Multi-component systems

System	Source
BioRad Protein Assay kit	Bio-Rad
Expand High Fidelity PCR system	Roche
HiSpeed Plasmid Midi kit	QIAGEN
Platinum Taq PCR System	Invitrogen
PerfeCTa SYBR Green SuperMix, UNG, Low Rox	Quanta Biosciences
Phusion™ Site-Directed Mutagenesis kit	FINNZYMES
Pierce BCA Microplate Protein Assay Kit	Thermo Scientific
QIAEX II gel extraction kit	QIAGEN
QIAprep spin miniprep kit	QIAGEN
QIAquick PCR Purification kit	QIAGEN
QuickChange Multi Site-Directed Mutagenesis kit	Stratagene
Quick Start™ Bradford Protein Assay kit	Bio-Rad
SuperScript III Reverse Transcriptase system	Invitrogen

Table 2.3. DNA/RNA modifying enzymes

Enzyme	Source
Calf intestinal alkaline phosphatase	Invitrogen
DNase I, amplification grade	Invitrogen
Restriction endonucleases	New England BioLabs
Restriction endonucleases	Invitrogen
RNase Out	Invitrogen
Shrimp alkaline phosphatase	Invitrogen
T4 DNA ligase	Invitrogen

Table 2.4. Molecular size standards

Marker	Source
1 kb DNA Ladder	Invitrogen
10 kDa Prestained Protein Ladder	NEB
PageRule Pre-stained Ladder	Fermentas
Pre-stained Protein Ladder (10-180 kDa)	Fermentas

Table 2.5. Detection systems

System	Source
Axioskop2 plus with AxioCam MRc	ZEISS
Axioskop2 with CoolSNAP HQ Photometrics	ZEISS
Axiovert 200M	ZEISS
FluorChem ™ 8000	Alpha Innotech Corporation

Table 2.5. (Continued)

System	Source
Leica SP5	Leica microsystems
LSCM510	ZEISS
MX3005P	Stratagene
Molecular Imager GelDoc ^{TM} XR+ imaging system	BIO-RAD
NanoVue Spectrophotometer	GE
NanoDrop ND-1000 Spectrophotometer	Thermo Scientific
Nitrocellulose membrane, Trans-Blot Transfer Medium	BIO-RAD
Polyvinyldene difluoride (PVDF) membrane	Millipore
Rx film	Fuji
Supersignal West Pico chemiluminescent substrate	Thermo Scientific
Ultraspec 3100 pro UV/visible Spectrometer	GE Healthcare
Ultraviolet gel transilluminator	Thermo Fisher Scientific
UltraView ERS spinning disk confocal unit	Perkin Elmer Bioscience
Velocity acquisition software	Perkin Elmer Bioscience
Vmax kinetic microplate reader	Molecular Devices
XO-MAT Developer	Kodak

2.1.2. Commonly used buffers and media

The following buffers and yeast media were used; their composition is detailed below in Tables 2.6 and 2.7.

Table 2.6. Buffers and Solutions

Name	Ingredients
4x SDS Laemmli loading buffer	0.01% bromophenol blue, 40% glycerol, 3.34% (v/v) β-mercaptoethanol, 8% SDS, 200 mM Tris-HCl (pH 6.8)
5x Protein sample buffer	62.5 mM Tris-HCl (pH 6.8), 25% (v/v) glycerol, 2% (w/v) SDS, 0.01% (w/v) bromophenol blue, 5% (v/v) β-mercaptoethanol
5x First strand buffer	250 mM Tris-Cl (pH 8.3), 375 mM KCl, 15 mM $MgCl_2$
6 x DNA gel loading buffer	40% sucrose, 0.25% bromophenol blue, 0.25% xylene cyanol FF
10 x PCR buffer for colony PCR	500 mM KCl, 100 mM Tris-HCl (pH 9.0), 1.0% Triton X 100
AC buffer with 6 M guanidine-HCl (25 ml)	Glycerol (2.5 ml), 5M NaCl (0.5 ml), 1 M Tris pH7.5 (0.5 ml), 0.5M EDTA (0.05 ml), 10% Tween-20 (0.25 ml), 8 M Guanidine-HCl (18.75 ml), Milk powder (0.5 g), 1M DTT (25 µl), ddH_2O (2.45 ml)

Table 2.6. (Continued)

Name	Ingredients
Alkaline lysis buffer	200 mM NaOH, 1% (w/v) SDS
Bacteria resuspension buffer	50 mM Tris-HCl (pH 8.0), 10 mM EDTA, 100 µg/mL RNase A
Cracking buffer	8 M Urea, 5% (w/v) SDS, 40 mM Tris-HCl (pH 6.8), 0.1 mM EDTA, 0.4 mg/ml bromophenol blue
Diatomaceous earth solution	100 mg/mL diatomaceous earth, 6 M guanidine-HCl, 20 mM EDTA, 50 mM Tris -HCl (pH 8.0)
Diatomaceous earth wash buffer	50% (v/v) isopropanol, 200 mM NaCl, 5 mM EDTA, 20 mM Tris -HCl (pH 7.5)
Dilution buffer for GFP trap	50 mM (pH 7.5), 150 mM NaCl, 0.5 mM EDTA
LB growth media	1% (w/v) Bacto-tryptone, 0.5% (w/v) Bacto-yeast extract, 0.5% (w/v) NaCl, 0.1% (v/v) 1 M NaOH
Lysis buffer for TCA method	5 mM NaOH, 7.5% β-mercaptoethanol (v/v), 200 mM phenylmethylsulfonyl fluoride (PMSF)
Modified homogenization buffer (MHB)	2 mM DTT, 60 mM β-glycerophosphate, 15 mM EGRA, 15 mM $MgCl_2$, 0.1 mM NaVO4, 25 mM 3- Morpholinopropanesulfonic acid (MOPS) (pH 7.5), 15 mM p-nitrophenyl phosphate di-Tris salt (pNPP), and 1% Triton X-100
Neutralization buffer	3.0 M Potassium acetate (pH 5.5)
NP40 lysis buffer	50 mM Tris-HCl (pH 7.5), 150 mM NaCl, 0.5 mM EDTA, 0.5% (v/v) NP-40
NZY^+ broth (per Liter)	10 g NZ amine (casein hydrolysate), 5 g Yeast etract, 5 g NaCl, 1 M $MgCl_2$ (12.5 mL) 1 M $MgSO_4$ (12.5 mL), 2 M glucose (10 mL), (pH 7.5)
Phosphate buffered saline (PBS)	137 mM NaCl, 2.7 mM KCl, 8 mM Na_2HPO_4 (pH 7.4)
PBS-T	137 mM NaCl, 2.7 mM KCl, 8 mM Na2HPO4 (pH 7.4), 0.05% (v/v) Tween-20
PEM	100 mM PIPES, pH 6.9, 1 mM EGTA, 1 mM magnesium sulfate ($MgSO_4$)
PEMS	100 mM PIPES (pH 6.9), 1 mM EGTA and 1 mM magnesium sulfate ($MgSO_4$), 1 M sorbitol
PEMBAL	100 mM PIPES (pH 6.9), 1 mM EGTA and 1 mM magnesium sulfate ($MgSO_4$), 1% bovine serum albumin, 0.1% sodium azide, 0.1 M L-lysine
Protein-binding buffer	100 mM NaCl, 20 mM Tris (pH 7.6), 0.5 mM EDTA, 10% glycerol, 0.1% Tween-20, 2% skim milk powder, 1 mM DTT
Radioimmunoprecipitation (RIPA) buffer	50 mM Tris-HCl (pH 7.5), 150 mM NaCl, 0.1% SDS, 1% Triton X-100, 1% sodioum deoxycholate, 5 mM EDTA
SDS-PAGE running buffer	250 mM glycine, 0.1% SDS, 100 mM Tris Base
SDS-PAGE resolving gel buffer	0.1% SDS, 374 mM Tris-HCl (pH 8.8)
SDS-PAGE stacking gel buffer	0.1% SDS, 250 mM Tris-HCl (pH 6.8)
Sodium citrate/ethanol solution	0.1 M sodium citrate in 10% ethanol (pH 8.5)

Table 2.6. (Continued)

Name	Ingredients
TAE	40 mM Tris acetate, 1 mM EDTA (pH 8.0)
Tris-buffered saline (TBS)	137 mM NaCl, 2.7 mM KCl, 24 mM Tris-HCl (pH 7.4)
TBS-T	137 mM NaCl, 2.7 mM KCl, 24 mM Tris-HCl (pH 7.4), 0.05% Tween 20
TE	1 mM EDTA, 10 mM Tris-HCl, pH 7.5
Transfer buffer	200 mM glycine, 25 mM Tris base (pH 8.3), 20% (v/v) methanol, 0.1% (w/v) SDS

Table 2.7. Yeast media

Media	Ingredients
Edinburg minimal media (EMM)	As per Stratagene or Bio 101 Systems + 225 mg/L adenine, histidine, leucine, uracil and lysine hydrochloride
Malt Extract (ME)	3 % (w/v) Bacto-malt extract (pH 5.5)
Yeast Extract (YE)	0.5% (w/v) Oxoid yeast extract, 3% (w/v) glucose
Yeast Extract + supplements (YES)	YE + 225 mg/L adenine, histidine, leucine, uracil and lysine hydrochloride
Yeast Extract + Adenine (YEA)	YE + 225 mg/L adenine
Yeast Extract + phloxin B (YEP)	YES+ 5 mg/L phloxin B
Solid media was made by adding 2% Difco Bacto Agar	

2.1.3. Oligonucleotides

Table 2.8. Oligonucleotides

Primer Name	Sequence	Engineered sites	Usage
Rdp1 Rev (SacI)	5’-ATATGACTTAAAAATTATTAGCAG TAAGCATGG-3’	SacI	RFP-Rdp1
Rdp1 For (KpnI)	5’-ATATGGTACCCACCATGGCAGTTT CGTTAAATGAC-3’	KpnI	RFP-Rdp1
Cherry-Not-5Gly-F	5’-ATATGCGGCCGCTGGTGGTGGTGG TGGTATGGTGAGCAAGGGCGAGG-3’	NotI	RFP-Rdp1
Cherry-Sst-R	5’-ATATGAGCTCTTACTTGTACAGCT CGTCCATG-3’	SstI	RFP-Rdp1

Table 2.8. (Continued)

Primer Name	Sequence	Engineered sites	Usage
Forward sequencing primer from adh	5’-CTCGGTTTGACGCCTCC-3’	N/A	sequencing
Reverse sequencing primer from ARS	5’-CTCTTACTTAGGGATTCTA TGC-3’	N/A	sequencing
Forward sequencing primer (3’ end of mCherry cassette)	5’-GAAATTGAAAGATGGTG GAC-3’	N/A	sequencing
Act-F-qPCR	5’-CCATTGAGCACGGTATT GTC-3’	N/A	RT-PCR actin mRNA
Act-R-qPCR	5’-CTTCTCACGGTTGGATT TGG-3’	N/A	RT-PCR actin mRNA
dg-For	5’-TGTGCCTCGTCAAATTAT CATCCATCC-3’	N/A	RT-PCR centromeric RNA
dg-Rev	5’-ACTTGGAATCGAATTGAG AACTTGTTATGC-3’	N/A	RT-PCR centromeric RNA
Rdp1-SV40-NLSApaI-F	5’-AGGCATGGGCCCATGACC ATGATAATCCGGAGGGGATA TTTG-3’	ApaI	RFP-Rdp1-SV40NLS
Rdp1-SV40-NLS-SacI-R	5’-ATATGAGCTCTTAGACCTT ACGCTTCTTCTTAGGAAAATT ATTAGCAGTAAGCATGGC-3’	SacI	RFP-Rdp1-SV40NLS
Nt-no-mtr-cut7-Not-F	5’-ATATGC GGCCGCACCATGTC ACTATTAACATTAGGCCGAG-3’	NotI	N-terminal NT-Cut7-RFP
Nt-no-mtr-cut7-Not-R	5’-ATATGCGGCCGCTATCAAT TCCGA AGAAATTCCATTTC-3’	NotI	C-terminal NT-Cut7-RFP
Ct-no-mtr-cut7-Not-F	5’-ATATGCGGCCGCACCATG GAATTG CAGAAAGACATGA AAG-3’	NotI	N-terminal CT-Cut7-RFP
Ct-no-mtr-cut7-Not-R	5’-ATA TGC GGC CGC TCG TT TCATTTTGGAATAGGC-3’	NotI	C-terminal CT-Cut7-RFP
Cherry-Not-5Gly-F	5’-ATATGCGGCCGCTGGTGGTG GTGGTGGTATGGTGAGCAAGG CGAGG-3’	NotI	N-terminal Cherry cassette
Cherry-Sst-R	5’-ATATGAGCTCTTACTTGTAC AGCTCGTCCATG-3’	SstI	C-terminal Cherry cassette
Cut7-Sal-F	5’-ATATGTCGACCACCATGGCC CCTAGAGTTGCAC-3’	SalI	N-terminal cut7-GFP
Cut7-Sal-Rev	5’-ATATGTCGACCCTCGTTTCAT TTTGGAATAGGC-3’	SalI	C-terminal cut7-GFP

Table 2.8. (Continued)

Primer Name	Sequence	Engineered sites	Usage
Y487F For	5’-GAGGGAGTGTTGAAGAACTATGTT TAACGTTATATAAAAAAGCTGAA-3’	N/A	Y487F mutation
Y487F Rev	5’-TTCAGCTTTTTTATATAACGTTAA ACATAGTTCTTCAACACTCCCTC-3’	N/A	Y487F mutation
Y487E For	5’-TAGAGGGAGTGTTGAAGAACTATG GAAAACGTTATATAAAAAAGCTGAA CAG-3’	N/A	Y487E mutation
Y487E Rev	5’-CTGTTCAGCTTTTTTATATAACGT TTTCCATAGTTCTTCAACACTCCCT CTA-3’	N/A	Y487E mutation
Y513F For	5’-GGATAAAAATTCGCCTGAACCATT TGGTTCCATTAAACGTGTT-3’	N/A	Y513F mutation
Y513F Rev	5’-AACACGTTTAATGGAACCAAATGG TTCAGGCGAATTTTTATCC-3’	N/A	Y513F mutation
Y513E For	5’-TTTGGATAAAAATTCGCCTGAACC AGAAGGTTCCATTAAACGTGTTTGC-3’	N/A	Y513E mutation
Y513E Rev	5’-GCAAACACGTTTAATGGAACCTTC TGGTTCAGGCGAATTTTTATCCAAA-3’	N/A	Y513E mutation

N/A, not applicable

2.1.4. Plasmids

Table 2.9. Plasmid vectors

Plasmid	Source
pAALN-GFP-Ago1	Lab Stock
pAAUN-Dcr1-GFP	Lab Stock
pAAUN-GFP-Rdp1	Lab Stock
pAAUN-RFP	Lab Stock
pAAUN-RFP-Rdp1	Lab Stock
pAAUN	Dr. D. Beach, Cold Spring Harbor Laboratory
pRep81	Dr. S. Forsburg, University of Southern California
pAALN	Dr. D. Young, University of Calgary
pGEX4T-1	GE Healthcare
pAALN-GFP-Ago1	Lab Stock
pAALN-RFP-Ago1	Lab Stock
pAAUN-Dcr1-GFP	Lab Stock
pREP41X-GFP	Dr. P. Young, Queens University
pAAUN-HA-Rdp1	Lab Stock
pREP41X-dcr1- HA	Dr. P. Provost, Centre de Recherche du CHUL
pAAUN-HA-Ago1	Lab Stock

2.1.5. Antibodies

Table 2.10. Primary antibodies

Antibody	Dilution	Application*	Source (Product ID)
Rabbit anti-Rdp1	1:500	IP, WB	Abcam (ab4577)
Rabbit anti-Ago1	1:1000	WB	Abcam (ab18190)
Rabbit anti-RFP	1:1000	WB	Abcam (ab34771)
Mouse anti-β-actin	1:1000	WB	Lab stock
Mouse anti-FLAG	1:1000	IP	Sigma (F3165)
Rat anti-HA	1:1000	IP, WB	Roche (3F10)
Mouse anti-GFP	1:500	IP, WB	Roche
Rabbit anti-GFP	1:20 000	IP, WB	Dr. L.G. Berthiaume, University of Alberta

*- WB: Westernblot; IP: immunoprecipitation

Table 2.11. Secondary antibodies

Antibody::Conjugate	Dilution	Application*	Source
Goat anti-mouse::HRP	1:5000	WB	Jackson ImmunoResearch Laboratories
Donkey anti-mouse::HRP	1:5000	WB	Jackson ImmunoResearch Laboratories
Goat anti-rabbit::HRP	1:5000	WB	Jackson ImmunoResearch Laboratories
Goat anti-rabbit::HRP	1:1000	WB	Santa Cruz Biotechnology
Goat anti-mouse::HRP	1:1000	WB	Santa Cruz Biothechnology

*- WB: Westernblot

2.1.6. *Schizosaccharomyces pombe* strains used

Table 2.12 *Schizosaccharomyces pombe* strains

Strain	Genotype	Source	Institution
FY254 (wild type)	can1-1 leu1-32 ade6-M210 ura4-D18 h−	Dr. S. Forsburg	University of Southern California
TV292 (Δ*ago1*)	*ago1*::kanMX6 ura4-D18 DS/E h−	Dr. T. Volpe	Northwestern University
TV296 (Δ*rdp1*)	*rdp1*::kanMX6 ura4-D18 DS/E h−	Dr. T. Volpe	Northwestern University

Table 2.12. (Continued)

Strain	Genotype	Source	Institution
Δ*sal3**	*sal3*::kanMX4 ade6-M210/ade6-M216 ura4-D18/ura4-D18 leu1- 32/leu1-32	Bioneer Corporation	
Δ*kap111**	*kap111*::kanMX4 ade6-M210/ade6-M216 ura4-D18/ura4-D18 leu1-32 /leu1-32	Bioneer Corporation	
Δ*kap113**	*kap113*::kanMX4 ade6-M210 ura4-D18 leu1-32	Bioneer Corporation	
Δ*kap114*	*kap114*::kanMX4 ade6-M216 ura4-D18 leu1-32	Bioneer Corporation	
Δ*kap123**	*kap123*::kanMX4 ade6-M210/ade6-M216 ura4-D18/ura4-D18 leu1-32 /leu1-32	Bioneer Corporation	
Q2007 (Δ*sal3*)	*sal3*::ura4 ura4-D18 leu1-32 h+	Dr. P. Young	Queens University
Q1082	*sal3-33* ura4-D18 leu1-32 h+	Dr. P. Young	Queens University
Q4207	Sal3-GFP int *sal3-33 rdp1*::ura4 pADH:RFP:Rdp1 ura4-D18	This study	
Δ*cse1*(Importin 8 homolog)	*cse1*::kanMX4 ade6-M210 (or M216) ura4-D18 leu1-32	Bioneer Corporation	
FY9778	*leu1 cut7-24* h−	Dr. M. Yanagida	Yeast Genetic Resource Center Japan, Kyoto
G1A	*dhc1*::ura4+ , *klp1*::his3+ , *klp2*::ura4+ , nmt1GFP-Atb2::lys , ade6-M216, leu1-32	Dr. R. Carazo-Salas	Cancer Research UK, London Research Institute
G2	*klp3*::ura4+ , *his3*-D1 , nmt1GFP-Atb2::lys , leu1-32	Dr. R. Carazo-Salas	Cancer Research UK, London Research Institute
G3	*klp5*::ura4+ , *klp6*::his3+ , nmt1GFP-Atb2::lys , leu1-32	Dr. R. Carazo-Salas	Cancer Research UK, London Research Institute
G5	*tea2/klp4*::his3+ , nmt1GFP-Atb2::lys , leu1-32 , ura4-D18	Dr. R. Carazo-Salas	Cancer Research UK, London Research Institute
G6	*klp8*::kanR , nmt1GFP-Atb2::lys , ade6-M216 , leu1-32 , ura4-D1	Dr. R. Carazo-Salas	Cancer Research UK, London Research Institute
3774	nmt1 GFP alpha tubulin integrant (Atb2)::lys , leu1-32 , ura4-D18 , h−	Dr. R. Carazo-Salas	Cancer Research UK, London Research Institute
FY648	otr1R(SphI)::ura4+ura4-DS/E leu1-32 ade6-M210, h+	Dr. D.Moazed	Harvard University
SPY1976	leu1-32, ura4-D18, ade6-216M, imr1R(NotI)::ura4$^+$ 3xFLAG-clr4-clr4ter::natR, h$^+$	Dr. D.Moazed	Harvard University

*Strains were purchased as diploids and then haploidized for experiments.

2.1.7. *Schizosaccharomyces pombe* online resources

Table 2.13. *S. pombe* online resources (Sabatinos and Forsburg 2010)

Name: General information, Links, Resources	URL
PombeNet: Protocols, resources, people, general information (Forsburg Lab)	http://www.pombe.net/
Sanger Centre	http://www.sanger.ac.uk/Projects/S_pombe/links.shtml
NIH *S. pombe* page	http://www.nih.gov/science/models/Schizosaccharomyces/index.html
Genome information:GeneDB (Genome browser and database)	http://genedb.org/genedb/pombe/
Genome information: Epigenome home page (Grewal lab)	http://pombe.nci.nih.gov/genome/
Sequences of related species Fungal genomes at the Broad Institute	http://broadinstitute.org/science/projects/fungal-genome-initiative/
Expression data: Bahler lab data, UCL (UK)	http://www.bahlerlab.info/
Gene Expression Viewer	http://www.bahlerlab.info/cgi-bin/SPGE/geexview
Transcriptome Viewer	http://www.bahlerlab.info/TranscriptomeViewer/
Software links (disruption, tagging)	http://www.bahlerlab.info/resources
Strains and plasmids: ATCC	http://www.atcc.org/Schizosaccharomycespombe/tabid/680/Default.aspx
Strains: Bioneer (commercial gene deletions)	http://www.bioneer.com
National Collection of Yeast Cultures (Norwich, UK)	http://www.ncyc.co.uk/
RIKEN, GFP-tagged ORFeome Yeast Resource Centre, Japan	http://yeast.lab.nig.ac.jp/nig/index_en.html
Pombelist (community list-serv)	http://lists.sanger.ac.uk/mailman/listinfo/pombelist

2.2. Methods

2.2.1. Yeast techniques

2.2.1.1. Growth, maintenance, and long-term storage of *S. pombe*

2.2.1.1.1. Yeast cultures at permissive and restrictive temperatures

A list of *S. pombe* strains used in this study and their corresponding genotypes are shown in Table 2.12. Unless otherwise indicated, yeast were cultured at 29–30°C in YES or EMM lacking nutritional supplements (Table 2.7). To induce expression of genes under the control of the no message in thiamine (*nmt*) promoter (Alfa C, and Warbrick E, 1993), yeast strains were grown overnight in EMM lacking thiamine. When using transformants of the temperature-sensitive *(ts)* strain *cut7-24,* yeast were first cultured at the permissive temperature (23°C) and, where indicated, shifted to 29°C for 18 hours before processing for live cell imaging.

2.2.1.1.2. Measuring cell growth rates

Overnight cultures (5 mL) were grown using a rotating wheel apparatus and used to inoculate fresh media to an OD_{600} of ~0.05. The cultures (1 L) were then grown at 29–30°C in a shaking incubator (225 rpm). The optical density for each strain was measured every 12 hours for 72 hours using an Ultraspec 3100 pro UV/visible Spectrometer (Table 2.5).

2.2.1.1.3. Maintenance of yeast strains

Yeast cultures grown in YES to late-logarithmic phase were mixed with an equal volume of sterile glycerol in a screw cap tube and placed in dry-ice with ethanol, followed by storage in a -80°C freezer. For short-term storage, strains were kept as patches on YES or EMM plates at 4°C for a maximum of two months. The plates were sealed with parafilm to prevent drying out.

2.2.1.1.4. Re-isolation of frozen cultures

To start cultures from frozen stocks, a small amount of frozen glycerol stock was scraped off with a sterile spatula and streaked onto YES plates, which were then incubated at 25°C–30°C for 2–4 days until single colonies appeared. When necessary, the phenotype of each strain was verified as described in Sections 2.2.1.3 or 2.2.4.1.

2.2.1.2. Yeast transformation

Transformation of yeast strains was performed using the following methods.

2.2.1.2.1. Quick TRAFO method

For small-scale transformation, yeast cells were grown in 5 mL cultures to a maximum density of 1 x 10^7 cells/mL. Cells were pelleted by centrifugation at 13,000 rpm for 1 minute, resuspended in 500 µL of 100 mM LiAc (pH 4.9), then

incubated for 30 minutes at room temperature. Alternatively, a toothpick full of fresh (less than one week old) colony was used. During the incubation with LiAc, carrier DNA (10 mg/mL) stock solution was boiled for 10 minutes and then chilled on ice for 5 minutes. Yeast cells were pelleted and resuspended in 240 µL of 50% (w/v) PEG 4000 and the following components were added: 36 µL of 1.0 M LiAc, 50 µL of 2 mg/mL single-stranded (SS) carrier DNA, 1 µg of plasmid DNA, and sterile water up to a total volume of 360 µL. The transformation mixtures were incubated for 60–90 minutes in a 42°C water bath, pelleted, resuspended in sterile water, and plated onto appropriate selection media plates, which were then incubated for 4–7 days at 29°C–30°C.

2.2.1.2.2. Lithium Acetate method

Fission yeast cells were grown in YE up to 1 x 10^7 cells/mL and harvested at 3,000 x g for 10 minutes. Cells were washed once with sterile water and then with 1 mL of 100 mM LiAc-TE (0.1 M Lithium acetate, 10 mM Tris [pH 7.5] and 1 mM EDTA). Cell pellets were resuspended in 250 µL of 1 M LiAc-TE, to which 2 µL of SS carrier DNA (10 mg/mL) and 1 µg of transforming DNA (per 100 µL of suspension) were added. Mixtures were incubated for 10 minutes at room temperature, after which 260 µL of 40% PEG-Lithium acetate-TE was added. Mixtures were incubated for 30 minutes at 30°C, and then 43 µL of pre-warmed DMSO was added before the cells were heat shocked for 5 minutes at 42°C. The transforming cell mixtures were pelleted at 3,000 x g for 5 minutes,

resuspended in 500 µL of sterile water, and plated onto appropriate selection media plates, which were then incubated for 4–7 days at 29°C–30°C.

2.2.1.2.3. Electroporation

Yeast cells were grown to early stationary phase (OD_{600} of 1.2–1.5) at permissive temperature, pelleted by centrifugation at 5,000 rpm for 5 minutes, washed once in an equal volume of ice-cold water, and then washed once in cold water (½ volume). Ice-cold sorbitol ($^1/_{25}$ volume) was added before the cell mixtures were adjusted with DTT (25 mM) and incubated for 10 minutes at room temperature. Cells were then washed with 1 M cold sorbitol ($^1/_{10}$ volume) and resuspended in $^1/_{100}$ the volume of cold 1 M sorbitol. Fifty µL of the cell suspensions were transferred to pre-chilled cuvettes containing 100 ng of DNA which were incubated on ice for 5 minutes, and then pulsed at 1.5 kV, 200 Æ, 25 µFadadays for Å5 miliseconds using a Bio-Rad electroporator. Immediately after the electrical pulse, 1 mL of 1M sorbitol was added to the cuvette to recover the cells. The content was transferred to a microfuge tube and incubated for 1 hour at the permissive temperature. Cells were then resuspended in 1 mL of 1 M sorbitol before plating on selective media plates, which were incubated for 4–7 days at 29°C–30°C.

2.2.1.3. Haploidizing yeast strains

Yeast from glycerol stocks were streaked on YES/G418 (25 µg/mL) or YES plates until single colonies were visible. Single colonies were then streaked

onto YES/thiabendazole (TBZ, 20 µg/mL) plates, which were incubated at 30°C for 24 hours. Patches of cells from YES/TBZ plates were re-streaked onto YES plates, which were then incubated at 30°C for 2–3 days until single colonies were visible. Replica-plates on YES/G418, YES/Phloxin B (5 µg/mL), and EMM - Ura - Leu plates (without Ade) were made to select for haploids. The colonies were incubated at 30°C for 2–4 days. Haploid and diploid colonies were distinguished as follows: haploids appeared white on YES/Phloxin B plates and did not grow on EMM- Ura - Leu plates; diploids appeared red on YES/Phloxin B plates and grew on EMM - Ura - Leu plates. To confirm haploid status, the putative haploid colonies were re-streaked onto YES/G418 and EMM - Ura - Leu plates, then were incubated at 30°C for 1–2 days. Haploids only grew on the YES/G418 plates.

Alternatively, Phloxin B (Table 2.1) was used to test cell ploidy after re-isolation of the frozen stock cells or obtaining new *S. pombe* strains from the suppliers. Phloxin B was spread on a plate to a final concentration of 5 mg/L from a stock of 10 g/L, which was made up in water, filter-sterilized, and kept covered with tin foil and stored at -20°C. After a few days of incubation at the permissive temperature, wild-type haploids formed pale pink colonies on phloxin B-containing plates. Diploid colonies were slightly darker. Dying cells formed darker colonies or patches and lethal mutants were often dark red (Forsburg and Rhind 2006). Ploidy was also confirmed by microscopic examination of the cells. Haploid cells divided at approximately 12–15 µm in length and were 3–4 µm in width (Sabatinos and Forsburg 2010).

2.2.1.4. Generating integrant strains

2.2.1.4.1. Illegitimate integration of plasmids

To produce integrant plasmid-bearing strains, the appropriate null mutants were transformed with plasmids encoding the gene of interest. Resulting colonies were screened using selective media such as EMM lacking uracil or leucine. Colonies were transferred to selective broth media (EMM lacking uracil or leucine) for 7 days before culturing in non-selective media (YEA) up to stationary phase—a process that results in loss of non-integrated plasmids. After approximately 1 week, aliquots of the cultures were plated onto EMM plates lacking the leucine or uracil. The process of plasmid dropping and selection cycles was repeated at least three times to enrich for cells chromosomally integrated plasmids.

2.2.1.4.2. Stability test

This test was used to check the stability of a transformed plasmid after generating integrant strains. If the plasmid was not integrated it was lost in the absence of selection. If the plasmid was integrated, the phenotype was maintained after relaxing the selection. After transformation and several cycles of plasmid dropping, the cells were plated on a YES plate to obtain clonal lines. Individual colonies were streaked out to single colonies on YES agar with no selection and incubated for several days until colonies formed. Replica plates were then made onto YEA and EMM lacking the selective marker to look for stability. Integrants exhibited 100% correspondence between the two plates.

2.2.1.5. Quantitation of lagging chromosomes

Yeast were grown in YES at the permissive temperature to mid-log phase and then shifted to 18°C for 6 hours to slow the rate of cell division (Pidoux et al. 2000). Cells were collected by centrifugation, fixed with 70% ethanol (v/v) at 4°C for over 60 minutes, then stained with DAPI (1 μg/mL) for 2 minutes. The cells were washed sequentially with PBS and water before viewing by fluorescence microscopy. The number of dividing cells with lagging chromosomes was counted for each condition or mutant (Pidoux et al. 2000).

2.2.1.6. Staurosporine treatment

Staurosporine (2 mM stock) was added to exponentially growing yeast cell cultures to a final concentration of 2 μM. After 16 hours, cells were viewed by fluorescence microscopy (Section 2.2.4.1).

2.2.1.7. Assay with thiabendazole (TBZ) treatment

Yeast strains were cultured at 30°C in YES or EMM lacking leucine or uracil until the OD_{600} reached approximately 0.8–1.0. Cell numbers were determined using a hemocytometer. Serial dilutions of the cultures were spotted onto YES or EMM (lacking leucine or uracil) plates containing 5–20 μg/mL TBZ. Plates were incubated at 29°C–30°C for 2–4 days. Fresh TBZ stocks (20 mg/mL) were prepared in dimethyl sulfoxide (DMSO) for each experiment.

2.2.2. Nucleic acid purification, analysis, and modification

2.2.2.1. Isolation of plasmid DNA from *Eschericia coli* (*E. coli*)

Isolation of plasmid DNA was performed using one of two methods: commercially available preparation kit, the QIAprep spin mini prep kit (Table 2.2), following the manufacturer's recommendations; or an in-house developed diatomaceous earth protocol (Table 2.6). Plasmid-transformed DH5α bacteria were grown overnight in 5 mL cultures of LB (Table 2.6) containing appropriate antibiotics at 37°C. For small-scale plasmid isolation, cultures were divided into 1.5 mL eppendorf tubes and were pelleted by centrifugation at 14,000 x *g* for 2 minutes. For the diatomaceous earth protocol, bacterial pellets were resuspended in 250 µL of bacteria resuspension buffer (Table 2.6). Following resuspension, 250 µL of alkaline lysis buffer (Table 2.6) was added. The tubes were inverted several times until the solution was clear and before incubation on ice for 5 minutes to allow complete cell lysis. Lysates were neutralized with 300 µL of neutralization buffer (Table 2.6). Insoluble materials (proteins and chromosomal DNA) were pelleted via centrifugation at 14,000 x *g* for 10 minutes. The supernatant fractions were transferred to fresh tubes containing 600 µl of diatomaceous earth slurry. The slurry/supernatant mixtures were incubated for at least 10 minutes at room temperature with rocking or rotation, then were applied to pre-wetted filter pipette tips on a vacuum manifold. Plasmid DNA bound to diatomaceous earth was washed in place on the filter pipette tip twice with diatomaceous earth wash buffer (Table 2.6). This was subsequently centrifuged at 5,000 x g for 1 minute to remove any residual column wash. Following the final

wash, tips were left to air dry for 10 minutes and then centrifuged at 10,000 x *g* for 1 minute to remove trace isopropanol. Tips were then transferred to fresh eppendorf tubes and the plasmid DNA was eluted from the diatomaceous earth with 50 µL of preheated 70^{o}C MilliQ H_2O (or TE buffer, pH7.5) and centrifuged at 13,000 x *g* for 1 minute. The concentrations of the plasmid DNAs were determined using a NanoVue or a NanoDrop ND-1000 Spectrophotometer (Table 2.5). When not in use, DNA samples were stored at -20°C.

2.2.2.2. Isolation of plasmid DNA from yeast

Yeast strains were grown to OD_{600} = 1.0 at the permissive temperature. Cells were harvested by centrifugation at 3,000 x g for 5 minutes, and 750 µL of TRIzol Reagent (Table 2.1) was added per 0.25 mL of sample (5 ~ 10 x 10^6 cells from yeast). Cells were lysed and homogenized by pipetting up and down several times. The homogenized cells were incubated for 5 minutes at room temperature to permit complete dissociation of the nucleoprotein complex. Two hundred µL of chloroform per 1 mL of TRIzol Reagent was added. The tubes were shaken vigorously by hand for 15 seconds and incubated for 2–3 minutes at room temperature. To separate phases, the samples were centrifuged at 12,000 x g for 15 minutes at 4°C. DNA was isolated from the interphase and the phenol-chloroform layer after the phase separation. Any remaining aqueous phase (contains RNA) overlaying the interphase was removed from the tubes and 300 µL of 100% ethanol per 1 mL TRIzol Reagent was added to the samples. After inverting several times and incubating for 2–3 minutes, the samples were pelleted

by centrifugation at 2,000 x g for 5 minutes at 4°C. The phenol-ethanol supernatant was removed before the DNA wash step. The DNA pellet was washed with 1 mL of sodium citrate/ethanol solution (Table 2.6) per 1 mL of TRIzol Reagent used for the initial homogenization. The samples were incubated for 30 minutes at room temperature and then pelleted by centrifugation at 2,000 x g for 5 minutes at 4°C. The supernatant was discarded and the wash steps were repeated one more time. DNA was recovered by ethanol precipitation and air-dried for 5–10 minutes before resuspension in 300–600 µL of 8 mM NaOH/ 1 x 10^7 cells. Insoluble material was removed by centrifugation at 12,000 x g for 10 minutes at 4°C. The DNA-containing supernatants were transferred to new tubes and the pH was adjusted with HEPES (Table 2.1). If not used immediately, the isolated DNAs were stored at -20°C.

2.2.2.3. Restriction endonuclease digestion

Reactions were typically carried out in a volume of 20 µL with 0.5–3 µg of plasmid DNA and 1–6 U of restriction endonuclease with appropriate reaction buffer (Table 2.3) at the recommended reaction temperature of the enzyme, as specified by the manufacturer.

2.2.2.4. Dephosphorylation of linearized vectors

To enrich the proportion of positive clones and to reduce the occurrence of vector self-ligation, particularly when using blunt-ended or single-cut vectors, vector DNA was dephosphorylated using calf intestinal alkaline phosphatase or

shrimp alkaline phosphatase (Table 2.3), according to the manufacturer's recommendations. The reaction was terminated by heat inactivation at 65^{o}C for 15 minutes.

2.2.2.5. Polymerase chain reaction (PCR)

DNA was amplified using indicated primers (Table 2.8) in conjunction with Expand High Fidelity PCR system or Platinum *Taq* PCR System (Table 2.2), according to the manufacturers' specifications. Reactions normally contained approximately 100 ng of plasmid DNA or 1 µg of genomic DNA templates, 10 µM dNTPs, 1–2 units of polymerase, and 1 x reaction buffer. Reactions were performed using either a Robocycler Gradient 40 Hot Top system (Stratagene) or a TC-312 thermocycler (Techne).

2.2.2.6. Agarose gel electrophoresis

2.2.2.6.1. DNA agarose gel electrophoresis

Electrophoresis-grade agarose was dissolved by heating in TAE (Table 2.6). Prior to pouring the gels (0.8%–1.5% agarose [w/v]) into casting trays, ethidium bromide was added to a final concentration of 0.5 µg/mL. DNA samples were mixed with 6x DNA gel loading buffer (Table 2.6), loaded into wells, and then electrophoretically resolved. Fragments were visualized using an ultraviolet gel transilluminator (Table 2.5), and the images were captured using a FluorChem ^{TM} 8000 imaging system or a Molecular Imager GelDoc ^{TM} XR+ imaging system (Table 2.5).

2.2.2.6.2. RNA agarose gel electrophoresis

The quality of the RNA used for reverse transcription polymerase chain reaction (RT-PCR) was examined by the method indicated in DNA agarose gel electrophoresis (Section 2.2.2.6.1). The appearance of distinct, non-smeared ribosomal RNA bands at approximately 1.8 and 3.5 kb indicated successful extraction of quality RNAs. The concentration of RANs was measured by using a NanoVue Spectrophotometer or a NanoDrop ND-1000 Spectrophotometer (Table 2.5).

2.2.2.7. Purification of DNA fragments

Prior to restriction endonuclease digestion, subsequent ligation, and/or gel electrophoresis, proteins and dNTPs were removed from PCR reactions using QIAquick PCR purification kits (Table 2.2). Restriction endonuclease digestions yielding larger DNA products—which were not compatible for exclusion by the QIAquick PCR purification kit—were separated by agarose gel electrophoresis. The bands of interest were visualized using an Ultraviolet gel transilluminator (Table 2.5) and were excised from the gel with a clean razor blade. DNA fragments were eluted from the agarose gel using the QIAEX II gel extraction kit (Table 2.2).

2.2.2.8. Ligation of DNA

T4 DNA ligase was used to ligate DNA fragments according to the manufacturer's specifications. DNA inserts and vectors were combined in molar ratios ranging from 2:1–6:1. Typically, a 15–20 µL reaction contained a minimum of 20 ng of vector DNA and 1–5 U of T4 DNA ligase (Table 2.3). For blunt-end reactions, the concentration of inserts and vectors was higher than in cohesive-end ligations. Reactions were performed for 1 hour at room temperature (for cohesive-end) or overnight at 16°C (for blunt-end).

2.2.2.8.1. Low melting agarose in gel-ligation

DNA fragments were separated on 1% agarose gels (UltraPure™ Low Melting Point, Table 2.1) in 1x TAE (Table 2.6). Gel pieces containing fragments of interest were isolated with a clean razor blade and put into separate microfuge tubes. The tubes containing gel pieces were put into a 70°C water bath for 5 minutes and after the gel had melted, the appropriate amount of fragments were aliquotted into new tubes which were transferred to a 37°C water bath. Pre-warmed ligation mix (10 µL) was added. For two-part ligations, the control reaction contained 10 µL of melted gel containing vector plus 10 µL ligation reaction mix. The experimental tubes contained 5 µL of vector gel piece, 5 µL of insert gel piece, and 10µL ligation reaction mix. Ligation mixtures were incubated at room temperature for 3–16 hours before they were used for transformation of bacteria. Two-part ligations of cohesive ends were incubated for 3 hours, whereas three-part or blunt-end ligation reactions were left for 16 hours.

2.2.2.9. Transformation of *E. coli*

2.2.2.9.1. Transformation of chemical-competent *E. coli*

SubCloning Efficiency™ DH5α™ Chemically Competent (Invitrogen) cells were normally used for routine subcloning. DNA (1–10 ng) was added to ice-thawed competent cells, and the mixtures were incubated on ice for 30 minutes, subjected to heat shock for 45 seconds in a 42°C water bath, and then incubated on ice for 2 minutes. Pre-warmed growth media (950 µL) was added to each tube, and the samples were incubated at 37°C for 1 hour while shaking at 225 rpm. The transformants were spread onto LB agar plates containing the appropriate antibiotics. In some cases, OneShot Chemical Competent (Invitrogen), XL10- Gold Ultracompetent cells (Stratagene), or Library Efficiency® DH5α™ Competent cells (Invitrogen) were used.

2.2.2.9.2. Transformation of electro-competent *E. coli*

Electro-competent *E. coli* DH5α cells were prepared as follows: Bacterial cultures (100 mL) were grown in LB at 37°C with shaking until OD_{600} = 0.5–0.8. Cells were collected by centrifugation at 4,000 x g for 15 minutes at 4°C. They were washed twice with 500 ml ice-cold water and then once in ice-cold 10% glycerol (v/v). The cells were subsequently resuspended in 1 mL of ice-cold 10% glycerol and then divided into 50 µL aliquots that were frozen in a dry ice-ethanol bath and stored at -80°C until further use. Electro-competent cells were thawed on ice prior to transformation with 0.5% of a ligation mixture. Cells and DNA were incubated together on ice for 5 minutes and transferred to an ice-cold 0.1 cm gap

electroporation cuvette (Bio-Rad). The cuvette and contents were subjected to the manufacturer's pre-set electrical pulse using a Micropulser (Bio-Rad). Immediately after the electrical pulse, 1 mL of LB was added to the cuvette and the contents were transferred to a microfuge tube, which was incubated for 1 hour at 37°C. Cells were plated onto an LB agar plate containing the appropriate antibiotics.

2.2.2.10. Colony PCR

Colony PCR was done to quickly screen for plasmid inserts. Typical reactions contained the following components: 38 μL of sterile ddH_2O, 5 μL of 10X PCR buffer (Table 2.6), 3 μL of 25 mM $MgCl_2$, 1 μL of 10 mM dNTPs, and 1 μL of 20 μM each forward and reverse primer. A small amount of bacterial colony was added to each PCR tube, which contained 49 μL of PCR reaction. The contents of the tube were mixed by pipetting up and down to increase lysis, after which 1 μL Taq polymerase was added. Reactions were performed using either a Robocycler Gradient 40 Hot Top system (Stratagene) or a TC-312 thermocycler (Techne), followed by separation by agarose gel electrophoresis, as described in Section 2.2.2.6.1.

2.2.3. Construction of recombinant plasmids

All primers and plasmids used for the construction are documented in Tables 2.8 and 2.9, respectively. The following expression constructs were made by polymerase chain reaction, as follows:

2.2.3.1. RFP-Rdp1

Primers Rdp1-Kpn-I-F and Rdp1-Sac-I-Rev were used to amplify an intronless genomic DNA fragment encoding the entire Rdp1 protein. The resulting product was digested with SacI and KpnI, and then ligated in frame with the monomeric cherry RFP cassette into the yeast expression plasmid pAAUN (Table 2.9).

2.2.3.2. RFP-Rdp1-SV40-NLS

Primers Rdp1-SV40-NLS-ApaI-F and Rdp1-SV40-NLS-SacI-R were used to amplify a ~ 700 bp genomic DNA fragment encoding the carboxyl-terminal region of Rdp1, followed by the SV40 nuclear localization signal (NLS) (Kalderon et al. 1984). The resulting PCR product was digested with ApaI and SacI and then used to replace the analogous 700 bp ApaI/SacI fragment released from the pAAUN-RFP-Rdp1 plasmid.

2.2.3.3. pAAUN-RFP

Primers Cherry-Not-5Gly-F and Cherry-Sst-R were used to amplify the mCherry RFP cassette from the expression construct pAAUN-RFP-Ago1 (Carmichael et al. 2006). The resulting fragment was digested with NotI and SstI and then sub-cloned into pAAUN (Table 2.9).

2.2.3.4. NT-Cut7-RFP

Constructions of Cut7 expression vectors were performed by C. Stoica and S. Willows (University of Alberta).

NT-Cut7-RFP: Primers Nt-no-mtr-cut7-Not-F and Nt-no-mtr-cut7-Not-R were used to amplify an intronless genomic DNA fragment encoding amino acid residues 353 to 720 of the Cut7 protein. The resulting product was digested with NotI and then ligated in-frame with RFP in the *S. pombe* expression vector pAALN-RFP.

2.2.3.5. CT-Cut7-RFP

CT-cut7-RFP: Primers Ct-no-mtr-cut7-Not-F and Ct-no-mtr-cut7-Not-R were used to amplify an intronless genomic DNA fragment encoding amino acid residues 721 to 1085 of the Cut7 protein. The resulting product was digested with NotI and then ligated in-frame with RFP in the *S. pombe* expression vector pAALN-RFP.

2.2.3.6. Cut7-GFP

Cut7-GFP: Primers Cut7-Sal-F and Cut7-Sal-Rev were used to amplify a genomic DNA fragment encoding the entire Cut7 protein. The resulting product was digested with SalI and then ligated in-frame with GFP in the *S. pombe* expression vector pREP41X-GFP.

2.2.3.7. Site-directed Mutagenesis

The primers described in Table 2.8 and the QuickChange Multi Site-Directed Mutagenesis kit were used to create point mutations in the Ago1 cDNA according to the manufacturer's recommendations. A typical PCR reaction contained the following components: 13.75 µL of sterile ddH_2O, 2.5 µL of 10X PCR buffer, 0.75 µL of QuickSolution, 1 µL of dNTPs, 2 µL of each forward and reverse primer (100 ng/µL), and 2 µL of DNA template (100 ng/µL). The samples were mixed by pipetting up and down and 1 µL QuickChange Multi enzyme blend was added to each sample tube, followed by PCR reactions using either a Robocycler Gradient 40 Hot Top system (Stratagene) or a TC-312 thermocycler (Techne). Following the mutant strand synthesis, amplified products were treated with DpnI restriction enzyme to digest methylated and hemimethylated DNA. The samples were centrifuged for 1 minute and 1 µL of DpnI enzyme was added to each sample. The samples were incubated at 37°C for 1 hour. After DpnI digestion, the samples were transformed with XL10- Gold Ultracompetent cells (Stratagene). NZY^+ broth (Table 2.6) was preferentially used for transformation with XL10- Gold Ultracompetent cells.

2.2.3.7.1. GFP-Ago1(Y487F)

Primers Y487F For and Y487F Rev were used to create a cDNA encoding a GFP-Ago1 protein with F substituted for Y at position 487. The template for the PCR reactions was pAAUN-GFP-Ago1.

2.2.3.7.2. GFP-Ago1(Y487E)

Primers Y487E For and Y487E Rev were used to create a cDNA encoding a GFP-Ago1 protein with E substituted for Y at position 487. The template for the PCR reactions was pAAUN-GFP-Ago1.

2.2.3.7.3. GFP-Ago1(Y513F)

Primers Y513F For and Y513F Rev were used to create a cDNA encoding a GFP-Ago1 protein with F substituted for Y at position 513. The template for the PCR reactions was pAAUN-GFP-Ago1.

2.2.3.7.4. GFP-Ago1(Y513E)

Primers Y513E For and Y513E Rev were used to create a cDNA encoding a GFP-Ago1 protein with F substituted for Y at position 513. The template for the PCR reactions was pAAUN-GFP-Ago1.

2.2.3.8. Automated DNA sequencing

DNA fragments amplified by PCR were verified by sequencing at the Molecular Biology Facility (Department of Biological Sciences, University of Alberta) or at The Applied Genomics Centre (TAGC, Department of Medical Genetics, University of Alberta). The sequencing facilities use a protocol based on the incorporation of fluorescently labeled dideoxy terminators during the elongation stage.

2.2.4. Microscopy

2.2.4.1. Fluorescent microscopy

After fixation (Sections 2.2.4.1.1 or 2.2.4.1.2) and DAPI staining (Section 2.2.4.1.4), cells were resuspended in 300–500 µL of ice-cold ddH_2O and 5–10 µL of the suspension was pipetted onto a poly-L-lysine coated microscope slide. Samples were viewed using an Axioskop2 plus (Table 2.5). Images were captured with an AxioCam MRc or a CoolSNAP HQ Photometrics camera. In some cases, a Leica SP5 confocal microscope was employed.

2.2.4.1.1. Aldehyde fixation

Yeast strains expressing GFP- and/or RFP-tagged chimeras were grown in EMM lacking corresponding nutritional supplements to an OD_{600} = 0.5–0.8. They were fixed at 1:10 in 37% paraformaldehyde for ~30 minutes or longer at 4°C in a rotating rack. After fixation, samples were pelleted by centrifugation and washed once in PEMBAL (Table 2.6) for 30 minutes on a rotating device, then washed twice with PEM (Table 2.6).

2.2.4.1.2. Solvent fixation

In some cases, ethanol fixation of cells was employed. This method is particularly good for maintaining nuclear structure. Yeast cells were grown in an appropriate media up to an OD_{600} = 0.5–0.8 and 1.0 OD unit of cells were harvested and fixed with 70% (v/v) ethanol. Cells were pelleted by centrifugation

and then resuspended by vortexing in a microfuge tube containing 1mL of cold 70% ethanol. Samples were allowed to fix incubation in this solution for at least 1 hour in a rotating device at 4°C. After fixation, samples were pelleted by centrifugation and washed once in PBS for 30 minutes on a rotating device, then washed twice with ice-cold ddH_2O.

2.2.4.1.3. Poly-L-lysine mounting

Poly-L-lysine (2 mg/mL) solution (200 µl) was pipetted onto microscope slides, which were then incubated for 30 minutes at room temperature. After washing with water and aspirating residual liquid, the slides were ready for yeast samples to be mounted.

2.2.4.1.4. DAPI staining of nuclei

DAPI stock solution (1 mg/ml) was kept in aliquots at -20°C. Fixed yeast cells were pelleted by centrifugation and resuspended in DAPI solution (1 µg/mL), then incubated at room temperature for 2–5 minutes. Cells were washed twice with PBS and then once with ice-cold ddH_2O before resuspension in 300–500 µL of ice-cold water. Approximately 5–10 µL of cell suspension was pipetted onto a poly-L-lysine coated microscope slide followed by examination by fluorescence microscopy.

2.2.4.2. Live-cell imaging

Unless otherwise indicated, yeast strains expressing GFP- and/or RFP-tagged chimeras were grown in selective EMM media to an OD_{600} = 0.5–0.8 at 30°C. When using temperature-sensitive *cut7-24* mutants expressing GFP-Ago1 or RFP-Ago1, yeast were cultured at the permissive temperature (23°C) and then were shifted to 29°C for 18 hours before processing for live-cell imaging. Live yeast cells were immobilized on slides coated with 0.7% agarose or 0.2% low melting agarose. Samples were examined using an Ultraview ERS spinning disc confocal imager attached to an Axiovert 200M microscope.

2.2.4.2.1. DASPMI staining of mitochondria

For visualization of mitochondria, 0.2 mL of yeast culture was mixed with 30 μL of 2-(4-dimethylaminostyryl)-1-methylpyridinium iodide (DASPMI; Table 2.1) that was prepared in DMSO or methanol (0.5 mg/mL). Samples were incubated at 36°C for 5 minutes. Cells were recovered by centrifugation at 1000 x g for 5 minutes and then resuspended in 0.2 mL YE media. Yeast cells were immobilized on microscope slides using agarose (Section 2.2.4.2.2) and examined using an Ultraview ERS spinning disc confocal imager (Perkin Elmer) attached to an Axiovert 200M microscope (Zeiss).

2.2.4.2.2. Immobilization of live yeast cells using agarose

Low melting agarose (0.2%) was melted in 1 mL of YE or EMM media at 70°C by mixing the contents every 10 minutes. The tube containing molten agarose was cooled to 37°C–42°C in a water bath, after which an equal volume of cell suspension was added. The mixture was pipetted onto a microscope slide and then covered with a cover slip. Samples were then immediately examined using an Ultraview ERS spinning disc confocal imager (Perkin Elmer) attached to an Axiovert 200M microscope.

2.2.4.3. Quantification of microscopic data

When statistical analysis was employed, at least 100 cells in microscopic fields from three independent experiments were counted. Images were acquired using Volocity image acquisition software, after which cells were accessed manually or with Imaris x64 (with the MeasurementPro module, Bitplane). Statistics were exported in Microsoft Excel file format, and then averages and standard errors were calculated.

2.2.5. Protein gel electrophoresis and detection

2.2.5.1. Protein preparations

Yeast stains were grown in liquid culture until the OD_{600} reached 1.0–1.2. Unless otherwise stated, protein samples were kept on ice. For each strain, a total of 100 OD_{600} units of cells were recovered by centrifugation at 4,000 x g for 5

minutes at 4°C in pre-chilled 50 mL centrifuge tubes. The cell pellets were washed twice with 50 mL of ice-cold H_2O containing Complete™ Protease Inhibitor Cocktail (EDTA-free) (Roche) and recovered by centrifugation at 1,000 x g for 5 minutes at 4°C. Cells were incubated with 2.0 M lithium acetate for 10 minutes on ice (Zhang et al. 2011), centrifuged, and resuspended in SDS-PAGE sample buffer (Table 2.6). The cell suspension was boiled for 5 minutes, then was subjected to sonication (Branson Sonifier 250). Lysates were clarified by centrifugation at 12,470 x g in the microfuge for 10 minutes, after which the 5% of total sample supernatants was subjected to SDS-PAGE or stored at -80°C.

Alternatively, for a small-scale blot, yeast stains were grown in 5 mL liquid media until the OD_{600} reached ~1.0. They were then pelleted by centrifugation at 2,000 rpm for 1 minute and washed once with water. The pellet was resuspended in 500 µL of Mili-Q H_2O containing 0.2mM of sodium orthovanadate (Na_3VO_4), 5 mM sodium fluoride (NaF), and 90 µL freshly made lysis buffer (Table 2.6). The cells were broken by a 30-second vortex twice and incubated on ice for 10 minutes. One hundred percent TCA (250 µL) was added and incubated on ice for 10 more minutes. The cells were collected by centrifugation at 14,000 x g for 10 minutes at 4°C and washed twice with 500 µL of 80% acetone. Dry pellet was dissolved in sample buffer (Table 2.6), boiled for 5 minutes at 95°C, and then subjected to SDS-PAGE.

2.2.5.2. Sodium dodecyl-sulphate polyacrylamide gel electrophoresis (SDS-PAGE)

Protein samples were mixed with 0.2 volumes of 5x Protein sample buffer (Table 2.6) and heated at 95°C for 5 minutes. Proteins were separated by discontinuous gel electrophoresis (4% stacking gel and 5% or 8% resolving gel). Stacking gels were prepared by adding acrylamide/bis-acrylamide to a final concentration of 4%, to SDS-PAGE stacking buffer (Table 2.6), 0.1% ammonium persulphate (w/v), and 0.1% TEMED (v/v). Resolving gels were prepared by combining acrylamide/bis-acrylamide to an appropriate final concentration, in SDS-PAGE resolving buffer (Table 2.6), 0.1% ammonium persulphate (w/v), and 0.1% TEMED (v/v). Electrophoresis was performed using the Bio-Rad mini-protean III system in SDS-PAGE running buffer (Table 2.6) at 80–140 V. After electrophoresis, the gels were processed for immunoblot analysis, as described below (Section 2.2.5.3).

2.2.5.3. Immunoblot analyses

2.2.5.3.1. Protein transfer

After SDS-PAGE, proteins were transferred from the gels to either 0.45 µm polyvinylidene fluoride (PVDF) or nitrocellulose membranes. For Far-Western blotting analysis, PVDF membranes were used. PVDF membranes were wet with methanol for 10 minutes and then equilibrated in transfer buffer (Table 2.6) for 15 minutes. Protein transfer was performed using a traditional sandwich method and a Mini Trans-Blot^{TM} Electrophoresis Transfer Cell apparatus (Bio-

Rad) in pre-chilled transfer buffer (Table 2.6) at 140 V (or 320 mA) for 2 hours at 4°C or in an ice-filled bucket. Following completion of the transfer, the membranes were air-dried, re-wetted with methanol (not applicable for nitrocellulose membrane), and then blocked in PBS-T or TBS-T (Table 2.6) containing 5% (w/v) skim milk powder for 1 hour at room temperature or overnight at 4°C on a rocking device.

2.2.5.3.2. Immunoblotting

Following the blocking step, the membranes were incubated with primary antibodies in PBS-T or TBS-T containing 5% (w/v) skim milk powder for 1–2 hours at room temperature or overnight at 4°C. RFP-Rdp1 in immunoprecipitates or cell lysates was detected with rabbit anti-Rdp1 (1:500). Immunoprecipitated Sal3-GFP was detected with mouse monoclonal anti-GFP (1:500). β-actin in cell lysates was detected with a mouse monoclonal antibody (Table 2.10). After three 15-minute washes with PBS-T, the membranes were incubated with the secondary antibody in PBS-T containing 5% (w/v) skim milk powder for 40 minutes at room temperature. The membranes were washed three times with PBS-T and then immunoreactive proteins were detected using Supersignal West Pico chemiluminescent substrate (Table 2.5) for 60 seconds, after which they were exposed to Rx film (Table 2.5).

2.2.6. Analysis of protein-protein interactions

2.2.6.1. Ball mill grinding of yeast

Each yeast strain (FY648 containing FLAG-Ago1, Spy1976 FLAG-Clr4, and FY254 [wild-type strain with no FLAG-tagged protein]; Table 2.12) was grown in rich media (1 L) until the OD_{600} reached 1.0. After grinding, this provided ~1.5 g of cell powder for one IP experiment. Cells were pelleted by centrifugation using a JLA 10.5 rotor at 5,000 rpm for 5 minutes at 4°C and washed twice with 200 mL ddH_2O containing Complete™ Protease Inhibitor Cocktail (EDTA-free) (Roche). During the last centrifugation spin, empty 50 mL Falcon tubes were weighed. The tubes and spatulas were placed in a 600 mL glass beaker containing liquid nitrogen. The cell pellets were scooped into 30 mL syringes and slowly discharged into the liquid nitrogen-containing 50 mL tubes to form long spaghetti-like shapes (note: forming clumps or round ball-shapes should be avoided, as they are difficult to grind in the machine). Excess liquid nitrogen from 50 mL Falcon tube was poured off and large strings of frozen cells were broken with a spatula after which they could be immediately ground or stored at -80°C until further use.

In preparation for grinding the frozen cells, a grinding jar (12 mL for 1 L culture), 5 balls, a jar lid, and a spatula were placed into an ice bucket containing liquid nitrogen, for 15 minutes prior to adding the frozen spaghetti cells. It should be noted that the jars should be ~50% full for grinding purposes. Otherwise, virtually no lysis occurs as the grinding balls do not rotate within the jar. Grinding jars containing frozen cells were stacked on the top of one another and the

counterweight of the grinding machine (Retsch PM100) was adjusted to be equal to the weight of the jars. Typically, the frozen cells were ground for 12–20 cycles for 1 minute and 58 seconds per cycle at 400–550 rpm. In between cycles, the jars were placed into ice buckets with liquid nitrogen to keep them cool. Hardened powder on the sides of each jar was scraped off with a spatula. After grinding cycles, the powder was examined under a microscope to monitor cell breakage. Once breakage was verified, the cell powder was transferred to a new, pre-chilled, and pre-weighted 50 ml Falcon tube using pre-cooled aluminum foil. The foil had been pre-weighed so that the cell mass could be calculated. The powder was stored at -80°C for a maximum of 3 days.

2.2.6.2. Immunoprecipitation of FLAG-Ago1

Cell powder (Section 2.2.6.1) was resuspended by vortexing in 2 mL of NP-40 lysis buffer (Table 2.6) per gram of powder and then incubated on ice for 30 minutes with vigorous vortexing every 5 minutes. Complete Protease Inhibitor Cocktail (EDTA-free, Roche) and antiform (1:5000 v/v) were added to the lysis buffer immediately prior to use. Insoluble material was removed by centrifugation at 14,000 x g for 15 minutes at 4°C. Total protein concentrations were determined with either a Quick Start™ Bradford Protein Assay kit (Bio-Rad) or a Pierce BCA Microplate Protein Assay kit (Thermo Scientific) (Table 2.2). Cell lysate containing FLAG-Ago1 was divided into three different tubes. Each sample was pretreated with lambda protein phosphatase (1 hour at 30°C), phosphatase inhibitor (at room temperature), and no treatment, respectively (Peng and

Weisman 2008). During the preparation of cell lysate, 100 µL of Anti-FLAG M2 Magnetic Beads slurry was collected in a new tube on the magnetic separator and equilibrated by washing twice with 10 packed volumes of TBS buffer (Table 2.6). During the course of the washing steps, the end of the pipette tip was cut to reduce damage to the magnetic beads. After washing, the resin was resuspended in 500 µL TBS buffer and divided according to the number of samples tested. The TBS buffer was removed on the magnetic separator. Cell lysate was added to the equilibrated resin beads, and all samples and controls were gently agitated in a roller shaker for 3 hours at 4°C. In order to increase the binding efficiency, the binding step was extended overnight. After binding incubation, the tubes were placed on the magnetic separator to collect the beads, and the supernatant was removed to a new tube and used for IP control. The resin was washed three times with TBS (Table 2.6) at room temperature. The bound FLAG fusion proteins were eluted with 50 µL 0.1 M glycine-HCl (pH 2.5), incubated for 5 minutes at room temperature with gentle shaking or on a rotator, and then neutralized by addition of 5 µl 1 M Tris-base (pH 10). Alternatively, the bound proteins were eluted by boiling in the sample buffer (Table 2.6) for immediate loading on SDS-PAGE and immunoblotting using Anti-FLAG or specific antibodies against the fusion protein, as described in Section 2.2.5.3.

2.2.6.3. Immunoprecipitation of RFP-Rdp1

Immunoprecipitation of RFP-Rdp1 and detection of association with Sal3 by immunoblot analysis was performed by S. Freitag (Queen's University).

Cells (Q4207; Table 2.12) expressing single-copy genome integrated Sal3-GFP expressing from its native promoter (derived from Q2015, (Chua et al. 2002)) and single-copy genome integrated RFP-Rdp1 expressing from *S. cerevisiae* ADH promoter (derived by illegitimate integration at an unknown locus of pAAUN-RFP-Rdp1 in rdp1::kanMX6 ura4:D18 leu1-32 background; Table 2.12) were grown to the mid-logarithmic growth phase at 30°C in a total of 2,000 mL YEA medium. After harvesting cells by centrifugation at 4,150 x g for 16 minutes at 4°C, cells were washed with 5 mL ice-cold modified homogenization buffer (MHB) (Table 2.6) containing Complete Protease Inhibitor Cocktail (EDTA-free) (Roche), 25 mM NaCl, and 1 mM phenylmethanesulfonylfluoride (PMSF), centrifuged again at 664 x g for 5 minutes, and then resuspended in 5 mL of fresh MHB. One minute of mechanical disruption with glass beads (Biospec 5 mm) and a cell disrupter (MiniBeadBeater-8 Cell Disrupter, Biospec) was followed by 1 minute of cooling in ice-water slush. Disruption and cooling cycles were alternated until ~ 90% of the cells were lysed. Lysates were cleared of cell debris by ultracentrifugation (TLA 100.2 rotor, Beckman Optima TL) at 84,688.5 x g for 40 minutes at 4°C. Total protein concentrations were determined with a BioRad Protein Assay kit (Table 2.2). A portion of whole protein extract was mixed with 4x SDS Laemmli loading buffer (0.25 volume) (Table 2.6) and boiled at 100°C for 5 minutes.

To eliminate non-specific binding of *S. pombe* proteins to Protein G Sepharose-beads (GE), 100 µL of the beads was washed three times with 1 mL MHB and added to the remaining protein lysate. Extracts were then incubated in

an end-over-end aliquot mixer for 1 hour at 4°C. Beads were removed by centrifugation and the remaining lysate was divided into four equal aliquots. Lysates were incubated overnight in the end-over-end aliquot mixer at 4°C after addition of either 15 µL of anti-RdRP (rabbit) antibody (0.2 µg/µL; polyclonal; Table 2.10), 15 µL anti-GFP (mouse) antibody (0.2 µg/µL; monoclonal; Table 2.10), or controls containing no antibody. MHB-washed Sepharose-G-beads (120 µL, 1:1 bead and buffer slurry) was added to each aliquot, followed by 2 hours of incubation at 4°C in the end-over-end aliquot mixer. Beads were collected by brief centrifugation at 664 x g for 1 minute and then washed six times with 1 mL MHB. Protein complexes were released by incubation with 40 µL of 0.2 M glycine (pH 2.2) for 15 minutes at 4°C, then the pH was neutralized by adding saturated Tris (pH 10). After the beads were removed by brief centrifugation, supernatants were mixed with the 4x SDS Laemmli loading buffer (0.25 volume) (Table 2.6) and boiled at 100°C for 5 minutes.

2.2.6.4. Far Western Blot

Yeast strains with or without *sal3* were grown in liquid culture until the OD_{600} reached 1.0. Cell lysates were prepared via methods described in Section 2.2.5.1. The protein samples were resolved by discontinuous gel electrophoresis, as described in Section 2.2.5.2. The samples were then transferred to a PVDF membrane (Section 2.2.5.3.1). Following transfer, the membrane was stained with Ponceau S (0.1%) to check if proteins were transferred from the gel to the membrane. The proteins on the membrane were denatured and renatured in AC

buffer (Table 2.6) by gradually reducing the guanidine-HCl concentration (6 M, 3 M, 1 M, 0.1 M, and 0 M). Proteins were denatured by incubating the membrane in the AC buffer containing 6 M guanidine-HCl for 30 min at room temperature, then washed with the AC buffer containing 3 M guanidine-HCl for 30 min at room temperature. This was followed by washing with the AC buffer containing 0.1 M and the guanidine-HCl-free AC buffer at 4°C for 30 min and overnight, respectively. The membrane was blocked with 5% milk in the PBS-T buffer (Table 2.6) for 1 hour at room temperature. During the separation of prey protein by SDS-PAGE, bait proteins were purified from each yeast strain expressing GFP-Rdp1, GFP, and no GFP by using Chromotek-GFP-Trap® (Table 2.1). The membrane containing prey proteins was incubated with purified bait proteins in 5 mL of protein-binding buffer (Table 2.6) overnight at 4°C, then washed off unbound bait proteins with PBS-T buffer (Table 2.6) three times, each for 10 minutes followed by immunoblotting analysis, as described in Section 2.2.5.3.

2.2.7. RNA techniques

2.2.7.1. Isolation of *S. pombe* RNA

Yeast cell pellets (100 µL) were resuspended in 1 mL of either TRIzol or TRI Reagent (Invitrogen). Acid-washed glass beads (Sigma) were added to samples (30% volume), which were then subjected to two cycles of homogenization at 4°C by bead beating (MiniBeadbeater-8, BioSpec Products). Samples were incubated for 5 minutes at room temperature, then underwent the addition of 0.2 mL chloroform in the hood. Tubes were mixed vigorously by hand

for 15 seconds, incubated at room temperature for 3 minutes, and centrifuged at 12,000 x g for 15 minutes at 4°C. The aqueous phase (400 µL) was transferred to fresh tubes and isopropanol (500 µL) was added to precipitate total RNA. Samples were incubated at room temperature for 10 minutes, then centrifuged at 12,000 x g for 10 minutes at 4°C. The RNA pellet was washed once with 1 mL of 75% ethanol and centrifuged at 7,500 x g for 5 minutes at 4°C. The RNA pellets were air dried and then dissolved in 50 µL of RNase-free water at 55–60°C for 10 minutes. Samples were stored at -80°C until further use.

2.2.7.2. Reverse transcriptase-polymerase chain reaction (RT-PCR)

Before the RT-PCR reaction, RNA samples were treated with amplification-grade DNaseI (Invitrogen) as per the manufacturer's recommendations. The DNase-treated RNA samples were used as templates for RT-PCR reactions. SuperScriptIII Reverse Transcriptase system (Invitrogen, Table 2.2) and the primers Act-F-qPCR, Act-R-qPCR, dg-For, and dg-Rev (Table 2.8) were used for cDNA generation. Before adding reverse transcriptase, the DNase-treated templates were treated with RNase Out (Invitrogen) as per the manufacturer's recommendations.

2.2.7.3. Real-time quantitative PCR (qPCR)

Relative levels of centromeric transcripts compared to actin mRNA were determined by qPCR (40 cycles) using the PerfeCTa™ SYBR® Green SuperMix, UNG, Low Rox (Quanta BIOSCIENCES™) assay mix in a STRATAGENE

MX3005P™ cycler (Table 2.5). Each sample was run in triplicate to control for variation. To ensure the qPCR reaction specificity and lack of genomic DNA contamination, no reverse transcriptase (NRT) and no template control (NTC) samples were included in these assays.

2.2.7.4. Analysis of qPCR data

Quantitative PCR reaction efficiency was monitored by a standard curve, which ran in triplicate in each assay. Only a linear standard curve fit with an R squared (Rsq) value > 0.985 was accepted for quantification analysis. Because a linear standard curve implies that efficiency of amplification is consistent at varying template concentrations, the Rsq value, which denotes the linearity of standard curve, should be very close to 1 (> 0.985). In addition, a dissociation curve was used to determine if anything other than the gene of interest was amplified in the qPCR reaction. The temperature range used was 55°C to 95°C. If secondary peaks are present in the NTC control wells, it may indicate primer dimer formation in the reaction. qPCR data from reactions exhibiting primer dimers were excluded from further analysis. Data were analyzed with the two standard curve method (Livak and Schmittgen 2001) to quantify the levels of pericentromeric transcripts (as determined by *dg* specific primers) relative to the β-actin control. The comparison of wild-type and the *dg* forward- and reverse-transcript levels allowed us to determine the effect of Sal3 or Cut7 activities in TGS and PTGS defects, respectively.

CHAPTER 3:
The karyopherin Sal3 is required for nuclear import of the core RNA interference pathway protein Rdp1

A version of this chapter has been published in
"Park J, Freitag SI, Young PG, Hobman TC. (2012). The karyopherin Sal3 is required for nuclear import of the core RNA interference pathway protein Rdp1. *Traffic*. 13(4):520-531."

3.1. Rationale and hypothesis

In the fission yeast *S. pombe*, Ago1, Dcr1, and Rdp1 are required for TGS and PTGS. Deletion of any one of the cognate genes (*ago1, dcr1*, or *rdp1*) impairs these processes (Sugiyama et al. 2005). Previous studies from our laboratory showed that most Rdp1 is primarily localized in the nucleus, but it is also associated with motile cytoplasmic puncta; whereas the bulk of Ago1 and Dcr1 is primarily cytoplasmic (Carmichael et al. 2006). Since Rdp1 functions in both TGS and PTGS, I hypothesized that the targeting of Rdp1 into the nucleus is required for TGS.

Currently, nothing is known about the nuclear trafficking pathway of Rdp1, although a number of studies have recently been published discussing the association of Argonaute proteins with nuclear events (Weinmann et al. 2009; Guang et al. 2008). For example, Weinmann *et al*. reported that the karyopherin importin 8 is required for the nuclear import of mammalian Argonaute proteins and miRNA-dependent targeting of Argonautes to mRNAs in the cytoplasm (Weinmann et al. 2009). Guang *et al*. showed that a nuclear localization signal in the Argonaute protein NRDE-3 of *C. elegans* is required for the transport of siRNAs, which are generated by the action of RDRP on cytoplasmic mRNA templates. However, the factors that govern the transport of NRDE-3 or other RNAi components are not known.

Transport between the nucleus and cytoplasm through nuclear pores is a highly regulated process. Although ions, metabolites, and small molecules can passively diffuse across nuclear pores, most macromolecules over 40 kDa are

selectively transported via active mechanisms [reviewed in (Chook and Suel 2011; O'Reilly et al. 2011; Terry et al. 2007; Lusk et al. 2004; Fried and Kutay 2003; Weis 2003), also refer to Section 1.4.2.2]. Active transport of most macromolecules is mediated by β-karyopherin family of nuclear transport receptors and small guanosine triphosphatase (GTPase) Ran. Because of its large size (139.4 kDa), Rdp1 cannot passively diffuse across nuclear pores and must therefore utilize nuclear transport machinery. With this in mind, I sought to determine the role of Rdp1 import to the nucleus on the RNAi mechanism in *S. pombe*. First, I investigated which karyopherin(s) is required for Rdp1 nuclear localization. Second, I examined how TGS and PTGS are affected by the localization of Rdp1.

3.2. Results

3.2.1. Sal3 is important for the nuclear import of Rdp1

Based on our previous studies regarding Rdp1 localization (Carmichael et al. 2006), it is assumed that the majority of Rdp1 in the nucleus functions as part of the RDRC, which is associated with nascent centromeric transcripts. As discussed in Section 1.2.3, the primary function of Rdp1 is the generation of dsRNAs which are critical for the RNAi process. The dsRNAs are then processed by Dcr1 into siRNAs that direct TGS and consequent heterochromatin formation [reviewed in (Djupedal and Ekwall 2009), also refer to Section 1.3.1.1].

To identify which karyopherin(s) is required for the nuclear import of Rdp1, the protein was N-terminally tagged with cherry RFP or GFP and its

localization was monitored in a subset of karyopherin null mutants and wild-type yeast. There are 13 karyopherins encoded by *S. pombe,* the majority of which are not essential for viability (Chen et al. 2004). I first chose to examine whether the importin-β3 homologue Sal3 (Chua et al. 2002) was required for the nuclear localization of Rdp1. I selected this protein because a previous study from our laboratory revealed an intriguing albeit indirect link between this karyopherin and the RNAi apparatus (Stoica et al. 2006). It was shown that the Ago1 truncation mutant impaired the nuclear import of Cdc25, which is well-known cargo of the Sal3 karyopherin (Chua et al. 2002).

A plasmid encoding green fluorescent protein (GFP)-tagged Rdp1 was transformed into wild-type, Δ*rdp1,* and *sal3* null mutants. As shown in Figure 3.1A, GFP-Rdp1 was concentrated in the nuclei of wild-type and Δ*rdp1 S. pombe*. In contrast, nuclear accumulation of GFP-Rdp1 was rarely observed in two different *sal3* null mutants [a targeted gene deletion strain (Δ*sal3*) and a point mutant (*sal3-33*)]. In the majority of cells in *sal3* mutants, GFP-Rdp1 was mislocalized and exhibited the diffused pattern in the cytoplasm.

I quantified the percentage of cells with distinct Rdp1 nuclear localization in wild-type and karyopherin null strains (Figure 3.1B). For each strain, at least 100 fluorescent Rdp1-expressing cells from three independent experiments were assessed as exhibiting only nuclear localization, nuclear and cytoplasmic localization, or cytoplasmic localization. It should also be noted that there was variability among the experiments. As shown in Figure 3.1B, some of the nuclear localization of Rdp1 was evident in the *sal3* mutants, but this was much lower

than in the wild-type strain. One interpretation of this result is that additional transport factors are involved in Rdp1 nuclear import. Indeed, redundancy is often observed in the nuclear import pathways (Fried and Kutay 2003). For example, histone proteins H2A and H2B require at least five different importin proteins for their nuclear transport both *in vitro* (Muhlhausser et al. 2001) and *in vivo* (Mosammaparast et al. 2001).

Next, I tested whether the ectopic expression of Sal3 karyopherin rescues Rdp1 nuclear localization. My data showed that the plasmid-based expression of Sal3 restored the localization of GFP-Rdp1 to the nucleus in the *sal3* mutants (Figure 3.1C). This indicates that Sal3 funciton is involved in GFP-Rdp1 targeting to the nucleus. The quantification data showed (Figure 3.1B) that the rescuing level was also significantly increased, though Rdp1 nuclear accumulation was not increased to the level of the wild-type.

In some cases, the fluorescent Rdp1 signal in *sal3* mutants was less intense (Figure 3.1A and C), which may reflect the diffused cytoplasmic localization. To examine if the difference in the signal intensity was related to the level of protein expression, I performed western blotting to determine the relative levels of Rdp1 protein in wild-type and *sal3* mutants (Figure 3.1D). Yeast lysates were subjected to immunoblot analyses with rabbit-Rdp1 and mouse anti-β-actin (Table 2.10). Although the level of Rdp1 protein was not consistant in all stranis, the level of Rdp1 was not dramatically altered in the *sal3* mutants (Figure 3.1D). For unknown reasons, the proportion of yeast cells containing plasmid encoding GFP-tagged Rdp1 transformed into wild-type, Δ*rdp1*, and *sal3* null mutants

varied from experiment to experiment. One possibility is that the difference in the signal intensities of the fluorescent Rdp1 is due to the instability of the proteins or the proteolytic cleavage of the fluorescent epitope tag. Further quantification assays would be needed to provide conclusive data. However, it is evident that Rdp1 proteins were detected in all transformed yeast strains used in the microscope analyses; wild-type, Δ*rdp1*, and *sal3* mutants transformed with GFP-Rdp1. Thus it is likely that the RNAi defects associated with *sal3* mutants can be explained by the loss of Rdp1 nuclear targeting.

Figure 3.1. Sal3 is required for nuclear import of Rdp1. A. Localization of GFP-Rdp1 in wild-type (WT), Δ*rdp1*, and two *sal3* null strains (Δ*sal3* and *sal3-33*). Yeasts were transformed with a plasmid encoding GFP-Rdp1 and grown in liquid culture to log phase before fixation and staining with DAPI (1 μg/mL). The localizations of the proteins were viewed by fluorescence microscopy. **B.** Quantification of microscopic data. For each sample, at least 100 cells from three independent experiments were counted. Standard error bars are shown. **C.** The null strain *sal3-33* expressing GFP-Rdp1 was transformed with plasmids encoding Sal3 (pSal3) or empty vector pRep81 (V). Cells were processed for fluorescence microscopy. Bars = 3 μm. **D.** Relative levels of Rdp1 protein in *sal3* mutants. Yeast lysates were subjected to immunoblot analyses with rabbit anti-Rdp1 and mouse anti-β-actin. Where indicated, yeast strains were transformed with plasmids encoding GFP-Rdp1 (+pRdp1), Sal3 (+pSal3), or vector alone (+V).

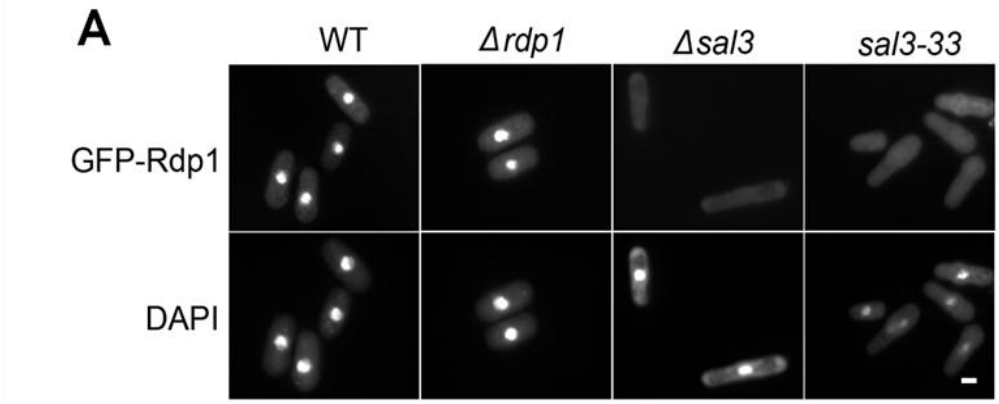
A
WT
Δrdp1
Δsal3
sal3-33
GFP-Rdp1
DAPI

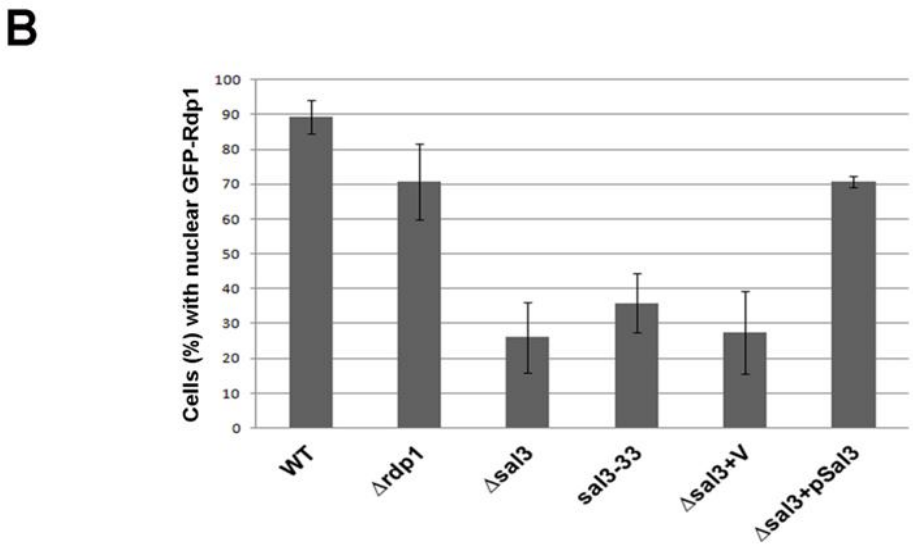
B
Cells (%) with nuclear GFP-Rdp1
100
90
80
70
60
50
40
30
20
10
0
WT
Δrdp1
Δsal3
sal3-33
Δsal3+V
Δsal3+pSal3

C

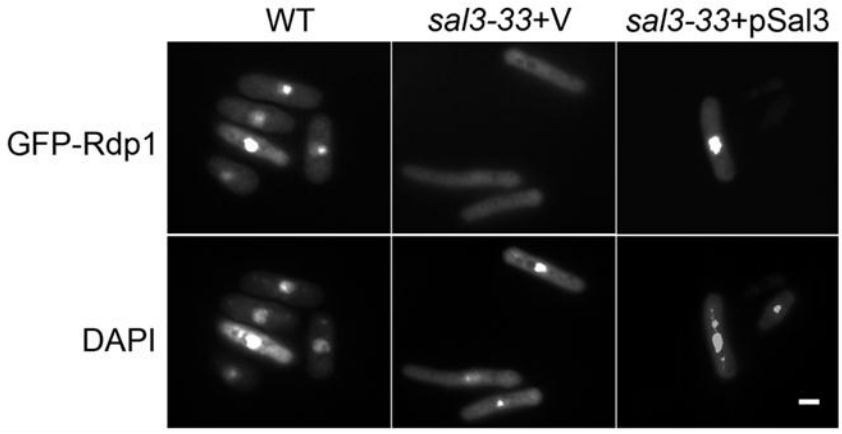
WT
sal3-33+V
sal3-33+pSal3
GFP-Rdp1
DAPI

D

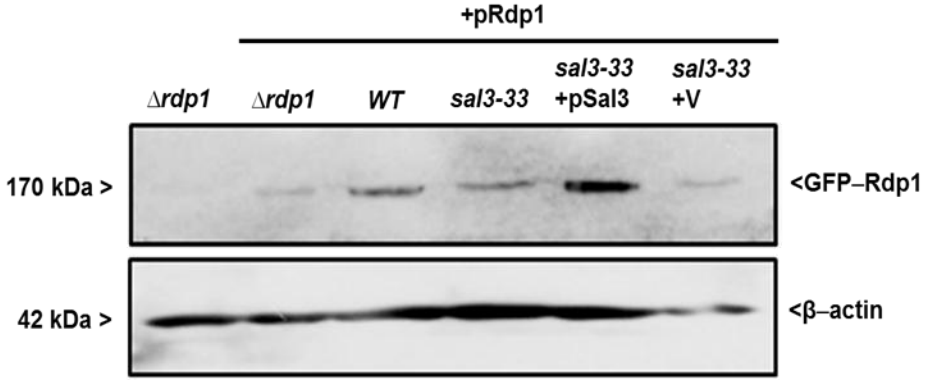
+pRdp1
Δrdp1
Δrdp1
WT
sal3-33
sal3-33 +pSal3
sal3-33 +V
170 kDa >
<GFP–Rdp1
42 kDa >
<β–actin

3.2.2. Kap111, Kap113, Kap114, and Kap123 are not required for the nuclear import of RFP-Rdp1

As a control, localization of RFP-Rdp1 was assessed in four other strains that lacked genes encoding nuclear import factors: Kap111, Kap123, Kap113, and Kap114 (Figure 3.2). These strains were chosen as my experimental controls because, similar to Sal3, they belong to the importin-β group of karyopherins (Mosammaparast and Pemberton 2004). In addition, these mutations are not lethal for *S. pombe*. In all four of these mutant strains, the bulk of Rdp1 was localized to the nucleus, as seen in wild-type *S. pombe* (Figure 3.2). Taken together, these results suggest that karyopherin Sal3 is important for the nuclear localization of Rdp1.

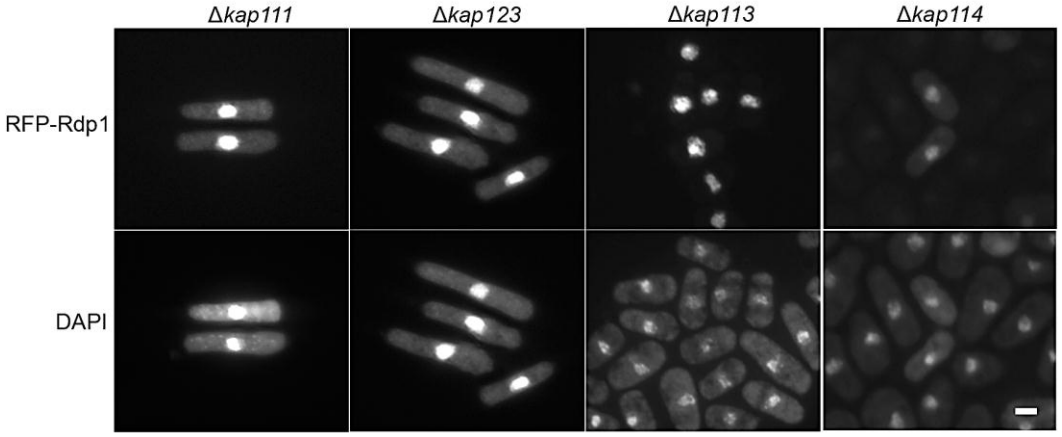

Figure 3.2. Karyopherins Kap111, Kap113, Kap114, and Kap123 are not required for nuclear import of RFP-Rdp1. Δ*kap111*, Δ*kap123*, Δ*kap113*, and Δ*kap114* strains were transformed with a plasmid encoding RFP-Rdp1. Cells were grown in liquid culture until log phase before fixation and staining with DAPI (1 µg/mL). The localizations of the proteins were viewed by fluorescence microscopy. Bar = 3 µm.

3.2.3. Rdp1 forms a complex with karyopherin Sal3

Next, I examined whether the karyopherin Sal3 forms a stable complex with Rdp1, as many known karyopherin-β family members bind directly to their substrates (Terry et al. 2007). A coimmunoprecipitation (co-IP) assay was employed to examine interaction between Rdp1 and Sal3. An illegitimately integrated strain was created for the co-IP assay (refer to Sections 2.2.1.4 and 2.2.6.3). A red fluorescent protein (RFP)-tagged Rdp1 was randomly integrated into the genome of an *S. pombe* strain encoding GFP-tagged Sal3 (Chua et al. 2002).

Preceding the co-IP assays, the localization signals of the two fluorescent labeled proteins were examined (Figure 3.3A). As shown in Figure 3.3A, the localization signals of GFP-Sal3 and RFP-Rdp1 overlapped extensively in the nucleus. Next, *S. pombe* strain expressing GFP-Sal3 and RFP-Rdp1 was grown to mid-logarithmic growth phase after which cell lysates were prepared. The data from the reciprocal co-IP immunoblot experiments indicate that Sal3-GFP form a stable complex with RFP-Rdp1 (Figure 3.3B). Although we cannot assess whether or not Rdp1 interacts directly with Sal3, these data suggest that Rdp1 may be another cargo for Sal3 karyopherin.

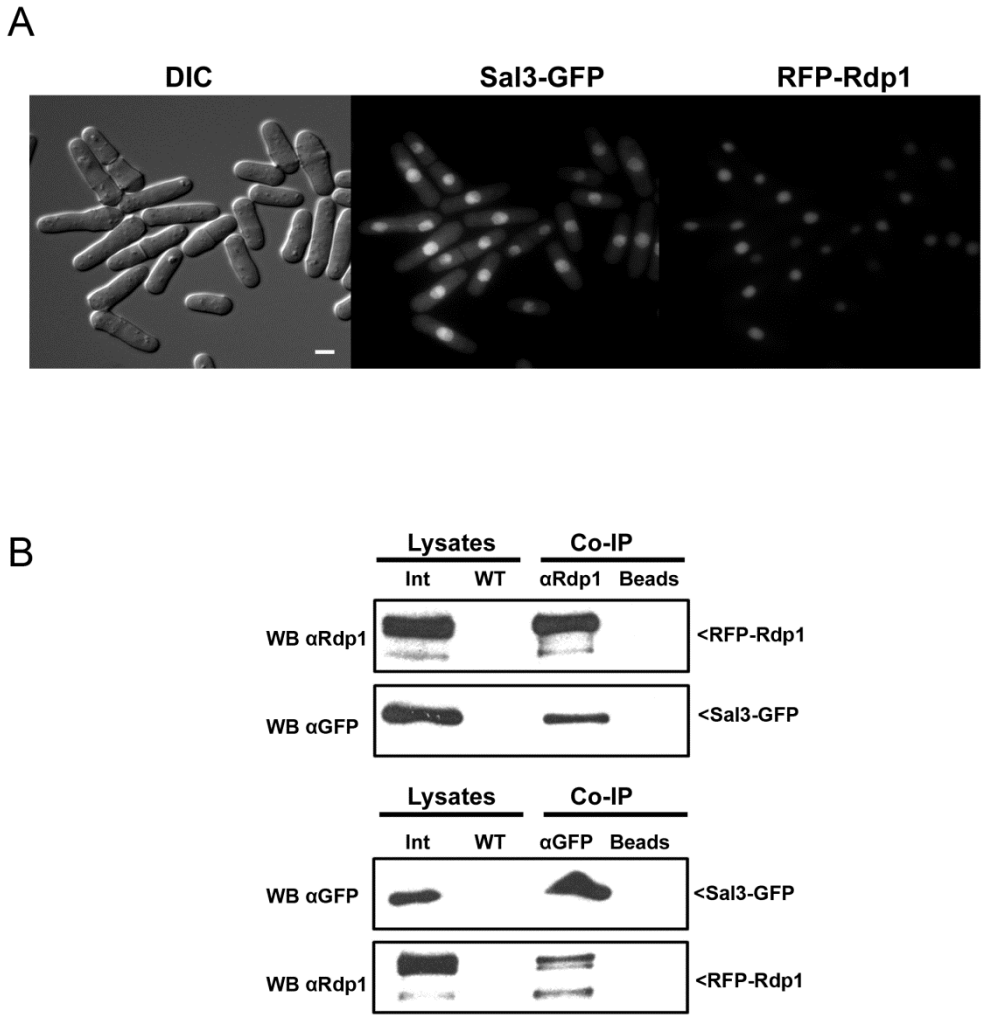

Figure 3.3. Rdp1 forms a complex with Sal3. A. A pool of RFP-Rdp1 colocalizes with Sal3-GFP in nuclei. DIC (differential interference contrast) image is shown. Scale bar = 3 µm. **B.** Total cell lysates (20 µg) prepared from wild-type (WT) or a strain containing integrated RFP-Rdp1 and Sal3-GFP cassettes (Int) were subjected to SDS-PAGE and western blotting (WB) with mouse anti-GFP or rabbit anti-Rdp1. Lysate from the RFP-Rdp1 and Sal3-GFP integrant strains was also immunoprecipitated with anti-GFP, anti-Rdp1, or no primary antibody (Beads) and then WB with antibodies to GFP or Rdp1 (courtesy of S. Freitag).

3.2.4. The levels of pericentromeric transcripts are increased in *sal3* mutants

Rdp1 is a major component of the RDRC in the nucleus of fission yeast (Motamedi et al. 2004). Together with RITS, RDRC mediates the silencing of centromeric loci (Sugiyama et al. 2005). Accordingly, I predicted that blocking the nuclear import of Rdp1 would result in defects in TGS, but not in PTGS. Because PTGS is thought to occur in the cytoplasm, it should not be significantly affected by a lack of Rdp1 targeting to the nucleus.

RNAi mediated heterochromatin formation has been studied extensively in *S. pombe* (Volpe et al. 2002) (refer to Section 1.3.1.1). Fission yeast chromosomes contain extensive heterochromatic regions that are associated with underlying repetitive DNA elements at centromeres (Grewal 2010; Pidoux and Allshire 2004). The centromeres consist of central cores that are composed of non-repeat sequences flanked by *imr* and *otr* (refer to Section 1.3.1.1.1). The *otr* contains a single copy of *dg* and *dh* repeats, which are transcribed in both directions to produce forward and reverse RNA transcripts (Moazed et al. 2006). These transcripts form dsRNAs that are processed by Dcr1 to generate siRNAs and that trigger RNAi (Volpe et al. 2002).

Although the RNAi machinery is essential for repressing the levels of both forward and reverse transcripts, the regulation of these transcripts is different. Transcription of forward transcripts is negatively regulated by a Swi6-dependent mechanism. The processed dsRNAs (and resulting siRNAs) recruit HMT Clr4, thereby promoting H3K9me and allowing the binding of heterochromatin protein Swi6. This leads to a block in forward transcription (refer to Figure 1.4). The

reverse transcripts are constantly transcribed, but are efficiently degraded through an RNAi-dependent process at the post-transcriptional level. Therefore, both forward and reverse transcripts do not accumulate to appreciable amounts in wild-type *S. pombe* (Volpe et al. 2002). However, loss of activity of the major RNAi proteins (Ago1, Dcr1, and Rdp1) results in the aberrant accumulation of long dsRNAs transcribed from centromeric repeats (Volpe et al. 2002).

I performed real-time quantitative PCR (qPCR) to examine whether the inability to target Rdp1 to the nucleus results in changes in the level of these centromeric transcripts. By using specific primers designed to amplify centromeric DNA repeats (Volpe et al. 2002), I measured the relative levels of centromeric transcripts in wild-type and mutant *S. pombe* strains. As a positive control for the loss of RNAi, I used a Δ*rdp1* mutant. Results from qPCR showed that relative levels of forward and reverse centromeric transcripts were significantly higher in the Δ*rdp1* mutant compared to the wild-type strain (Figure 3.4). TGS was more impaired than PTGS by a lack of Rdp1 activity. Specifically, the level of forward transcripts was >1,000-fold higher in Δ*rdp1* mutants, whereas reverse transcripts were increased by >70-fold.

I examined TGS and PTGS activity in two different *sal3* null mutants. Compared to wild-type, the levels of both forward and reverse centromeric transcripts were significantly higher in the *sal3* mutant strains. On average, forward transcripts were 20-fold higher in the *sal3* mutants as compared to the wild-type strain; whereas reverse transcripts were increased by ~12-fold. This

indicates that, similar to the RNAi mutant Δ*rdp1*, TGS was more affected than PTGS in the *sal3* mutants.

As controls, I measured forward and reverse transcripts in *kap111, kap123, imp8, kap113,* and *kap114* null strains. In both Δ*kap111* and Δ*kap123*, TGS was slightly impaired. The possibility that Kap111 and Kap123 are required for nuclear import of other factors that have minor functions in RNAi pathways cannot be rule out at this point. However, in all other strains, neither TGS nor PTGS was significantly different from wild-type. Together, these data suggest that the Sal3-dependent nuclear import of Rdp1 is important for the transcriptional and post-transcriptional silencing of the centromeric transcripts in *S. pombe*.

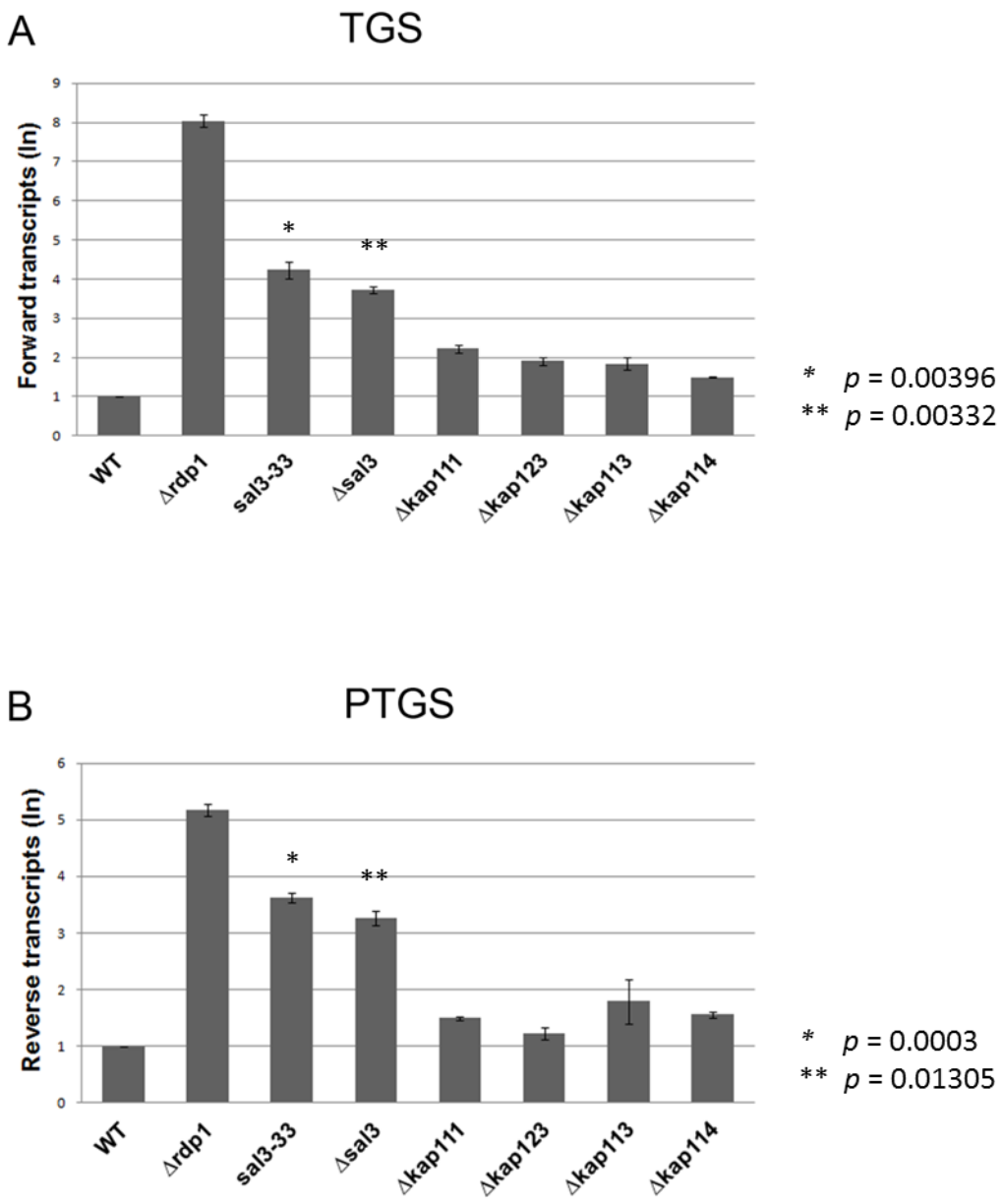

Figure 3.4. Sal3 is important for silencing centromeric transcripts. Total RNA extracted from the indicated strains was subjected to reverse transcription and then real-time quantitative PCR. Levels of forward and reverse centromeric transcripts were normalized to levels of actin transcripts. For controls, the levels of centromeric transcripts were determined in wild-type (WT), Δ*rdp1*, Δ*kap111*, Δ*kap113*, Δ*kap114*, and Δ*kap123* strains. **A.** The relative levels of forward centromeric transcripts, which are regulated by transcriptional gene silencing (TGS), are indicated. **B.** The relative levels of reverse centromeric transcripts, which are regulated by post-transcriptional gene silencing (PTGS), are indicated. *p* values are indicated (samples were compared to the WT control). $n = 3$. (Note: *y*-axis is in natural log [ln] scale).

3.2.5. *sal3* mutants are sensitive to the microtubule poison thiabendazole

As described above, previous work from Volpe *et al*. showed that the RNAi machinery is involved in the formation and maintenance of heterochromatin in *S. pombe* (Volpe et al. 2002) (refer to Section 1.3.1.1.2). Loss of genes encoding RNAi proteins results in the aberrant accumulation of complementary transcripts from centromeric heterochromatic repeats and the consequent loss of H3K9me, transcriptional derepression of centromeric loci, and impairment of centromere function (Sugiyama et al. 2005; Volpe et al. 2003; Volpe et al. 2002). As a result, the loss of Rdp1 activity or other core RNAi proteins, such as Ago1 and Dcr1, results in chromosome segregation defects (Volpe et al. 2003). Accordingly, RNAi mutants are extremely sensitive to microtubule destabilizing drugs, such as thiabendazole (TBZ).

In order to determine if Rdp1 nuclear import into the nucleus is important for RNAi-dependent transcriptional gene silencing, I performed another well-described gene silencing assay for *S. pombe*: a TBZ sensitivity assay. Wild-type, *sal3,* and RNAi mutant strains of *S. pombe* were plated onto media containing various concentrations of TBZ, and relative growth rates were determined. Compared to wild-type and RNAi mutant Δ*rdp1* strains, *sal3* mutants displayed an intermediate sensitivity to TBZ (Figure 3.5A). Importantly, plasmid-driven ectopic expression of Sal3 rescued the TBZ-sensitivity of *sal3* mutant strains (Figure 3.5C).

As controls, I tested the sensitivity of other karyopherin mutants. Similar to wild-type yeast, strains that lacked *kap111, kap123, kap113,* and *kap114* activity were not sensitive to TBZ (Figures 3.5A and B). In fact, for unknown

reasons, the mutant strain lacking *kap113* was more resistant to the drug than wild-type *S. pombe*. Together, these data may suggest that the TBZ sensitivity of *sal3* mutants is not due to general defects in nuclear import.

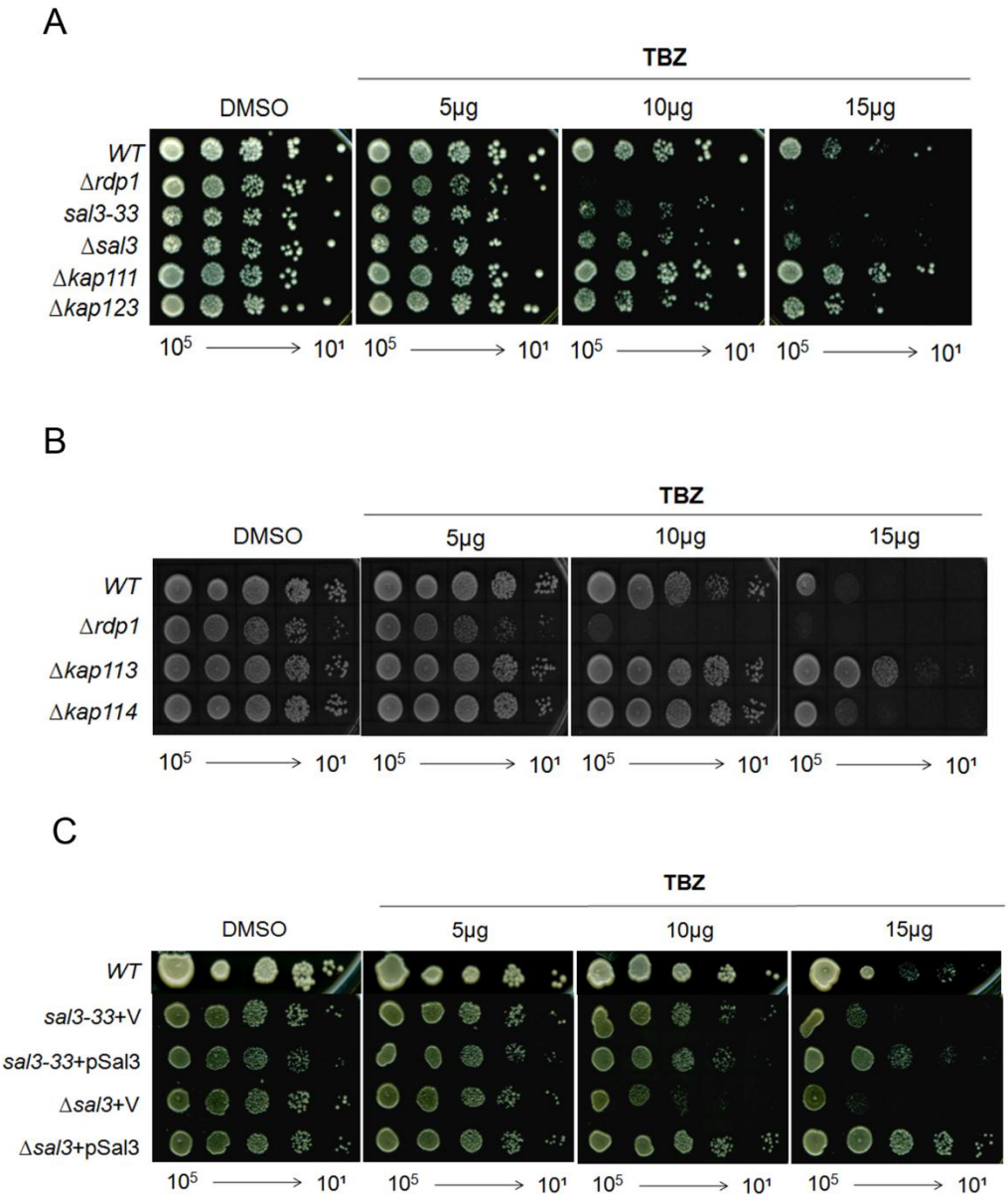

Figure 3.5. *sal3* mutants are sensitive to the microtubule poison thiabendazole (TBZ). A and **B.** Ten-fold dilutions of wild-type (WT), Δ*rdp1*, Δ*sal3*, *sal3-33*, Δ*kap111*, Δ*kap123*, Δ*kap113*, and Δ*kap114* were spotted onto media containing TBZ (5–15 µg/mL) or solvent (DMSO). Plates were incubated at 30°C for 2–3 days. **C.** *sal3* null mutants harboring the vector pRep81 (V) or pRep81-Sal3 (pSal3) were spotted onto uracil-deficient media containing TBZ or DMSO. Cultures were incubated at 30°C for 3–5 days.

3.2.6. *sal3* mutants exhibit chromosome segregation defects

I performed a direct assay to determine whether chromosome segregation defects were higher in *sal3* mutants. As described, the loss of Rdp1 activity or other core RNAi proteins, Dcr1 and Ago1, results in mis-segregation of chromosomes in a large proportion (30%) of cells (Volpe et al. 2003). Wild-type, *sal3,* and RNAi mutant cells were grown at a permissive temperature, then quickly transferred to 18°C for 6 hours to decrease the speed of cell division (Pidoux et al. 2000). Cells were fixed with ethanol and then stained with 4', 6-diamidino-2-phenylindole (DAPI) (Forsburg and Rhind 2006). I viewed the cells by fluorescence microscopy and counted the percentage of dividing cells with lagging chromosomes.

As shown in Figure 3.6A, RNAi and *sal3* null mutant strains exhibited aberrant chromosome segregation defects during cell division. In contrast, most of the wild-type cells and two other karyopherin mutants lacking *kap111* and *kap123* did not show such defects. I quantified the data from these experiments; the results are shown in Figure 3.6B. Similar to a previous study (Volpe et al. 2003), an average of 29% of the RNAi mutant Δ*ago1* and 3.5% of wild-type cells exhibited lagging chromosomes during cell division. The *sal3* mutants exhibited an intermediate proportion of lagging chromosomes at 14%, on average. As controls, I quantified the proportion of lagging chromosomes in two other karyopherin mutants lacking *kap111* and *kap123*. In these mutants, chromosomal segregation defects were slightly higher than in wild-type, but these differences were not significant.

I also characterized the most abundant phenotypes of the chromosome segregation defects in the *sal3* mutants. Previously, Pidoux *et al*. showed several classes of lagging chromosomes in mutant strains with defective chromosome segregation (Pidoux et al. 2000). Accordingly, I compared the phenotypes detected in *sal3* with those reported in the previous study (Pidoux et al. 2000). I found that most *sal3* mutants exhibit uneven segregation or that the *sal3* chromosome often fails to move toward either pole (Figure 3.6A arrows in Δ*sal3* and *sal3-33*).

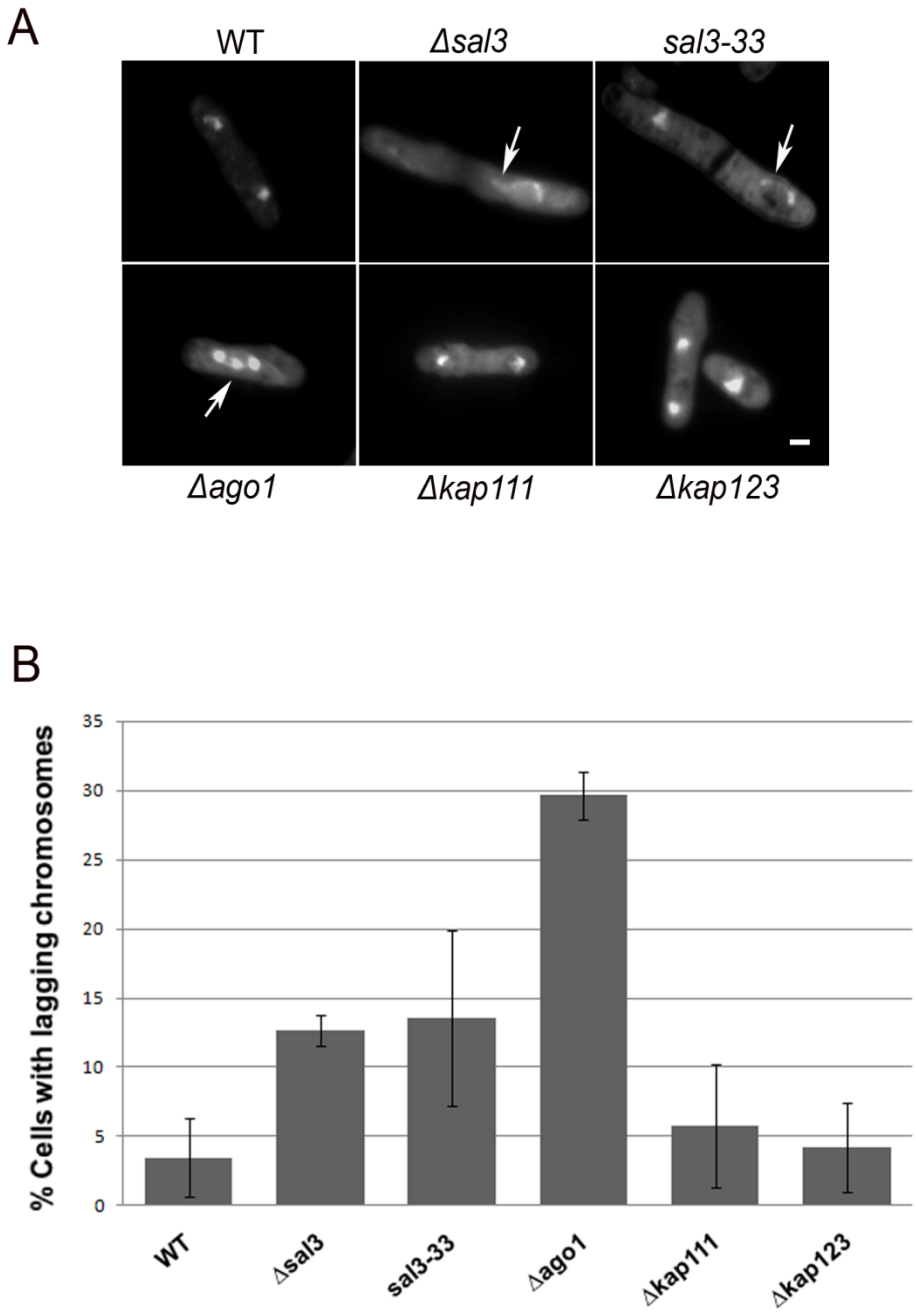

Figure 3.6. *sal3* mutants exhibit chromosome segregation defects. A. Wild-type (WT), *ago1*, *sal3*, *kap111*, and *kap123* null mutant strains were grown at 30°C until reaching log phase, after which they were shifted to 18°C for 6 hours. Cells were fixed and stained with DAPI (1 µg/mL) and examined by fluorescence microscopy. Scale bar = 3 µm. **B.** The percentages of dividing cells with lagging chromosomes were determined for wild-type and mutant strains. Standard error bars are shown. $n = 3$.

3.2.7. Sal3-independent nuclear import of Rdp1 rescues RNAi defects

As mentioned in Section 3.2.1, Sal3 is required for the nuclear import of other critical cargo proteins, including the mitotic regulator phosphatase Cdc25 (Chua et al. 2002). Accordingly, it was important to determine whether nuclear import of Rdp1 by a non-Sal3-dependent mechanism could rescue the RNAi defects in *sal3* mutants. To enable Sal3-independent nuclear import of Rdp1, I constructed a plasmid in which the SV40 large T antigen nuclear localization signal (NLS) (Kalderon et al. 1984) was fused to the carboxyl-terminus of the Rdp1 protein. *sal3* null mutants were transformed with this plasmid and the cells were examined by fluorescence microscopy.

Fluorescence microscopic analyses revealed that the fusion of SV40-NLS to the Rdp1 moderately rescued the nuclear import of Rdp1 in *sal3* null mutants (Figure 3.7 arrows). Similarly, results from qPCR assays showed that expression of the SV40-NLS-containing Rdp1 efficiently rescued the TGS and PTGS defects of the *sal3-33* strain (Figures 3.8A and B). Interestingly, expression of the fusion protein Rdp1-SV40-NLS appeared to suppress centromeric transcript levels below that of those found in wild-type *S. pombe*. These results were at first puzzling because the nuclear localization of Rdp1-SV40-NLS was not as distinct as in wild-type cells, as shown in Figure 3.1A. However, subsequent investigation revealed that compared to non-transformed wild-type *S. pombe*, the levels of centromeric transcripts were higher in wild-type *S. pombe* that were transformed with plasmid vector alone. The reason for this is not clear, but it provides a plausible explanation as to why the expression of the Rdp1-SV40-NLS construct

appears to suppress centromeric transcripts to such low levels, below that of those found in wild-type *S. pombe* (Figures 3.7B and C). One possibility is that because the plasmid encodes different promoter and origin of replication than *S. pombe,* expression of plasmid can somehow afftect the growth condition, altering the profile of the cell transcription. In addition, the wild-type *S. pombe* cells that were transformed with plasmid vector alone were grown in different media than media for non-transformed wild-type *S. pombe*.

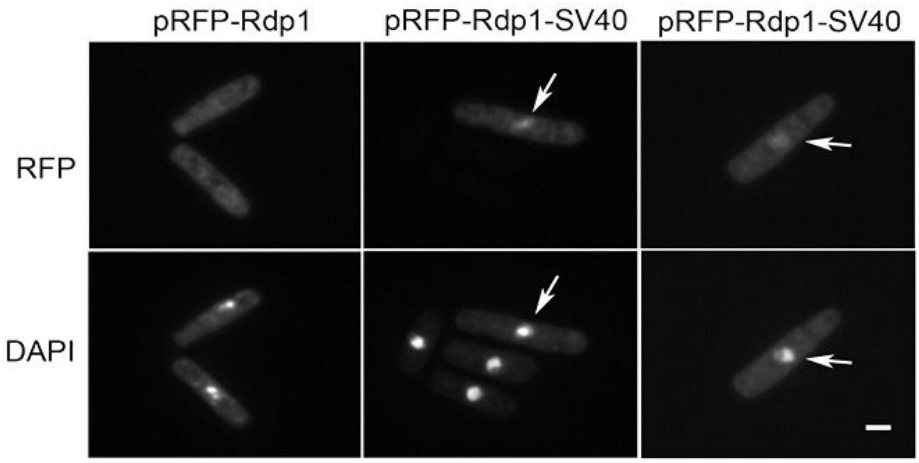

Figure 3.7. Sal3-independent nuclear import of Rdp1 rescues the protein targeting to the nucleus. Plasmids encoding RFP fused to Rdp1 (pRFP-Rdp1) or a modified version of Rdp1 containing the SV40-NLS (pRFP-Rdp1-SV40) were transformed into *sal3* null strains. The localizations of the proteins were monitored by fluorescence microscopy. Nuclear DNA was stained with DAPI (1 µg/mL). Bar = 3 µm. Arrows indicate localization of Rdp1 in the nucleus.

Figure 3.8. Sal3-independent nuclear import of Rdp1 rescues RNAi and chromosome segregation defects A, B. Pericentric transcript levels were decreased in a *sal3* mutant that expressed an SV40-NLS-containing Rdp1 (Rdp1-SV40), but not when expressing Rdp1 or vector alone (V). Total RNA was extracted from *sal3* null strains containing vector alone, RFP-Rdp1, and RFP-Rdp1-SV40-NLS. Samples were subjected to real-time quantitative PCR and levels of forward and reverse centromeric transcripts were normalized to actin transcripts. (Note: *y*-axis is in natural log [ln] scale.) As controls, levels of centromeric transcripts were assayed in wild-type containing vector alone (WT/V). The relative levels of centromeric forward transcripts (TGS) and reverse transcripts (PTGS) are shown in panels B and C, respectively. (Note: When grown on selective media to maintain plasmids in the yeast strains, I consistently observed smaller differences in TGS and PTGS between wild-type and *sal3* mutants, in part due to the higher levels of transcripts in the control wild-type strain). *p* values are indicated (samples were compared to the WT control). $n = 3$. **C.** Chromosome segregation defects in *sal3* mutants are partially rescued by expression of Rdp1-SV40-NLS construct, which does not require Sal3 for nuclear import. The percentages of dividing cells with lagging chromosomes were determined for each sample. Standard error bars are shown. *p* values are indicated (sample was compared to the *sal3-33* controls). $n = 3$.

A

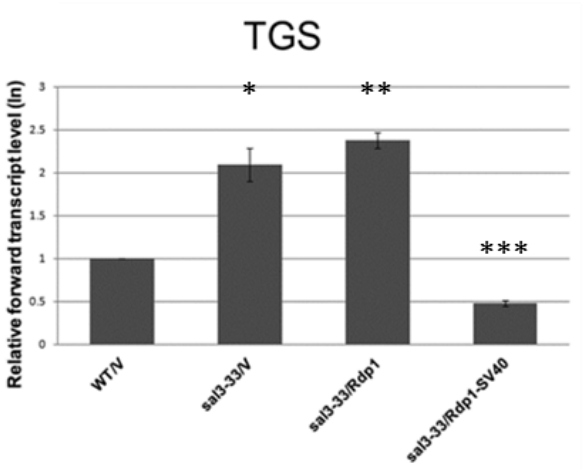

* $p = 0.025$
** $p = 0.0083$
*** $p = 0.067$

B

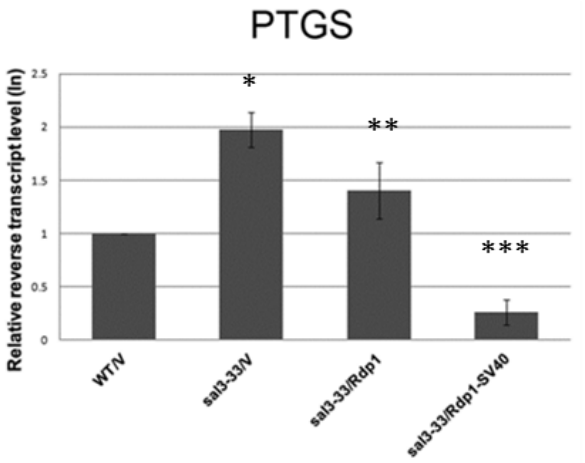

* $p = 0.0005$
** $p = 0.1170$
*** $p = 0.0004$

C

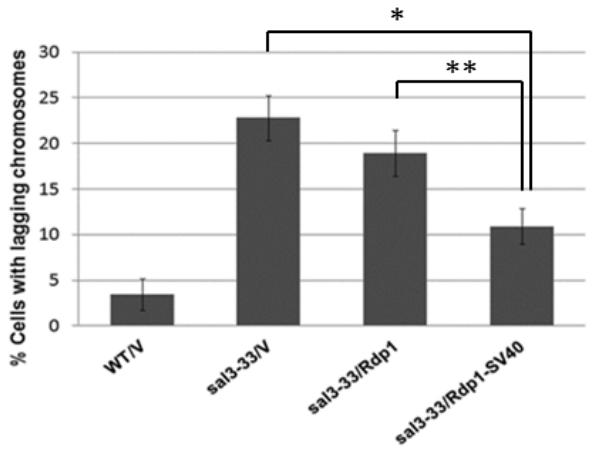

* $p = 0.0027$
** $p = 0.0113$

3.2.8. Chromosome segregation defects of *sal3* mutants are partially rescued by expression of Rdp1-SV40-NLS

Sal3 is required for nuclear import of the critical mitotic modulator, phosphatase Cdc25 (Chua et al. 2002). Accordingly, it is possible that the chromosome segregation defects are not solely due to the loss of Rdp1 nuclear targeting. Therefore, I examined whether the expression of Rdp1-SV40-NLS rescues chromosome segregation defects in *sal3* null mutants. Similar to the nuclear targeting results shown in Figure 3.7, the phenotype of the chromosome segregation defects was rescued by the expression of the Rdp1-SV40-NLS fusion protein (Figure 3.8C). My data showed that the chromosome segregation defects were significantly decreased in the *sal3* mutant expressing the fusion protein, as compared to the mutant cells expressing the vector alone or expressing only Rdp1. However, the defects were higher than in the wild-type strain expressing the vector alone. Taken together, these data suggest that the chromosome segregation defects are due primarily to lack of Rdp1 activity in the nucleus, rather than altered targeting of other Sal3 cargoes, such as Cdc25.

3.2.9. Importin 8 function is not required for silencing centromeric transcripts in *S. pombe*

During the course of this study, Weinmann et al. reported that the karyopherin importin 8 is required for nuclear import of Argonaute proteins and miRNA-dependent targeting of Argonautes to mRNAs in the cytoplasm of mammalian cells (Weinmann et al. 2009). Accordingly, I assayed the localization of GFP-Ago1, Dcr1-GFP, and RFP-Rdp1 in an *S. pombe* mutant that lacked Cse1, a homolog of importin 8. As shown in Figure 3.9A, there were no apparent differences in the localization of fluorescently tagged Ago1, Dcr1, or Rdp1 in the wild-type or *cse1* mutant. Furthermore, the *cse1* null mutant was not sensitive to microtubule disrupting agent TBZ and the levels of both forward and reverse centromeric transcripts were normal (Figures 3.9B and C). These indicate that TGS and PTGS are not affected by the loss of importin 8 activity in this organism. These data suggest that unlike in mammalian cells, importin 8 function is not required for proper localization of RNAi core proteins, nor for siRNA-mediated gene silencing mechanisms in *S. pombe*.

Figure 3.9. Loss of the importin 8 ortholog gene does not affect the localizations of RNAi core proteins or silencing of centromeric loci. A. Wild-type and Δ*imp8* strains were transformed with plasmids encoding GFP-Ago1, Dcr1-GFP, or RFP-Rdp1. Cells were grown in liquid culture until log phase before fixation and staining with DAPI (1 µg/mL). Images were captured using a spinning disc confocal microscope. Bar = 3 µm. **B.** Yeast were spotted onto media containing TBZ (5–15 µg/mL) or solvent (DMSO). Cultures were incubated at 30°C for 2–3 days. **C.** Total yeast RNA was subjected to real-time quantitative PCR and levels of forward and reverse centromeric transcripts were normalized to actin transcripts. As a control for derepression of centromeric transcripts, Δ*rdp1* and Δ*ago1* strains were used. The relative levels of centromeric forward (TGS) and reverse transcripts (PTGS) are indicated. (Note: *y*-axis is in natural log [ln] scale.) Standard error bars are shown. *p* values are indicated (sample was compared to the WT control). $n = 3$.

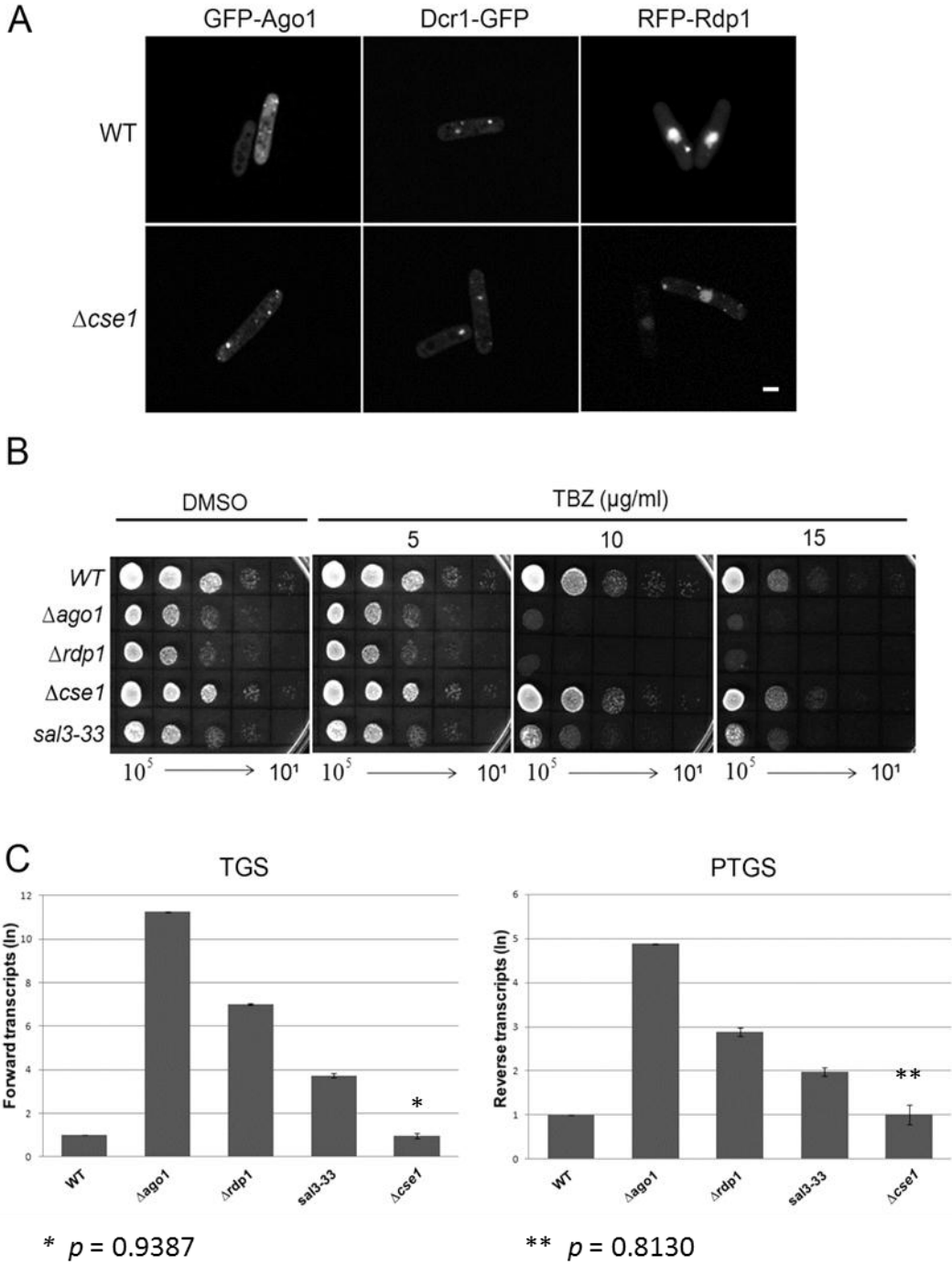
A
GFP-Ago1
Dcr1-GFP
RFP-Rdp1
WT
Δcse1
B
DMSO
TBZ (μg/ml)
5
10
15
WT
Δago1
Δrdp1
Δcse1
sal3-33
10⁵ → 10¹
C
TGS
PTGS
Forward transcripts (ln)
Reverse transcripts (ln)
WT
Δago1
Δrdp1
sal3-33
Δcse1
* p = 0.9387
** p = 0.8130

3.2.10. Sal3 activity is not required for localization of Ago1 and Dcr1 to P-body (PB)-like structures

To further our understanding of the association of Sal3 karyopherin activity with RNAi, I examined the localization of the other two RNAi core proteins, Ago1 and Dcr1, in a *sal3* null background. Plasmids encoding fluorescently tagged Ago1 and Dcr1 were transformed into the *sal3-33* point mutant strain and the localizations of the proteins were monitored by confocal microscopy. As shown in Figure 3.10, GFP-Ago1 and Dcr1-GFP mostly localized to cytoplasmic puncta, a finding consistent with previous observations reported from our laboratory (Carmichael et al. 2006). These findings suggest that Sal3 function is not required for the localization of other RNAi proteins to PBs in yeast.

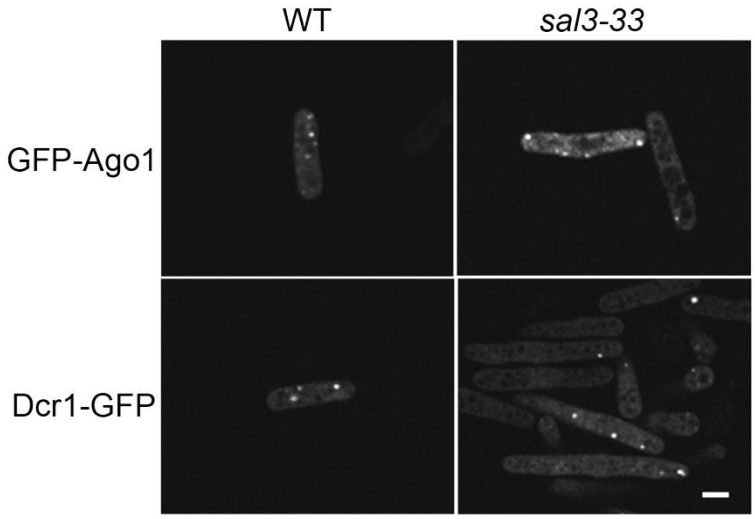

Figure 3.10. Localization of GFP-tagged Ago1 and Dcr1 is normal in *sal3* mutant. The *sal3-33* mutant was transformed with plasmids encoding GFP-Ago1 or Dcr1-GFP. Cells were grown in liquid culture to log phase before fixation and staining with DAPI (1 μg/mL). Images were captured using a spinning disc confocal microscope. Bar = 3 μm.

3.3. Summary

This chapter describes an important role for karyopherin Sal3 in regulation of RNAi activity through mediating nuclear import of the core RNAi protein Rdp1. By using yeast transformation and microscopic analysis, I found that karyopherin Sal3 is required for the nuclear localization of Rdp1. My data showed that nuclear accumulation of fluorescently tagged Rdp1 was rarely observed in *sal3* mutants. However, in five other strains lacking genes encoding nuclear import factors Kap111, Kap123, Kap113, Kap114, and importin 8 homolog, RFP-Rdp1 was localized to the nucleus, similar to wild-type *S. pombe*. However, loss of Sal3 activity did not affect PB localization of two other RNAi core proteins, Ago1 and Dcr1. My results also showed that karyopherin Sal3 forms a stable complex with Rdp1, suggesting that Rdp1 may be another cargo for Sal3.

Loss of Sal3 activity, but not of other karyopherin genes (*kap111*, *kap123, kap113, kap114,* or *importin 8* homolog), was accompanied by a significant increase in forward and reverse centromeric transcripts, which is indicative of defects in TGS and PTGS, respectively. *sal3* mutants also exhibited sensitivity to the microtubule poison TBZ and chromosome segregation defects, phenotypes that result from the loss of centromeric heterochromatin. These defects are often present among RNAi mutants (Volpe et al. 2002; Hall et al. 2002). Moreover, I demonstrated that these defects were rescued by the expression of an Rdp1 variant that was targeted to the nucleus independently of Sal3. In addition to identifying Sal3 as a modulator of Rdp1, my data suggest a potential link between nuclear import and PTGS in the cytoplasm.

CHAPTER 4:
The kinesin motor protein Cut7 regulates biogenesis and function of Ago1-complexes

A version of this chapter has been published in
"C. Stoica (†), J. Park (†), J. Pare, S. Willows, T. Hobman (2010), The Kinesin Motor Protein Cut7 Regulates Biogenesis and Function of Ago1-Complexes, *Traffic*. 11(1):25-36." (†These authors contributed equally to this work)

4.1. Rationale and hypothesis

Argonaute proteins are the major effectors of small RNA-dependent gene-silencing pathways (Hock and Meister 2008) (refer to Section 1.2.1.1). In *S. pombe*, Ago1 and the other core RNAi proteins, Dcr1 and Rdp1, are incorporated into large cytoplasmic mobile ribonucleoprotein (RNP) complexes that are thought to be the yeast counterparts of PBs (Carmichael et al. 2006). PBs are enriched in enzymes that mediate mRNA decay (Sheth and Parker 2003) and are highly dynamic in that their number and size fluctuate in a cell cycle-dependent manner (Aizer and Shav-Tal 2008; Lian et al. 2006) (refer to Section 1.2.1.4). In addition, it has been shown that the Argonaute-containing RNPs undergo rapid assembly and disassembly in the cytoplasm, and that the disruption of microtubules results in the increased size and number of these structures in *S. pombe* (Carmichael et al. 2006). Studies from other groups using different organisms confirmed that PB formation is stimulated when microtubule networks are disrupted (Sweet et al. 2007; Mallik and Gross 2004; Miki et al. 2001). These studies can be interpreted to mean that functions of microtubule-associated motor proteins are involved in the regulation of PB homeostasis. Until this study, however, there has been no direct evidence for the involvement of microtubule motor proteins in RNAi pathways. Based on previous studies, I hypothesized that functions of microtubule-associated motor proteins are involved in the regulation of Ago1-containing PB homeostasis and further regulate the RNAi pathways in *S. pombe*.

It was necessary to first identify the motor proteins associated with the major RNAi effectors in *S. pombe*. There are two families of microtubule-associated motor proteins present in eukaryotic cells: dyneins and kinesins [reviewed in (Mallik and Gross 2004)]. Most kinesins move cargo toward the plus-end of microtubules that extend to the cell periphery, whereas dyneins move cargo toward the cell center or nucleus. My model system, *S. pombe,* encodes only one dynein chain and nine kinesin heavy chains (Schoch et al. 2003); whereas mammalian genomes encode multiple dyneins and at least 45 kinesin genes (Miki et al. 2001). Some of the mammalian motor proteins are essential for viability and a number of them are cell-type specific. Functional redundancy thus may be an issue in mammalian model systems. *S. pombe* is, therefore, an excellent experimental model system to study the function of the molecular motor(s) that associates with RNAi effector complexes in the cytoplasm.

4.2. Results

4.2.1. Cut7 activity is important for regulating the number and size of Ago1-containing RNPs

To identify the microtubule-associated motors that regulate movement and/or morphology of Ago1-containing RNPs in *S. pombe*, I utilized a candidate gene approach. With the exception of one kinesin-like protein (SPBC15D4), genetic mutants for the remaining eight kinesin-like proteins and one dynein protein have been characterized to varying degrees (Table 4.1). Only one of the kinesin-like proteins, Cut7, is essential for viability (Hagan and Yanagida 1992),

but temperature-sensitive (*ts*) mutant *cut7-24* is available. Deletion and *ts* mutants (Tables 2.12 and 4.1) were transformed with plasmids encoding red (RFP)- or green fluorescent protein (GFP)-tagged Ago1 (Carmichael et al. 2006). Live-cell imaging was used to monitor the morphologies and movements of Ago1-containing RNPs in the various genetic backgrounds. Unless otherwise indicated, transformed yeast cells were grown at 29°C.

As shown in Figure 4.1A, in wild-type *S. pombe*, pools of RFP-Ago1 were localized to cytoplasmic puncta that presumably correspond to PBs, as the distribution was typical for Argonaute proteins in yeast and mammalian cells (Carmichael et al. 2006; Jakymiw et al. 2005; Liu et al. 2005; Sen and Blau 2005). Consistent with our previous data (Carmichael et al. 2006), these structures were highly mobile within confined areas of the cytoplasm. I found that nonessential microtubule motor proteins are not required for movement of PBs in fission yeast. For example, the distribution of RFP-Ago1 in the G1A strain (Table 4.1), which lacks the genes encoding the dynein heavy chain (Dhc1) and the kinesin-like proteins, Klp1 and Klp2, was similar to those seen in the wild-type strain (Figure 4.1A). Similarly, the absence of Klp3, Klp4/Tea2, Klp5, Klp6, and Klp8 did not significantly affect the distribution or movement of RFP-Ago1-containing PBs.

I examined whether the remaining motor protein, Cut7, functions in the distribution and/or movement of PBs. My results showed that the distribution of RFP-Ago1-labeled puncta was similar to those observed in the wild-type and other kinesin mutants at the permissive temperature of 23°C. Also, the Ago1-positive puncta exhibited normal movement patterns at 23°C. However, when the

cut7-24 strain was cultured at 29°C, the bulk of RFP-Ago1 was associated with large, immobile puncta and very few RFP-labeled PBs were visible. Even though the remaining PBs exhibited some degree of motility at this temperature, their movement was less extensive than that of similarly-sized RNPs seen in wild-type cells. It should be noted that 29°C is not a true restrictive temperature for the *cut7-24* allele (Hagan and Yanagida 1992) and as such, some Cut7 activity likely remains at this temperature. However, because aggregation of RFP-Ago1 into large foci was observed in wild-type cells at 36°C, I chose to conduct the experiments at lower temperatures to minimize the aggregation of RFP-Ago1.

I also confirmed that the formation of large Ago1-positive structures at 29°C in the *cut7-24* strain was not an artifact of RFP tagging. Data in Figure 4.1B showed that at 29°C, GFP-Ago1 also formed large aggregates in *cut7-24* cells and the number of PB-like structures was markedly reduced in these cells. However, the large aggregates were not observed at the permissive temperature of 23°C.

Lastly, I quantified the fluorescent-labeled PBs in wild-type, Δ*klp4*, and *cut7-24* strains at 23°C and 29°C to see if loss of Cut7 activity affects PB formation. Quantification data showed that the number of GFP-positive PBs decreased fourfold when *cut7-24* cells were shifted to 29°C, whereas the number of PBs in wild-type and Δ*klp4* strains was not dramatically affected by the same shift (Figure 4.1C). Taken together, these data suggest that Cut7 activity plays an important role in PB homeostasis in *S. pombe*.

Table 4.1. Known motor proteins in *S. pombe*

Protein name	Description	Accession number	References
Cut7p	Kinesin-like protein Cut7	CAA40738	(Hagan and Yanagida 1990)
Dhc1p	Cytoplasmic dynein heavy chain	AB006784	(Yamamoto et al. 1999)
Klp2p	Kinesin-like protein 2	CAAB65811	(Wood et al. 2002)
Klp3p	Kinesin-like protein 3	AAF14525	(Brazer et al. 2000)
Klp5p	Kinesin-like protein 5	BAB69885	(West et al. 2001)
Klp6p	Kinesin-like protein 6	BAB69886	(West et al. 2001)
Klp8p	Kinesin-like protein 8	CAB59694	(Wood et al. 2002)
Klp1/Pkl1p	Kinesin-like protein 1	AAB88235	(Pidoux et al. 1996)
SPBC15D4	Kinesin-like protein	CAA20476	–
Tea2p	Kinesin-like protein Tea2	CAA22353	(Browning et al. 2000)

Figure 4.1. Cut7 activity is important for regulating the number and size of Ago1-containing RNPs. *S. pombe* strains lacking activity of one or more dynein and kinesin proteins were transformed with a plasmid encoding RFP-Ago1. **A.** Live-cell imaging was employed to analyze the localization of RFP-Ago1 in wild-type (WT) and mutant strains lacking *dhc1*, *klp1* and *klp2*; *klp3*; *klp5* and *klp6*; *klp4*; *klp8;* or in the temperature-sensitive strain *cut7-24*. Unless otherwise indicated, images were obtained from yeast grown at 29°C. Bar = 3 μm. **B.** Live-cell imaging of GFP-Ago1 in wild-type (WT) and *cut7-24* strains at 23°C and 29°C. Bars = 3 μm. **C.** Quantitation of PB numbers in wild-type (WT), *Δklp4*, and *cut7-24* strains at 23°C and 29°C. n = number of cells counted with at least one GFP-Ago1 positive PB.

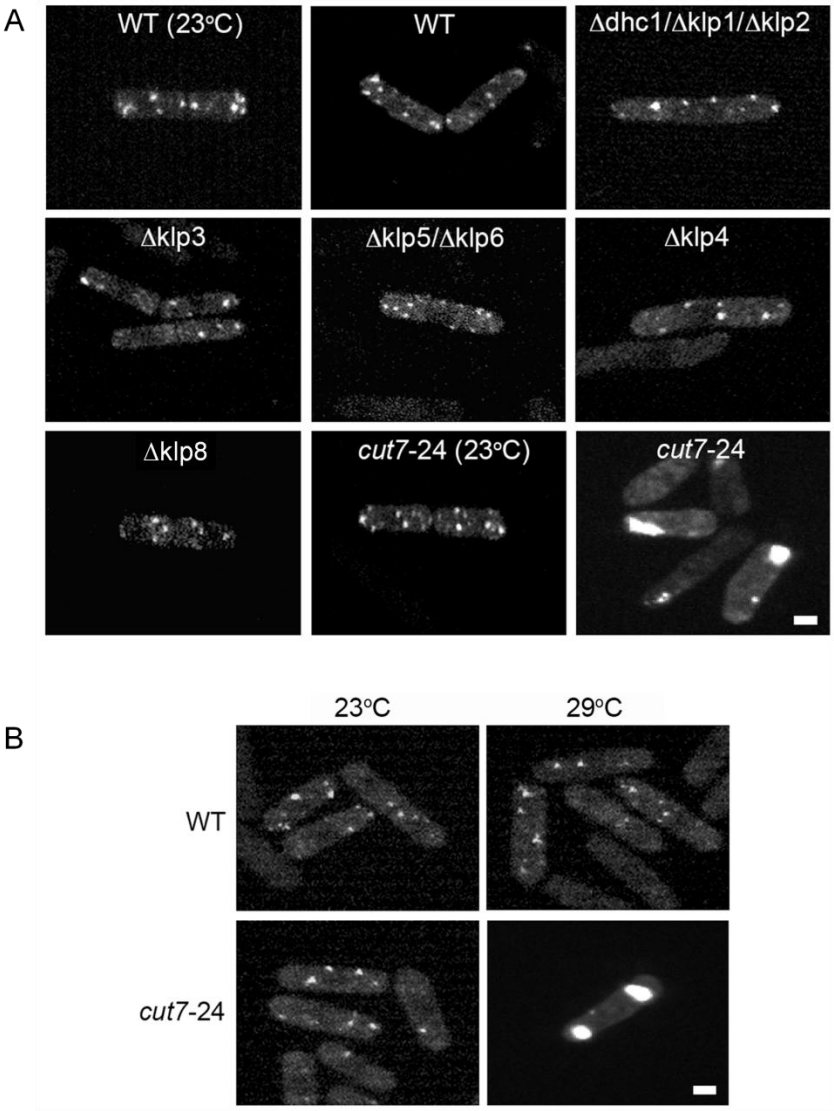
A
WT (23°C)
WT
Δdhc1/Δklp1/Δklp2
Δklp3
Δklp5/Δklp6
Δklp4
Δklp8
cut7-24 (23°C)
cut7-24
B
23°C
29°C
WT
cut7-24
C
PB number as function of temperature
Average number of PBs/cell
14
12
10
8
6
4
2
0
n=129
n=109
n=112
n=126
n=64
n=105
WT
Δklp4
cut7-24
23°C
29°C

4.2.2. Cut7 forms a complex with components of the RNAi machinery

If Cut7 protein indeed functions in PB homeostasis, a direct or indirect interaction between this motor protein and PB component(s) is expected. To test whether Cut7 interacts with the RNAi apparatus in *S. pombe*, a Cut7-GFP chimera was constructed. One of the functions of Cut7 is that of a spindle pole motor. Cut7 mutant cells cannot form a functional mitotic spindle when cells are grown at the restrictive temperature (36°C), resulting in an unfaithful proceeding of mitosis (Hagan and Yanagida 1992; Hagan and Yanagida 1990). The functionality of the Cut7-GFP chimera was tested; it was confirmed that the Cut7-GFP was able to rescue the growth defect of the *cut7-24* at 36°C (Figure 4.2A).

I examined whether Cut7-GFP localizes to RFP-Ago1-containing structures in living cells. The *ts cut7-24* mutant was transformed with plasmids encoding Cut7-GFP and RFP-Ago1. The localization of the Cut7-GFP was monitored by confocal microscopy (Figure 4.2B). The number of cells co-expressing Cut7-GFP and RFP-Ago1 was relatively low; however, colocalization of Cut7-GFP and RFP-Ago1 was evident when both proteins were expressed at similar levels. In these cells, large pools of the Cut7-GFP were associated with the Ago1-positive structures (Figure 4.2B, arrowheads).

In addition, *in vitro* binding assays were employed to see if Cut7 motor proteins interact with Ago1 proteins. Lysates were prepared from yeast cells overexpressing Cut7-GFP, GFP alone, or hemagglutinin (HA)-tagged Ago1. Interactions were detected by immunoprecipitation with anti-GFP, followed by immunoblotting with anti-HA. As seen in Figure 4.2C, HA-Ago1 binds to Cut7-

GFP, but not to GFP alone. To investigate if the Ago1 and Cut7 interaction was dependent on intact RNA, the co-immunoprecipitation assays were employed in the presence of micrococcal nuclease. The result showed that treatment of the immunoprecipitates with micrococcal nuclease did not reduce the amount of HA-Ago1 recovered in the pulldowns, indicating that RNA is not required for the interaction between Ago1 and Cut7 proteins (Figure 4.2C).

A previous study from our lab showed that the other core RNAi proteins, Dcr1 and Rdp1, colocalize with Ago1 in PB-like structures in the cytoplasm (Carmichael et al. 2006), and therefore, interactions between Cut7 with these two proteins were also examined. The co-immunoprecipitation experiments were repeated using lysates prepared from yeast overexpressing HA-Dcr1 and HA-Rdp1. Both HA-Dcr1 and HA-Rdp1 proteins formed nuclease-resistant complexes with Cut7-GFP. The two proteins did not interact with GFP alone, a negative control (Figure 4.2D). Taken together, these results indicate that the core RNAi proteins in *S. pombe* form a complex with the Cut7 motor protein.

Figure 4.2. Cut7 forms a complex with components of the RNAi machinery. **A.** To demonstrate that Cut7-GFP is functional, the *cut7-24* strain was transformed with plasmids encoding GFP alone or Cut7-GFP. Serial dilutions were spotted onto selective media and cultures were maintained at 23°C or 36°C for 3–5 days. **B.** Cut7-GFP and RFP-Ago1 colocalize in cytoplasmic puncta. *S. pombe* transformed with plasmids encoding Cut7-GFP and RFP-Ago1 were viewed by confocal microscopy. Arrowheads indicate colocalization of Cut7-GFP and RFP-Ago1. Bar = 3 μm. **C.** Lysates from *S. pombe* strains expressing HA-Ago1 and GFP, GFP-Dcr1, or Cut7-GFP were subjected to co-immunoprecipitation with antibodies to GFP. The immunoprecipitates were treated with or without micrococcal nuclease, and then subjected to SDS–PAGE and immunoblotting with antibodies to HA. Lower panel is an immunoblot showing the levels of recovered GFP-fusion proteins. **D.** Lysates from *S. pombe* strains expressing HA-Rdp1 or HA-Dcr1 and GFP, GFP-Ago1, or Cut7-GFP were subjected to co-immunoprecipitation with antibodies to GFP. The immunoprecipitates were then subjected to SDS–PAGE and immunoblotting with antibodies to HA. Lower panel is an immunoblot showing the levels of recovered GFP-fusion proteins (courtesy of C. Stoica).

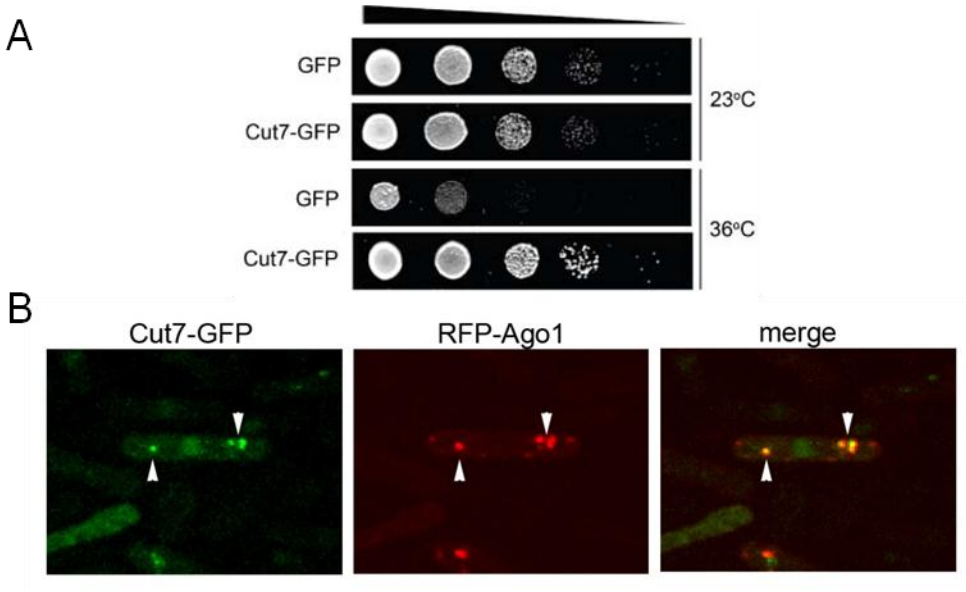
A
GFP
Cut7-GFP
GFP
Cut7-GFP
23°C
36°C
B
Cut7-GFP
RFP-Ago1
merge
C
HA-Ago1
GFP
GFP-Dcr1
Cut7-GFP
nuclease
-
+
-
+
-
+
anti-HA
GFP
D
HA-Rdp1
HA-Dcr1
GFP
GFP-Ago1
Cut7-GFP
GFP
GFP-Ago1
Cut7-GFP
anti-HA
GFP

4.2.3. *cut7-24* mutants are not sensitive to thiabendazole at the restrictive temperature

I examined how this kinesin protein Cut7 activity affects RNAi-dependent gene silencing. *S. pombe* Ago1 is a multifunctional protein that is required for TGS and PTGS in the nucleus and cytoplasm, respectively (Sigova et al. 2004; Volpe et al. 2002). To determine if Cut7 activity affects TGS and/or PTGS in *S. pombe*, I employed a number of well-characterized assays that are described in Sections 3.2.4 and 3.2.6. As previously mentioned, RNAi is required for the formation of pericentromeric heterochromatin in *S. pombe*. As such, Δ*ago1* and other RNAi null mutants, Δ*dcr1* and Δ*rdp1*, exhibit frequent chromosomal segregation defects and are extremely sensitive to the microtubule destabilizing drug, TBZ (Volpe et al. 2003; Volpe et al. 2002).

I first utilized the TBZ sensitivity assay as an indirect method to examine the requirement of Cut7 activity in gene silencing. Serial dilutions of wild-type, Δ*ago1,* and *cut7-24* cell cultures were spotted onto media containing TBZ (10 μg/mL) or solvent (DMSO). The plates were incubated at 23°C or 29°C for 5 or 3 days, respectively. The data show that, compared to wild-type *S. pombe*, *cut7-24* mutants were not sensitive to TBZ when grown at 29°C (Figure 4.3). Indeed, the *ts* mutant *cut7-24* was even more resistant to the drug than wild-type *S. pombe* at 29°C. As a control for TBZ, the Δ*ago1* mutant exhibited high sensitivity to this drug.

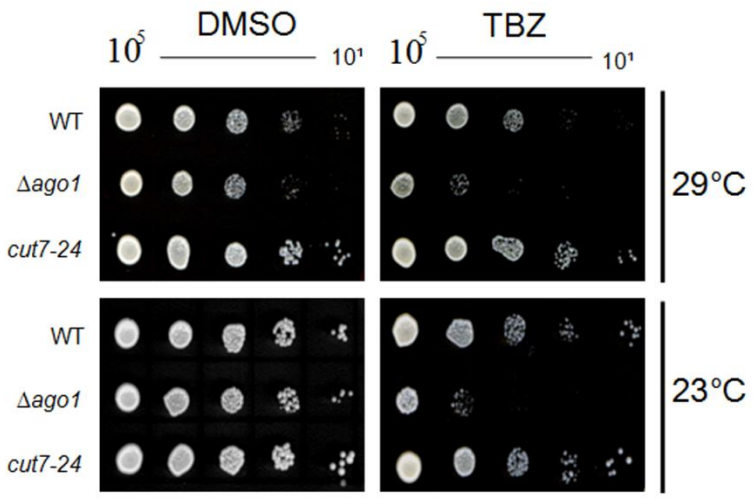

Figure 4.3. *cut7-24* mutants are not sensitive to thiabendazole at the restrictive temperature. Serial dilutions of wild-type (WT), Δ*ago1*, and *cut7-24* cell cultures were spotted onto media containing TBZ (10 μg/mL) or solvent (DMSO). Plates were incubated at 23°C or 29°C for 5 or 3 days, respectively.

4.2.4. Cut7 activity is important for post-transcriptional silencing of centromeric transcripts

The TBZ sensitivity assay is an indirect method to gauge TGS and therefore, I employed real-time qPCR to determine if the levels of centromeric transcripts in *cut7-24* mutants were temperature-dependent. As explained in Sections 1.3.1.1 and 3.2.4, the RNAi machinery is essential for repressing the levels of both forward and reverse transcripts from the pericentromeric *dg* or *dh* repeats; however, the regulation of these transcripts is different. Specifically, the forward transcripts are negatively regulated by a Swi6-dependent mechanism. In this case, the RNAi machinery indirectly regulates the levels of forward transcripts. Conversely, synthesis of reverse centromeric transcripts is a constant process in wild-type cells. However, these transcripts are degraded by the RNAi machinery, presumably in the cytoplasm. Therefore, neither forward nor reverse centromeric transcripts accumulate to appreciable levels in wild-type *S. pombe* (Volpe et al. 2002).

My results demonstrated that, when *cut7-24* and wild-type cells were cultured at 23°C or 36°C, there was no significant difference in the levels of forward centromeric transcripts (Figure 4.4A). In this particular experiment, a slight increase in the levels of forward centromeric transcripts was observed in *cut7-24* cells that were grown at 29°C, but this increase was relatively small. By comparison, the levels of forward centromeric transcripts were more than 1,000 times higher in the control Δ*ago1* mutant, regardless of the temperature. Although statistically significant, it is unlikely that the slight increase in the transcript levels

observed when the *cut7-24* strain was cultured at 29°C is biologically significant. This is because, as can be seen in Figure 4.3, these cells are not sensitive to TBZ when cultured at this temperature (29°C). Based on the results from the two assays (Figures 4.3 and 4.4A), I conclude that TGS is not dramatically affected by decreased Cut7 activity.

Though forward transcript levels did not vary greatly with temperature, the levels of reverse centromeric transcripts were significantly higher when *cut7-24* cells were cultured at elevated temperatures—both 29°C and 36°C (Figure 4.4B). Relative to wild-type cells cultured at 29°C and 36°C, the levels of reverse transcripts were two to five times higher in *cut7-24* mutants. In contrast, no difference was observed in the *cut7-24* cells cultured at 23°C (Figure 4.4B).

It is important to verify that the *cut7-24* cells used for my experiments were still viable and that there were no disruptions of other microtubule-associated networks in the cytoplasmic structures after being cultured for 18 hours at the restrictive temperature, 36°C. I utilized the vital mitochondrial stain 2-(4-dimethylaminostyryl)-1-methylpyridinium iodide (DASPMI). Wild-type and *cut7-24* cells were cultured at 23°C, 29°C, and 36°C for 18 hours before their mitochondria were stained with DASPMI (0.5 mg/mL) for 5 minutes. Samples were then subjected to live-cell imaging using a spinning disc confocal microscope. As shown in Figure 4.5, decreased Cut7 activity for 18 hours at the restrictive temperature did not result in a loss of viability or in gross disruption of the microtubule network. These results (described in Sections 4.2.3 and 4.2.4)

suggest that Cut7 activity is important for post-transcriptional gene silencing in *S. pombe*.

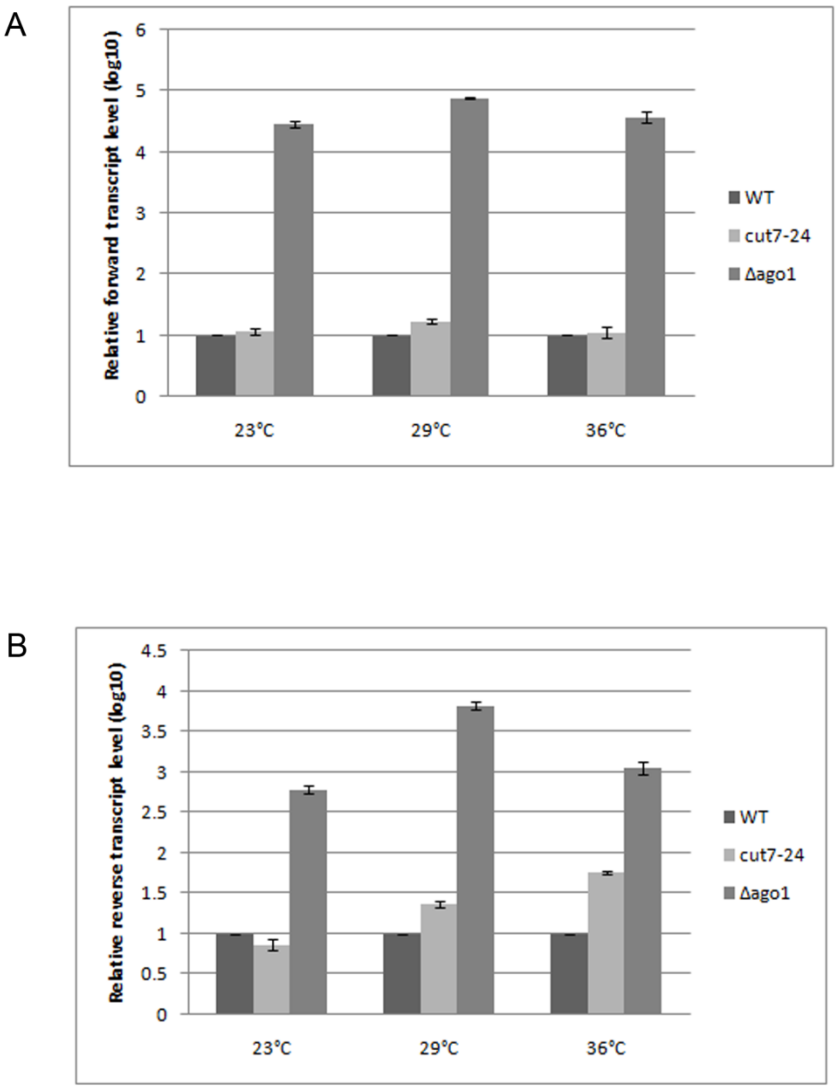

Figure 4.4. Cut7 activity is important for post-transcriptional silencing of centromeric transcripts. A. Total RNA was extracted from wild-type, Δ*ago1*, and *cut7-24* strains that were incubated at 23°C, 29°C, or 36°C for 18 hours. Samples were subjected to real-time quantitative PCR (qPCR) and the levels of forward centromeric transcripts were normalized to actin transcripts. The levels of transcripts in wild-type strains were set to 1.0. **B.** Normalized levels of reverse centromeric transcripts are shown. (Note: *y*-axis is in log10 scale.)

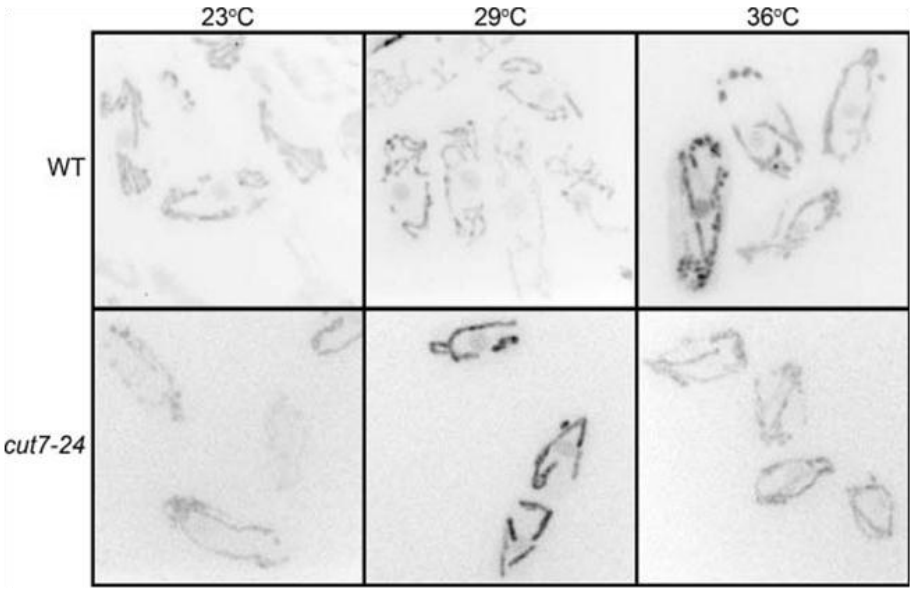

Figure 4.5. Disruption of Cut7 activity for 18 hours does not result in loss of viability or in gross disruption of the microtubule network. Wild-type (WT) and *cut7-24* cells were cultured at 23°C, 29°C, and 36°C for 18 hours before their mitochondria were stained with DASPMI (0.5 mg/mL) for 5 minutes. Samples were then subjected to live-cell imaging using a spinning disc confocal microscope. The colors in the images were inverted to provide maximum contrast. The mitochondrial network is black against a white background (courtesy of J. Pare).

4.2.5. Overexpression of the Ago1-binding domain of Cut7 affects the distribution of Ago1

To further our understanding of Cut7 motor protein function in PB homeostasis and/or RNAi, *in vitro* binding assays were used to identify the region of Cut7 that interacts with Ago1. The domain structure of Cut7 is shown in Figure 4.6A. As with most kinesin proteins, there is a large motor domain in the amino-terminal region of the protein. This domain is not expected to interact with cargo; rather, it is involved in microtubule binding. For the sake of simplicity, I refer to the non-motor carboxyl-terminal region of Cut7 as the cargo-binding region. The Ago1-binding site resides in the amino-terminal (NT) half of the cargo-binding region between amino acid residues 367 to 720 (Figure 4.6A).

After mapping the Ago1-binding site, a plasmid encoding the Ago1-binding domain of Cut7 (NT-Cut7-RFP) was constructed and the localization of the resulting chimera (NT-Cut7-RFP) was monitored by live-cell imaging in *S. pombe*. Because a pool of Cut7 interacts with Ago1 and colocalizes to Ago1-positive RNPs, it was expected that a fusion protein containing the Ago1-binding domain (NT-Cut7-RFP) would also target these structures. As shown in the bottom panel of Figure 4.6B, the NT-Cut7-RFP construct was excluded from nuclei and localized to discrete cytoplasmic foci. Even though these foci morphologically resembled PBs, unlike the Ago1-containing RNPs, the NT-Cut7-RFP-associated puncta did not exhibit motility.

Based on these observations, I hypothesized that the NT-Cut7-RFP construct would act as a dominant negative to prevent endogenous Cut7 from

interacting with PBs. I examined this possibility by monitoring the motility of GFP-Ago1 in yeast cells that co-expressed NT-Cut7-RFP. However, GFP-Ago1-positive puncta were not visible in the cytoplasm of NT-Cut7-RFP-expressing cells (Figure 4.6B). Rather, GFP-Ago1 was localized in a diffuse pattern throughout the cytoplasm. In contrast, GFP-Ago1-positive PBs were clearly visible in yeast cells expressing RFP alone (Figure 4.6B). These data suggest that overexpression of the Ago1-binding domain of Cut7 inhibits the association of Ago1 with PBs.

4.2.6. Overexpression of the Ago1-binding region of Cut7 does not affect the targeting of Dcr1 to PBs, nor the formation of PBs

A previous study from our laboratory showed that a large pool of Dcr1 is localized to PBs in *S. pombe* (Carmichael et al. 2006). Because overexpression of the Ago1-binding site of Cut7 (NT-Cut7-RFP) inhibited the recruitment of GFP-Ago1 to PBs (Figure 4.6B), I questioned whether the targeting of Dcr1 proteins to PBs is also affected by the overexpression of this construct. Interestingly, the targeting of Dcr1-GFP to PBs was not affected by the expression of the Ago1-binding domain of Cut7 (Figure 4.6C). The distribution of Dcr1-GFP-positive puncta was typical and the pattern was not noticeably different between the cells co-expressing the NT-Cut7-RFP construct and the cells co-expressing RFP alone.

Overexpression of the Ago1-binding domain of Cut7 (NT-Cut7-RFP) did not block the formation of PBs, as evidenced by the fact that the localization of Dcr1-GFP was not disrupted in yeast expressing this construct (Figure 4.6C). The results may suggest that association of Ago1 is not required for targeting of Dcr1 to PBs in *S. pombe* or that the PBs in wild-type cells expressing the NT-Cut7-RFP construct still contain enough endogenous Ago1 (which is non-fluorescent) that functions to recruit Dcr1-GFP to PBs. Because overexpression of the Ago1-binding domain of Cut7 strongly inhibited the recruitment of GFP-Ago1 to PBs, this may indicate that Cut7 activity is important for stable association of Ago1 with PBs.

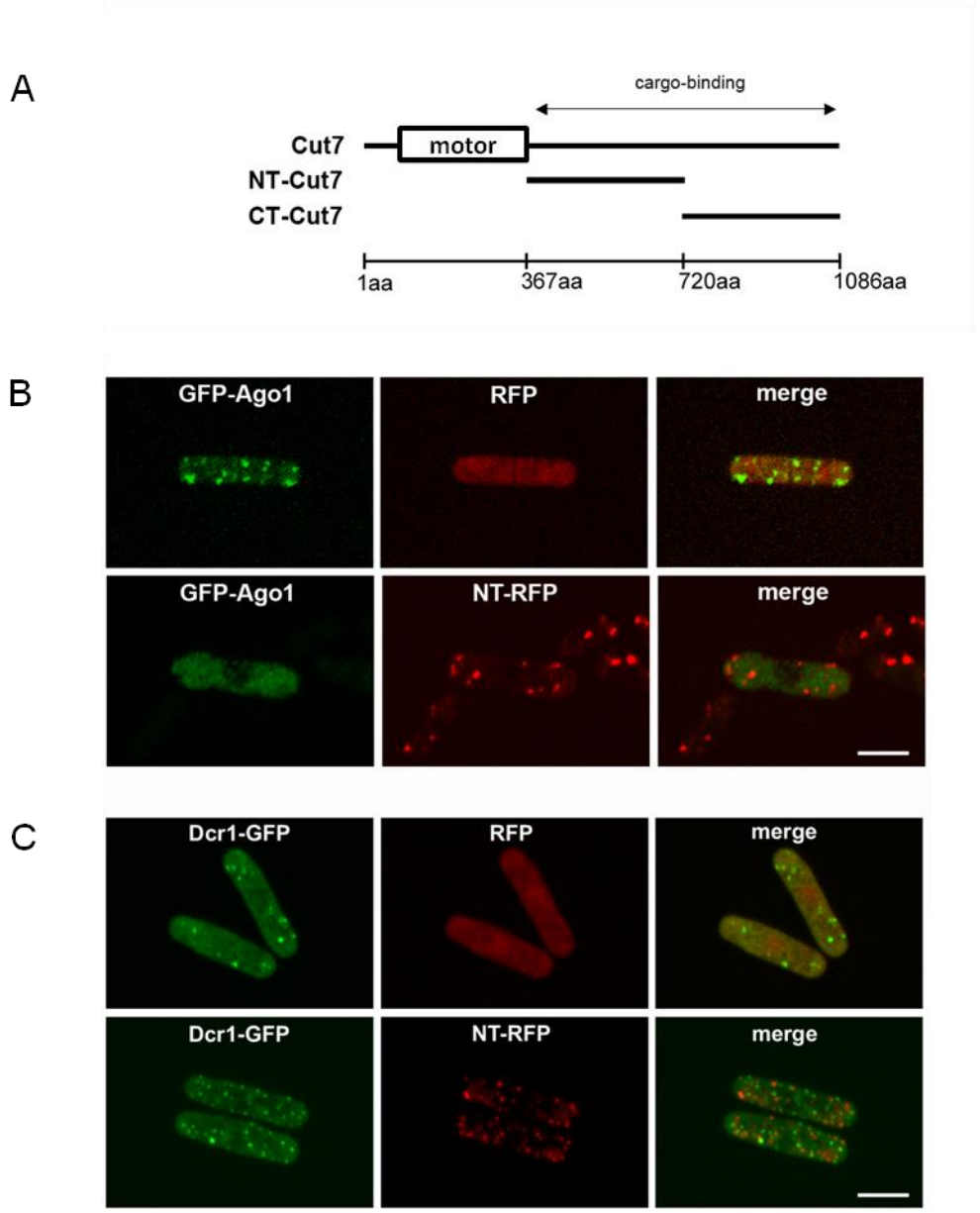

Figure 4.6. Overexpression of the Ago1-binding domain of Cut7 affects the distribution of Ago1, but not the formation of PBs. A. Schematic of Cut7 protein constructs. The motor and cargo-binding domains are indicated. **B, C.** NT-Cut7-RFP (NT-RFP) or RFP alone was expressed together with GFP-Ago1 (images in panel B; courtesy of C. Stoica), or Dcr1-GFP in wild-type *S. pombe*. The images were acquired from live cells using a spinning disc confocal microscope. Bar = 5 μm.

4.2.7. Overexpression of the Ago1-binding domain of Cut7 does not affect silencing of centromeric repeats

As shown in Section 4.2.5, overexpression of the NT-Cut7-RFP affects the intracellular distribution of Ago1. It was tempting to speculate whether the expression of this construct inhibits RNAi-dependent gene silencing.

Total RNA was extracted from wild-type *S. pombe* harboring plasmids encoding RFP alone (vector control), NT-Cut7-RFP (Ago1-binding region of Cut7; Figure 4.6A), or CT-Cut7-RFP (the rest of the cargo-binding region; Figure 4.6A). Samples were subjected to real-time qPCR and the levels of forward and reverse centromeric transcripts were normalized to actin transcripts as described in Section 4.2.4. As a control for the derepression of centromeric transcripts, a Δ*ago1* strain was employed. Results from the qPCR assays are shown in Figure 4.7. The relative levels of both forward and reverse centromeric transcripts in wild-type cells expressing NT-Cut7-RFP were not significantly different from those detected in cells expressing the vector alone or in cells expressing CT-Cut7-RFP. In the control RNAi mutant, Δ*ago1*, the levels of both forward and reverse centromeric transcripts were much higher than those in the wild-type strain or in cells expressing CT-Cut7-RFP.

Together, these results suggest that the expression of NT-Cut7-RFP does not affect the regulation of TGS- or PTGS-dependent silencing of centromeric transcripts. It is possible that the expression of NT-Cut7-RFP, which appears to block the association of Ago1 with PBs (Figure 4.6B), may give rise to a large pool of free cytosolic Ago1 that is able to function in PTGS.

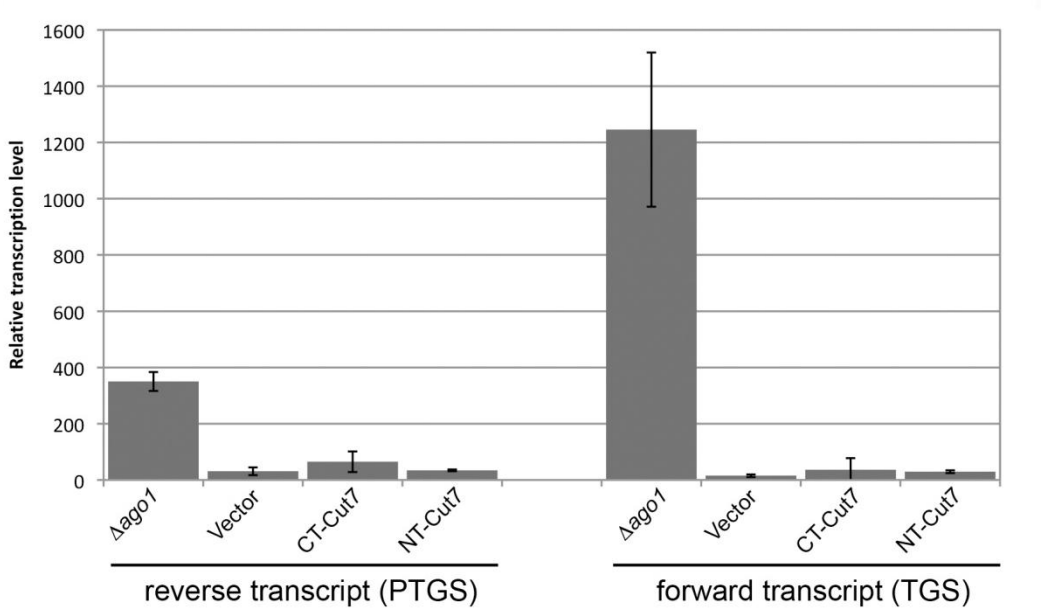

Figure 4.7. Over-expression of the Ago1-binding domain of Cut7 does not affect the silencing of centromeric repeats. Total RNA was extracted from wild-type *S. pombe* harboring plasmids encoding RFP alone (Vector), NT-Cut7-RFP (NT-Cut7), or CT-Cut7-RFP (CT-Cut7). Samples were subjected to real-time quantitative PCR (qPCR) and the levels of forward and reverse centromeric transcripts were normalized to actin transcripts. As a control for derepression of centromeric transcripts, a Δ*ago1* strain was employed. The relative levels of centromeric transcripts are indicated.

4.3. Summary

In this chapter, I described Cut7 motor protein functions in regulation of Ago1-containing PB homeostasis and RNAi activity in the cytoplasm. My results showed that the microtubule-associated kinesin protein Cut7 is associated with Ago1-positive RNPs, which are thought to be the equivalent of PBs in *S. pombe*. Cut7 activity was shown to be important for PB homeostasis. I observed a reduction in PB motility, a reduced number of Ago1-positive PBs, and a concomitant appearance of large Ago1-positive aggregates in *cut7-24* mutants that were cultured at elevated temperatures (29°C and 36°C). It was shown that this motor protein forms a stable complex with all three of the RNAi apparatus in *S. pombe*—Ago1, Dcr1, and Rdp1.

Although TGS was not significantly affected by the loss of Cut7 activity, PTGS was significantly impaired. Interestingly, overexpression of the Ago1-binding region of Cut7 specifically inhibited recruitment of GFP-Ago1 to PBs, but did not affect the distribution of Dcr1-GFP. This suggests that Cut7 may be important for stable association of Ago1 with these PBs. However, overexpression of the Ago1-binding region of the Cut7 construct did not significantly affect TGS or PTGS. It is possible that the remaining pool of cytosolic Ago1 is still functional in the cells expressing this construct. In summary, these findings provide evidence that microtubule motor proteins may be important regulators of RNAi in the cytoplasm.

CHAPTER 5:
Discussion

5.1. Overview

The focus of my thesis research was to characterize *trans*-acting factors that modulate small RNA-mediated gene silencing mechanisms in *S. pombe.* Although the basic roles of the core RNAi components, Ago1, Dcr1, and Rdp1, are well understood, efforts to investigate the regulation of the RNAi effector proteins, themselves, are much more recent. Understanding how *trans*-acting factors mediate the localization/activity of RNAi proteins will provide key insights into the modulation of gene expression on a global level. To this end, I hypothesized that there are multiple *trans*-acting factors which regulate the localization and/or activity of the RNAi apparatus in *S. pombe*.

Several studies have characterized multiple *trans*-acting factors that regulate the localization and activity of RNAi proteins. For example, in my recently published paper, it was shown that the karyopherin Sal3 is required for the nuclear import of Rdp1 in *S. pombe* (Park et al. 2012). Previously, our laboratory reported that targeting of hAgo2 to SGs and PBs is dependent upon the activity of the molecular chaperone Hsp90 in mammalian cells (Pare et al. 2009). It also has been shown that microtubule-associated motor proteins regulate the movement and homeostasis of Argonaute protein complexes in the cytoplasm (Stoica, Park et al. 2010; Loschi et al. 2009). Finally, it has been reported that localization, and presumably the functions of Argonaute proteins, are regulated by phosphorylation (Rudel et al. 2011; Zeng et al. 2008). These studies demonstrate that the RNAi apparatus is subject to intricate and extensive regulation.

5.2. Rdp1 nuclear localization is required for TGS in *S. pombe*

5.2.1. RNA-dependent RNA polymerase activity: a universal feature of RNAi?

In lower eukaryotes, such as *A. thaliana* (Dalmay et al. 2000; Schiebel et al. 1993), *C. elegans* (Sijen et al. 2001; Smardon et al. 2000), *S. pombe* (Volpe et al. 2002), and *N. crassa* (Martens et al. 2002; Cogoni and Macino 1999), RdRP is a required component of the RNAi pathway (Lipardi and Paterson 2010). The most important function of Rdp1 in *S. pombe* is providing substrates for Dcr1 by generating dsRNAs in order to increase the speed and magnitude of the RNAi response (Sigova et al. 2004).

Although Rdp1 homologs are not found in higher eukaryotes that employ RNAi, such as flies, mice, or humans (Shabalina and Koonin 2008; Okamura and Lai 2008), various functional homologs have been characterized experimentally (Pelczar et al. 2010; Maida et al. 2009; Lehmann et al. 2007; Lipardi et al. 2001). For example, it has been shown that human TERT (telomerase reverse transcriptase catalytic subunit) and RMRP (RNA component of mitochondrial RNA-processing endoribonuclease) form a ribonucleoprotein complex that has RdRP activity. This complex produces dsRNAs that can be processed into small interfering RNAs in a Dicer-dependent manner (Maida et al. 2009). The TERT-RMRP RdRP complex has a strong preference for RNA templates that form hairpin-like folds.

Recently, the *elp1* subunit of the RNAPII complex has also been shown to possess canonical RdRP activity (Lipardi and Paterson 2009). It is thought to be an important functional homolog as it is present in organisms ranging from *D.*

melanogaster to humans (Lipardi and Paterson 2010). D-elp1 associates with Dicer-2, similar to the Dicer-RdRP interaction observed in lower eukaryotes. However, miRNA function is not dependent on D-elp1, even though siRNA accumulation and function requires this enzyme (Lipardi and Paterson 2009). In this study, RdRP activity was identified using three assays to interrogate the reaction products: Dcr2 digestion, RNase sensitivity, and nearest neighbor analysis (Lipardi and Paterson 2009). However, the authors retracted this particular report due to their misinterpretation of the nearest neighbor analysis (Lipardi and Paterson 2011).

In some cases, suppression of transposon activity can be achieved by alternative pathways that are independent of RdRP activity (Crombach and Hogeweg 2011). Thus, although RdRP activity is common to most eukaryotic RNAi pathways (Birchler 2009), it is not required for RNAi in all organisms. However, together with my data, the experimental observations may suggest that modulation of RdRP activity is yet another means by which RNAi-dependent gene silencing is controlled in some organisms.

5.2.2. Importin 8 homolog is not involved in siRNA-mediated gene silencing, but is associated with miRNA-mediated RNAi

Even though there is evidence showing that *trans*-acting factors affect the targeting and/or functions of Argonaute proteins (Stoica, Park et al. 2010; Pare et al. 2009; Weinmann et al. 2009; Guang et al. 2008), little is known about how the localization and/or functions of Rdp1 and Dcr1 (or their homologs) are regulated.

The data in my recently published paper indicate that the karyopherin Sal3 is important for the nuclear import of Rdp1 (Park et al. 2012). Loss of *sal3* function was accompanied by a significant increase in forward centromeric transcripts, which is indicative of defects in TGS. The mutant cells also exhibited chromosome segregation defects (described in Sections 3.2.4, 3.2.5, and 3.2.6). This phenotype is common to RNAi mutants and results from the loss of centromeric heterochromatin (Volpe et al. 2002; Hall et al. 2002). It is assumed that the defects in TGS and in chromosome segregation pattern associated with *sal3* mutants were mainly due to a failure to target Rdp1 into the nucleus. The expression of an Rdp1 variant that is targeted to the nucleus via a Sal3-independent pathway partially rescued these defects.

The karyopherin importin 8, which governs the nuclear localization of Argonaute proteins in mammalian cells, is also required for their localization to PBs and SGs and miRNA-dependent gene silencing (Weinmann et al. 2009). However, my results indicate that importin 8 is not required for RNAi-dependent gene silencing in *S. pombe* (Figure 3.9). Fission yeast does not employ miRNA-based gene silencing, but rather siRNA-dependent cleavage (Irvine et al. 2006). The results may suggest that the co-opting of importin 8 as a regulatory factor for RNAi co-evolved with miRNA-dependent pathways in higher eukaryotes.

5.2.3. Existing Rdp1-independent pathway: the silencing defects associated with *Δago1* are more severe than those associated with *Δrdp1*

My results demonstrated that *sal3* mutants exhibited defects in gene silencing and chromosome segregation. However, these defects were not as severe as those of RNAi mutants. The results may be related to the fact that Rdp1 is not absolutely required for the generation of siRNAs in *S. pombe*. Indeed, Djupedal et al. reported that there are multiple types of siRNAs in fission yeast *S. pombe,* some of which are generated through an Rdp1-independent pathway (Djupedal et al. 2009). Ago1 seems to play an important role in the production of most, if not all, types of siRNAs. This may explain why the gene silencing defects associated with *ago1* mutants are more severe than those associated with *rdp1* mutants (Figure 3.9C). Djupedal *et al*. also demonstrated that, in the Rdp1-independent pathway, Dcr1 processes centromeric transcripts that adopt hairpin-like folds to produce siRNAs (primary siRNAs or 1° siRNAs, as shown in Figure 5.1). The siRNAs may then act to initiate heterochromatin formation (Djupedal et al. 2009).

In addition, Halic *et al*. showed that there is a distinct class of small RNAs, called primal siRNAs (priRNAs), which are Rdp1- and Dcr1-independent. They are thought to be the product of exosome-dependent trimming of mRNA transcripts and to interact with the Ago1 pools that mediate gene silencing at heterochromatic and possibly euchromatic (Halic and Moazed 2010). The findings indicate that endogenous siRNAs can be produced by several mechanisms.

Although Rdp1 is not essential for siRNA production, most siRNAs in fission yeast are in fact derived from Dcr1-dependent cleavage of Rdp1-amplified transcripts. Data from multiple studies are consistent with a scenario in which Rdp1-generated siRNAs are produced in *cis* to transcription of nascent centromeric RNAs (Djupedal et al. 2009; Sugiyama et al. 2005; Noma et al. 2004). Loading of these Rdp1-generated siRNAs (secondary siRNAs or 2° siRNAs) onto RITS then silences transcription locally through heterochromatin formation. However, siRNAs produced from RNA hairpin structures that are processed by Dcr1 (primary siRNA) can function in *trans* to silence genes at remote loci (Simmer et al. 2010). Accordingly, it is tempting to speculate that some of the siRNAs that are generated via Rdp1 (secondary siRNAs) are also loaded onto Ago1 complexes which function in PTGS in the cytoplasm. My results showed that PTGS was affected by the loss of Sal3 function, though the level of defects in PTGS was much lower than in TGS (Figure 3.4). The results may indicate a link between Rdp1-dependent siRNA production and Ago1-mediated cleavage of centromeric transcripts in the cytoplasm. That is, Rdp1-dependent siRNAs (secondary siRNAs) may also be loaded onto Ago1 in the cytoplasm (Figure 5.1).

Finally, my findings suggest that defects in the TGS-dependent suppression of centromeric transcripts were more pronounced in RNAi mutants than in PTGS. This is likely because reverse centromeric transcripts, which are degraded by PTGS, are more abundant in wild-type cells (Volpe et al. 2002). Accordingly, the loss of RNAi-dependent PTGS would not result in as large of an increase in centromeric transcripts.

5.2.4. A revised model for Sal3 involvement in fission yeast heterochromatin formation

In conclusion, the findings described in this thesis contribute to an understanding of how heterochromatic silencing is regulated by RNAi machinery in the *S. pombe* nucleus, in accordance with other previously published data (Irvine et al. 2006; Moazed et al. 2006; Zofall and Grewal 2006; Allshire 2002; Volpe et al. 2002) (Figure 5.1).

Heterochromatin formation is thought to be initiated by association of RITS complex with nascent transcripts and RDRC (Grewal 2010). Rdp1 of the RDRC generates dsRNAs and, in association with Dcr1, processes centromeric transcripts into siRNAs. Based on my findings, Rdp1 nuclear import by karyopherin Sal3 is required for Rdp1 function in the nucleus to generate dsRNAs that can serve as substrates for Dcr1 in *S. pombe* (Park et al. 2012). Downstream signaling of chromatin remodeling can then be activated by secondary siRNAs that are generated through an Rdp1-Dcr1-dependent pathway to accelerate the RNAi response, resulting in the spread of heterochromatin (Figure 5.1).

RITS complex associates with RDRC. It is known that the interaction between these complexes is dependent upon siRNAs that are produced in an Rdp1-Dcr1-dependent manner (Grewal 2010). If Rdp1 cannot function efficiently, it is plausible that the levels of dsRNAs, and subsequently siRNAs, are lower than those required to trigger the association of these RNAi complexes and to initiate the heterochromatin formation in *S. pombe*. This leads to defects in heterochromatic silencing of the peripheral region of centromere and

consequently, to centromere dysfunction. Primary siRNAs that are generated independently of Rdp1 activity can also facilitate TGS and PTGS. These siRNAs associate with Ago1-containing complexes, RITS and RISC, in the nucleus and in the cytoplasm, respectively (Djupedal et al. 2009) (Figure 5.1).

It is not clear why the loss of Sal3 activity exhibited only a moderate effect on PTGS, but it is possible that some secondary siRNAs are loaded onto Ago1 in the cytoplasm. It is also possible that the defects in PTGS in *sal3* mutants are the result of siRNAs not functioning efficiently in *trans* (Grewal 2010; Djupedal et al. 2009; Sugiyama et al. 2005; Noma et al. 2004). My data may have important implications for a potential link between nuclear import pathway and PTGS.

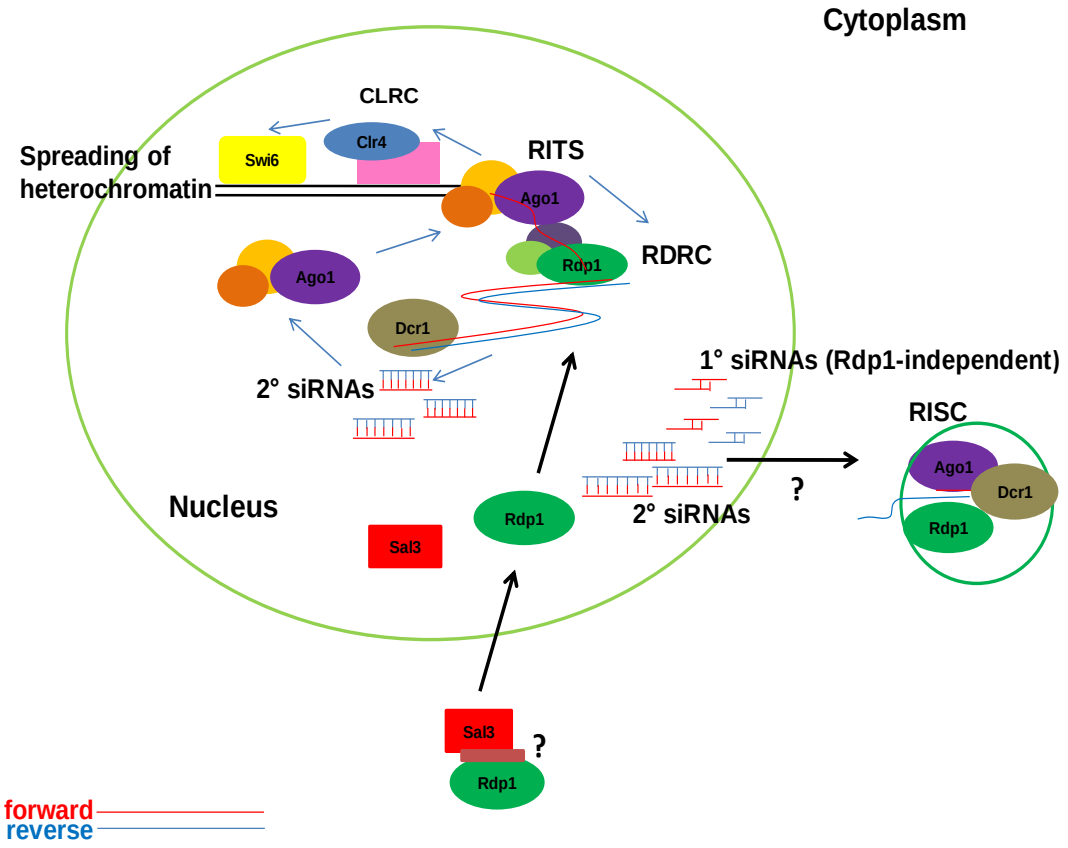

Figure 5.1. A revised model depicting Sal3 involvement in heterochromatin formation. Model depicting the role of Rdp1 in transcriptional (TGS) and post-transcriptional gene silencing (PTGS). The bidirectional transcription of centromeric repeats leads to dsRNAs that are cleaved by Dcr1 to produce primary siRNAs. These siRNAs do not need Rdp1 for production and can be incorporated into Ago1-containing RITS and RISC in the nucleus and in the cytoplasm, respectively. The Rdp1-dependent amplification of centromeric transcripts is required for the production of the secondary siRNAs that may be preferentially incorporated into Ago1-containing RITS complexes in the nucleus. RITS functions together with the chromatin silencing machinery (Clr4 and Swi6) to repress transcription from centromeric loci. Karyopherin Sal3 plays an important role in Rdp1 entering the nucleus. In the nucleus, Rdp1 boosts the RNAi response by secondary siRNA generation. Loss of Rdp1 activity in the nucleus results in TGS defects, leading to centromeric dysfunction.

5.3. Cut7 activity is required for PTGS in *S. pombe*

5.3.1. Cut7 activity is required for PB homeostasis

Besides the multiple *trans*-acting factors that affect the localization of Argonaute proteins (Johnston and Hutvagner 2011; Rudel et al. 2011; Weinmann et al. 2009; Pare et al. 2009; Guang et al. 2008), intriguing links between Argonautes and microtubules and their associated motor proteins have also emerged through a number of recent studies. It was first reported that Seawi, a sea urchin Piwi/Argonaute family member, associates with a microtubule-ribonucleoprotein complex (Rodriguez et al. 2005). Subsequently, the kinesin KIF17b, which is involved in the nucleocytoplasmic transport of RNA and of a transcriptional coactivator, was shown to physically interact with a testis-specific member of the PIWI/Argonaute family, MIWI. It is assumed that this interaction takes place in the context of chromatoid bodies, which are the putative germline equivalents of somatic PBs (Kotaja et al. 2006). However, the nature of the functional interplay between KIF17b and MIWI and their roles in biogenesis and/or motility of chromatoid bodies remain to be determined.

It has been shown that the motility of somatic PBs requires ATP and microtubules (Aizer and Shav-Tal 2008; Sweet et al. 2007; Carmichael et al. 2006), which suggests that there is an association between microtubule motors and these RNPs. Disruption of microtubules increases the size and number of PBs in a given cell (Aizer and Shav-Tal 2008; Sweet et al. 2007; Carmichael et al. 2006), indicating that PB disassembly requires microtubule networks. However, unlike PBs, assembly of SGs is a microtubule-dependent process and the

movement of individual SG components is facilitated by the motor protein (Nadezhdina et al. 2010; Ohn et al. 2008; Ivanov et al. 2003). Consistent with these observations, my earlier findings provided evidence that microtubule motor protein functions are required to prevent the aggregation of PBs. Specifically, the study showed a reduction in PB motility, reduced numbers of Ago1-positive PBs, and a concomitant appearance of Ago1 aggregates in the absence of Cut7 activity. Because the Cut7 protein cannot bind microtubules at the restrictive temperature (Hagan and Yanagida 1992), it would not be able to function in the disassembly of large PBs or aggregates.

5.3.2. Cut7 activity is important for enhancing PTGS

In addition to PB homeostasis, microtubule dynamics appear to play a role in post-transcriptional gene silencing. Specifically, tubulin and katanin—the latter of which is a microtubule-severing enzyme—are required for miRNA-dependent inhibition of translation (Brodersen et al. 2008; Parry et al. 2007). However, until the publication of our work (Stoica, Park et al. 2010), the potential role for motor proteins in RNAi had not been investigated. The findings in our paper are consistent with a scenario in which interactions between Cut7 and RNAi effector proteins are important for PTGS. I demonstrated that the loss of Cut7 activity is associated with increased levels of reverse centromeric transcripts. As discussed earlier, reverse centromeric transcripts are degraded by PTGS via a mechanism that requires the RNAi machinery Ago1, Dcr1, and Rdp1 (Sigova et al. 2004; Volpe et al. 2002).

The association between the kinesin motor protein Cut7 and Ago1-positive PBs is not absolutely essential for RNAi; rather, it is assumed that the activity of this protein enhances PTGS in the cytoplasm. There are two potential non-mutually exclusive mechanisms of how Cut7 enhances PTGS in the cytoplasm. First, Cut7-dependent movement of Ago1-positive RNPs along the microtubules could be required for efficient scanning and sampling of cytoplasmic RNAs, a process which may determine whether they are translated, stored, or degraded. Second, Cut7 appears to play a role in the homeostasis of Ago1-containing PBs, specifically, the disassembly of large PBs. Non-aggregated, smaller PBs may more efficiently regulate mRNAs dispersed over a larger area of the cell (Decker et al. 2007).

The precise role of Ago1-containing PBs in PTGS is not clear, but a previous study has shown that microscopic PBs are not required for small RNA-dependent gene silencing in metazoans. Blocking siRNA or miRNA silencing pathways at any step prevents PB formation, indicating that these structures arise as a consequence of RNAi activity (Eulalio et al. 2007). As such, it is likely that the remaining pool of free non-PB associated Ago1 can still perform siRNA-directed cleavage of centromeric transcripts in the absence of Cut7 activity, albeit less efficiently. In this respect, it is not surprising that overexpression of the Ago1-binding domain of Cut7 (NT-Cut7) did not have a significant effect on PTGS, even though it affected the distribution of Ago1. Rather, I believe that expression of the NT-Cut7, which appears to block the stable association of Ago1 with PBs, results in the generation of a large pool of cytosolic Ago1 that can

function in PTGS. In contrast, the aggregated Ago1 that builds up in *cut7-24* mutants may be less available for PTGS, resulting in buildup of reverse centromeric transcripts.

5.3.3. TGS is not significantly affected by decreased Cut7 activity

Although Cut7 activity appears to be important for enhancing PTGS (presumably in the cytoplasm), loss of Cut7 activity does not significantly affect TGS in the nucleus. As shown in my qPCR assays, a slight increase in forward centromeric transcript level was observed in *cut7-24* cells that were grown at an elevated temperature of 29°C. However, the forward centromeric transcript levels were not dramatically changed and it is unlikely that the slight increase in the transcript levels at this temperature is biologically significant because *cut7-24* cells were not sensitive to TBZ at this temperature. Even though some Cut7 localizes to the nucleus (Hagan and Yanagida 1992), it seems that the activity of this protein is not required for silencing forward centromeric transcripts, a process that is regulated at the transcriptional level in the nucleus (Volpe et al. 2002).

5.3.4. A proposed model for Cut7 activity in maintaining PB homeostasis and formation

Based on our observations and evidence from previous studies, we proposed a model to account for how Cut7 and microtubules regulate the size and/or number of Ago1-containing RNPs in the cytoplasm. The model is depicted in Figure 5.2. It is assumed that Cut7 forms a dumbbell-shaped homotetramer

similar to its mammalian ortholog Eg5 (Kapitein et al. 2005) and that this tetramer drives anti-parallel sliding of microtubules toward the plus-end. PBs bind to microtubules as well as to associated motors such as Cut7. If the binding between PBs and microtubules is stronger than the interaction between PBs and Cut7, then the anti-parallel sliding of microtubules by the plus-end-directed motor protein Cut7 would pull apart the large PBs and result in the fission of the PBs. To be consistent with our observations, it is assumed that overexpression of the Ago1-binding domain of Cut7 does not inhibit the interaction of endogenous Cut7 with microtubules and other PB components. Therefore, we suggest that Cut7 negatively regulates the size of the Ago1-containing PBs. Cut7-dependent movement of PBs along microtubules may also be required to efficiently scan cytoplasmic RNA transcripts prior to their degradation.

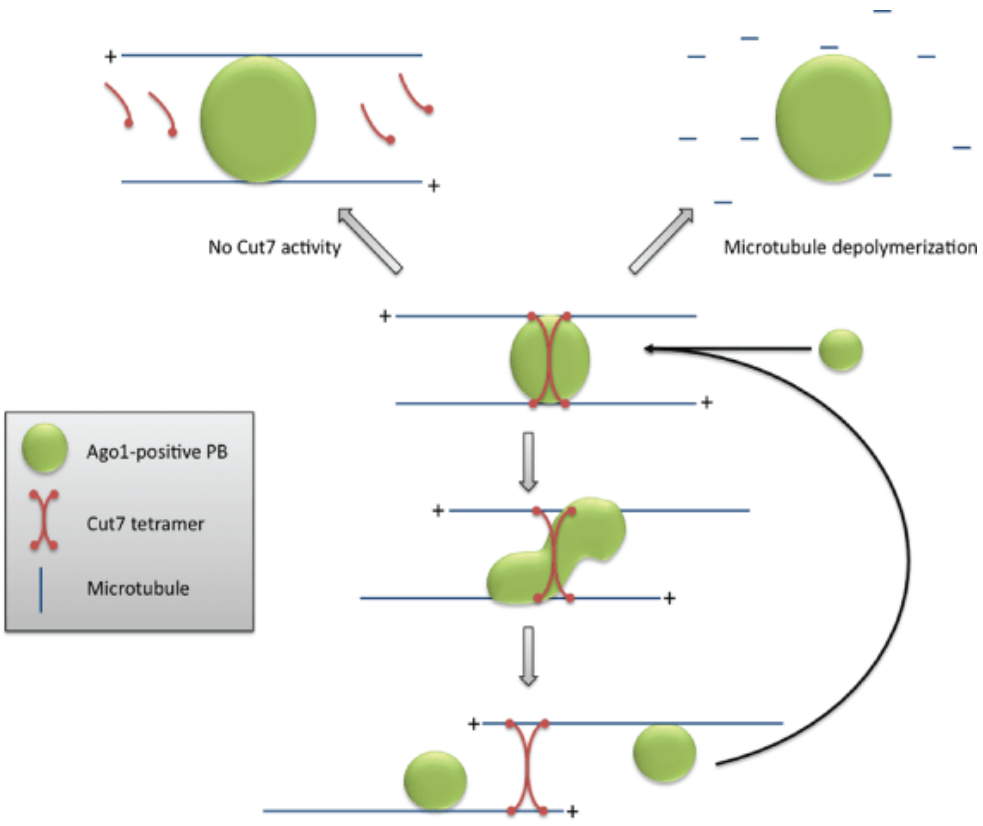

Figure 5.2. A proposed model depicting the role of the microtubule-associated motor protein Cut7 activity in regulating Ago1-containing PB homeostasis in *S. pombe*. The size of the PB is regulated by fission and fusion events. Microtubules and associated motors, such as Cut7, negatively regulate the size of Ago1-containing PBs. The model proposes that PBs bind to microtubules as well as to Cut7, though the association with microtubules is predicted to be stronger. Accordingly, the antiparallel sliding of microtubules by the plus-end-directed motor Cut7 results in fission of the PBs, which remain attached to the microtubules. Adapted from (Stoica, Park et al. 2010)

5.4. Phosphorylation states of Ago1 may affect targeting to PBs in *S. pombe*

5.4.1. Kinase and phosphatase activities; critical links between RNAi and other cell signaling pathways

Emerging data show that the activities and/or localization of gene-silencing factors are regulated by phosphorylation events (Johnston and Hutvagner 2011; Rudel et al. 2011; Paroo et al. 2009; Zeng et al. 2008). Reversible phosphorylation of proteins is the most common post-translational modification in a cell and is an important regulatory mechanism that is catalyzed by kinases and phosphatases (Bimbo et al. 2005). Phosphorylation and dephosphorylation represent a molecular on/off switch that regulates many key biological pathways within the cell, including signal transduction, cell division, apoptosis, and tumorigenesis (Fong et al. 2010; Bimbo et al. 2005; Surjit et al. 2005).

A potential regulatory mechanism for small RNA-mediated gene silencing by a kinase pathway was first described by Zeng *et al*. The study reported that hAgo2 phosphorylation can be induced by p38 MAPK pathway and is involved in mediating the protein localization to PBs (Zeng et al. 2008). My preliminary data showed that the number of Ago1-positive PBs is dramatically decreased after treatment with the kinase inhibitor staurosporine (refer to Appendix Figure A2). This may also indicate that specific kinase(s) and phosphatase(s) are involved in controlling Argonaute protein activity in response to different cellular conditions. However, given the controversy over the direct role of PBs in small RNA-

mediated gene silencing, the biological significance of PB localization of Argonaute proteins remains unclear (Kim et al. 2010).

Up until now, there is no direct evidence regarding the role of phosphatase(s) in RNAi. However, the fact that phosphorylation of hAgo2 on Y529 blocks loading of small RNAs (Rudel et al. 2011) implies that phosphatases can activate RNAi. Identification of the kinase(s)/phosphatase(s) that regulates Argonaute protein phosphorylation may be required to further understand the physiological significance of Argonaute protein localization and the Argonaute-mediated gene silencing process. In *S. pombe*, Spc1/Sty1/Phh1 and Pmk1 are homologs of mammalian p38 and ERK, respectively (Sugiura et al. 2011). Unpublished data from our lab has shown that Ssp2, an AMP-kinase, may be involved in Ago1-mediated gene silencing pathways (Dr. H. Parker, unpublished data). In addition, recent data has shown that kinase-specific Hsp90 cofactor Cdc37 is critical for RNAi in mammalian cells (Dr. J. Pare, unpublished data).

The fact that hAgo2 is phosphorylated, in part through the p38/MAPK pathway (Zeng et al. 2008), may indicate that Argonaute-mediated gene silencing is linked to specific signaling pathways, such as oncogenic pathways. MAPKs transfer extracellular signals from the cell membrane to the nucleus, allowing the cell to respond to extracellular stimuli. These types of signaling pathways are often affected in various types of cancer, leading to constitutive gene activation (Chen and Thorner 2007). More recently, aberrant expression of hAgo2 in tumor cells has been reported (Adams et al. 2009). It has been demonstrated that hAgo2 is up-regulated by an epidermal growth factor receptor (EGFR)/MAPK signaling

pathway in estrogen receptor (ER) negative breast cancer cell lines. MicroRNAs have also been implicated in cancer pathogenesis (Qi and Mu 2012; Esteller 2011).

5.4.2. Cellular localization of Argonaute protein and phosphorylation

Argonaute protein in the nucleus: In *S. pombe*, Ago1 functions in TGS together with the RITS complex in the nucleus (Motamedi et al. 2004; Sigova et al. 2004; Volpe et al. 2002). Although several studies have been reported regarding Argonaute nuclear events in other organisms (Weinmann et al. 2009; Guang et al. 2008), signals of Ago1 targeting to the nucleus in *S. pombe* have not been investigated. Although the *S. pombe* Ago1 sequence contains a potential NLS (KKKP motif starting at amino acid residue 150), it is also possible that its nuclear import is mediated by a non-classical type of signal similar to Rdp1. Unlike with hAgo2 (Weinmann et al. 2009), the Importin 8 ortholog in *S. pombe* is not required for Ago1 localization or function in the nucleus or PBs (Park et al. 2012).

Posttranslational modification of cargo has emerged as a common mechanism used to regulate nuclear transport (Mosammaparast and Pemberton 2004). For example, it has been shown that phosphorylation of the yeast transcription factor Pho4 regulates its association with karyopherins during both import and export (Kaffman et al. 1998a; Kaffman et al. 1998b). Phosphorylation also regulates the nuclear transport of several other proteins, including histone deacetylases, PDK-1, and Swi6 (Geymonat et al. 2004; Smillie et al. 2004; Lim et al. 2003).

With respect to miRNA processing, phosphorylation of the RNase III Drosha on S300 and S302 appears to play a role in targeting of this enzyme to the nucleus (Tang et al. 2010). However, while both endogenous and overexpressed Drosha localize to the nucleus constitutively, it is unclear whether or not phosphorylation at S300/S302 is a regulated process (Kim et al. 2010). Candidate kinases that could modify S300 and S302 include cyclin-dependent kinase 5, glycogen synthase kinase 3, mitogen-activated protein kinase 3, MAPK2, MAPK8, protein kinase A, protein kinase Cα, protein kinase B, and casein kinase I (Tang et al. 2010). This may indicate that S300/302 can be constitutively phosphorylated by multiple kinases. By analogy, nuclear localization of Ago1 may also be controlled in part by its phosphorylation state.

Argonaute protein in the cytoplasm: Ago1 is also engaged in PTGS in the cytoplasm (Sigova et al. 2004). A large pool of Ago1 localizes to PB-like structures in the cytoplasm (Carmichael et al. 2006). As mentioned above, Ago1 contains a putative NLS and the fact that a large pool of Ago1 localizes to the cytoplasm may indicate that a nuclear export signal (NES) in Ago1 is dominant over the NLS or that the NLS is normally masked. The NLS in Ago1 may also be non-functional. Although a number of *trans*-acting factors have been reported that regulate the targeting of Argonautes to PBs in mammalian cells (Rudel et al. 2011; Pare et al. 2009; Zeng et al. 2008), nothing is known about Ago1 targeting to yeast PBs. There is reason to suspect that the processes may be fundamentally different. For example, in mammalian cells, the binding of small RNAs to Argonautes is required for this process (PB localization), but in *S. pombe*, Ago1 is

still targeted to PBs in mutants that lack Dcr1 (and therefore lack siRNAs) (Carmichael et al. 2006). Recently, a body of evidence suggested that the processes of Argonaute targeting to PBs is regulated by phosphorylation (Johnston and Hutvagner 2011; Rudel et al. 2011; Zeng et al. 2008). It is possible that Ago1 targeting to PBs in *S. pombe* is regulated by its phosphorylation (refer to Appendix).

5.5. Future directions

Although many aspects of Argonaute protein function have been characterized, still many unanswered questions remain regarding the regulation of RNAi mechanisms. For example, there is much to learn about if/how Argonaute phosphorylation regulates protein localization and/or function. Recently, there have been reports on the homologous sequences that are phosphorylated in conserved 5'-siRNA binding region and PIWI domain in *S. pombe* (refer to Table 1.1) (Johnston and Hutvagner 2011; Rudel et al. 2011). Mutagenesis of putative phospho-serine, -threonine, and -tyrosine residues in the *S. pombe* Ago1 that are positionally conserved within the domains can be utilized for investigating physiological function of Ago1 phosphorylation. For example, Y513 in *S. pombe* Ago1, which corresponds to Y529 in the 5'-siRNA binding region of hAgo2 (Johnston and Hutvagner 2011; Rudel et al. 2011), can be changed to Phe/Glu. By utilizing the fluorescently tagged-Ago1 mutant strains and live-cell imaging, the localization of these mutants in *S. pombe* cells can be monitored to investigate

whether phosphorylation of Ago1 in this RNA binding region is required for its targeting to PBs in the cytoplasm.

In addition, the fluorescently tagged-Ago1 mutant strains can be utilized for further analysis to determine how a lack of phosphorylation and constitutive phosphorylation affect transcriptional and post-transcriptional gene silencing in this organism. Two well-established assays in our lab, a cell viability assay with microtubule disrupting drug and real-time qPCR, can be utilized to examine gene silencing defects in Ago1 mutant strains. Further, because phosphorylation often affects protein-protein interactions, it will be of interest to determine if/how phosphorylation affects the binding of known Ago1 partners, including Dcr1 and Rdp1 in *S. pombe*.

In the Appendix, I presented preliminary evidence suggesting both mutations (Y513F and Y513E) of amino acid residue in the 5'-siRNA binding pocket region of Ago1 disrupt the protein localization to PBs. This may suggest that dynamic phosphorylation states are required for Ago1 targeting to PBs. However, it is necessary to repeat the experiments to confirm the preliminary results. Further quantification assays will provide us with more conclusive data on these results. The preliminary data derived from the study of Ago1 mutants as well as kinase inhibitor experiments will serve as a foundation for future experiments designed to investigate the role of phosphorylation in Ago1 protein localization and function in *S. pombe*.

REFERENCES:

Adams, B. D., Claffey, K. P., & White, B. A. (2009). Argonaute-2 expression is regulated by epidermal growth factor receptor and mitogen-activated protein kinase signaling and correlates with a transformed phenotype in breast cancer cells. *Endocrinology, 150*(1), 14-23.

Aizer, A., Brody, Y., Ler, L. W., Sonenberg, N., Singer, R. H., & Shav-Tal, Y. (2008). The dynamics of mammalian P body transport, assembly, and disassembly in vivo. *Molecular Biology of the Cell, 19*(10), 4154-4166.

Aizer, A., & Shav-Tal, Y. (2008). Intracellular trafficking and dynamics of P bodies. *Prion, 2*(4), 131-134.

Alber, F., Dokudovskaya, S., Veenhoff, L. M., Zhang, W., Kipper, J., Devos, D., Suprapto, A., Karni-Schmidt, O., Williams, R., Chait, B. T., Sali, A., and Rout, M. P. (2007). The molecular architecture of the nuclear pore complex. *Nature,* 450(7170), 695-701.

Aleman, L. M., Doench, J., & Sharp, P. A. (2007). Comparison of siRNA-induced off-target RNA and protein effects. *RNA, 13*(3), 385-395.

Alfa, C., Fantes, P., Hyams, J., McLeod, M., & Warbrick, E. (1993). Experiments with Fission Yeast: A Laboratory Course Manual. *Plainview: Cold Spring Harbor Laboratory Press.*

Allshire, R. (2002). Molecular biology. RNAi and heterochromatin--a hushed-up affair. *Science, 297*(5588), 1818-1819.

Andrade, M. A., Petosa, C., O'Donoghue, S. I., Muller, C. W., and Bork, P. (2001). Comparison of ARM and HEAT protein repeats. *J.Mol.Biol., 309*(1), 1-18.

Andrei, M. A., Ingelfinger, D., Heintzmann, R., Achsel, T., Rivera-Pomar, R., & Luhrmann, R. (2005). A role for eIF4E and eIF4E-transporter in targeting mRNPs to mammalian processing bodies. *RNA, 11*(5), 717-727.

Apirion, D., & Miczak, A. (1993). RNA processing in prokaryotic cells. *BioEssays : News and Reviews in Molecular, Cellular and Developmental Biology, 15*(2), 113-120.

Aristarkhov, A., Mikulskis, A., Belasco, J. G., & Lin, E. C. (1996). Translation of the adhE transcript to produce ethanol dehydrogenase requires RNase III cleavage in escherichia coli. *Journal of Bacteriology, 178*(14), 4327-4332.

Arnold, M., Nath, A., Hauber, J., and Kehlenbach, R. H. (2006). Multiple importins function as nuclear transport receptors for the Rev protein of human immunodeficiency virus type 1. *J.Biol.Chem., 281*(30), 20883-20890.

Bagga, S., Bracht, J., Hunter, S., Massirer, K., Holtz, J., Eachus, R., et al. (2005). Regulation by let-7 and lin-4 miRNAs results in target mRNA degradation. *Cell, 122*(4), 553-563.

Bao, N., Lye, K. W., & Barton, M. K. (2004). MicroRNA binding sites in arabidopsis class III HD-ZIP mRNAs are required for methylation of the template chromosome. *Developmental Cell, 7*(5), 653-662.

Bashkirov, V. I., Scherthan, H., Solinger, J. A., Buerstedde, J. M., & Heyer, W. D. (1997). A mouse cytoplasmic exoribonuclease (mXRN1p) with preference for G4 tetraplex substrates. *The Journal of Cell Biology, 136*(4), 761-773.

Baulcombe, D. (2004). RNA silencing in plants. *Nature, 431*(7006), 356-363.

Bayne, E. H., White, S. A., Kagansky, A., Bijos, D. A., Sanchez-Pulido, L., Hoe, K. L., et al. (2010). Stc1: A critical link between RNAi and chromatin modification required for heterochromatin integrity. *Cell, 140*(5), 666-677.

Behm-Ansmant, I., Rehwinkel, J., Doerks, T., Stark, A., Bork, P., & Izaurralde, E. (2006). mRNA degradation by miRNAs and GW182 requires both CCR4:NOT deadenylase and DCP1:DCP2 decapping complexes. *Genes & Development, 20*(14), 1885-1898.

Beilharz, T. H., Humphreys, D. T., Clancy, J. L., Thermann, R., Martin, D. I., Hentze, M. W., et al. (2009). microRNA-mediated messenger RNA deadenylation contributes to translational repression in mammalian cells. *PloS One, 4*(8), e6783.

Benhamed, M., Herbig, U., Ye, T., Dejean, A., & Bischof, O. (2012). Senescence is an endogenous trigger for microRNA-directed transcriptional gene silencing in human cells. *Nature Cell Biology, 14*(3), 266-275.

Bernstein, E., Caudy, A. A., Hammond, S. M., & Hannon, G. J. (2001). Role for a bidentate ribonuclease in the initiation step of RNA interference. *Nature, 409*(6818), 363-366.

Bimbo, A., Jia, Y., Poh, S. L., Karuturi, R. K., den Elzen, N., Peng, X., et al. (2005). Systematic deletion analysis of fission yeast protein kinases. *Eukaryotic Cell, 4*(4), 799-813.

Birchler, J. A. (2009). Ubiquitous RNA-dependent RNA polymerase and gene silencing. *Genome Biology, 10*(11), 243.

Birmingham, A., Anderson, E. M., Reynolds, A., Ilsley-Tyree, D., Leake, D., Fedorov, Y., et al. (2006). 3' UTR seed matches, but not overall identity, are associated with RNAi off-targets. *Nature Methods, 3*(3), 199-204.

Bischoff, F. R., and Ponstingl, H. (1991). Catalysis of guanine nucleotide exchange on Ran by the mitotic regulator RCC1. Nature, 354(6348), 80-82.

Blaszczyk, J., Tropea, J. E., Bubunenko, M., Routzahn, K. M., Waugh, D. S., Court, D. L., et al. (2001). Crystallographic and modeling studies of RNase III suggest a mechanism for double-stranded RNA cleavage. *Structure, 9*(12), 1225-1236.

Bohmert, K., Camus, I., Bellini, C., Bouchez, D., Caboche, M., & Benning, C. (1998). AGO1 defines a novel locus of arabidopsis controlling leaf development. *The EMBO Journal, 17*(1), 170-180.

Brazer, S. C., Williams, H. P., Chappell, T. G., & Cande, W. Z. (2000). A fission yeast kinesin affects golgi membrane recycling. *Yeast, 16*(2), 149-166.

Bridge, A. J., Pebernard, S., Ducraux, A., Nicoulaz, A. L., & Iggo, R. (2003). Induction of an interferon response by RNAi vectors in mammalian cells. *Nature Genetics, 34*(3), 263-264.

Brodersen, P., Sakvarelidze-Achard, L., Bruun-Rasmussen, M., Dunoyer, P., Yamamoto, Y. Y., Sieburth, L., et al. (2008). Widespread translational inhibition by plant miRNAs and siRNAs. *Science, 320*(5880), 1185-1190.

Browning, H., Hayles, J., Mata, J., Aveline, L., Nurse, P., & McIntosh, J. R. (2000). Tea2p is a kinesin-like protein required to generate polarized growth in fission yeast. *The Journal of Cell Biology, 151*(1), 15-28.

Buhler, M., & Moazed, D. (2007). Transcription and RNAi in heterochromatic gene silencing. *Nature Structural & Molecular Biology, 14*(11), 1041-1048.

Buhler, M., Verdel, A., & Moazed, D. (2006). Tethering RITS to a nascent transcript initiates RNAi- and heterochromatin-dependent gene silencing. *Cell, 125*(5), 873-886.

Buker, S. M., Iida, T., Buhler, M., Villen, J., Gygi, S. P., Nakayama, J., et al. (2007). Two different argonaute complexes are required for siRNA generation and heterochromatin assembly in fission yeast. *Nature Structural & Molecular Biology, 14*(3), 200-207.

Carmell, M. A., Xuan, Z., Zhang, M. Q., & Hannon, G. J. (2002). The argonaute family: Tentacles that reach into RNAi, developmental control, stem cell maintenance, and tumorigenesis. *Genes & Development, 16*(21), 2733-2742.

Carmichael, J. B., Stoica, C., Parker, H., McCaffery, J. M., Simmonds, A. J., & Hobman, T. C. (2006). RNA interference effector proteins localize to mobile cytoplasmic puncta in schizosaccharomyces pombe. *Traffic, 7*(8), 1032-1044.

Carthew, R. W., & Sontheimer, E. J. (2009). Origins and mechanisms of miRNAs and siRNAs. *Cell, 136*(4), 642-655.

Catala, M., Lamontagne, B., Larose, S., Ghazal, G., & Elela, S. A. (2004). Cell cycle-dependent nuclear localization of yeast RNase III is required for efficient cell division. *Molecular Biology of the Cell, 15*(7), 3015-3030.

Cerutti, L., Mian, N., & Bateman, A. (2000). Domains in gene silencing and cell differentiation proteins: The novel PAZ domain and redefinition of the piwi domain. *Trends in Biochemical Sciences, 25*(10), 481-482.

Chanfreau, G., Legrain, P., & Jacquier, A. (1998). Yeast RNase III as a key processing enzyme in small nucleolar RNAs metabolism. *Journal of Molecular Biology, 284*(4), 975-988.

Chanfreau, G., Rotondo, G., Legrain, P., & Jacquier, A. (1998). Processing of a dicistronic small nucleolar RNA precursor by the RNA endonuclease Rnt1. *The EMBO Journal, 17*(13), 3726-3737.

Chang, S. S., Zhang, Z., & Liu, Y. (2012). RNA interference pathways in fungi: Mechanisms and functions. *Annual Review of Microbiology, 66*, 305-323.

Chen, C. C., Simard, M. J., Tabara, H., Brownell, D. R., McCollough, J. A., & Mello, C. C. (2005). A member of the polymerase beta nucleotidyltransferase superfamily is required for RNA interference in C. elegans. *Current Biology : CB, 15*(4), 378-383.

Chen, R. E., & Thorner, J. (2007). Function and regulation in MAPK signaling pathways: Lessons learned from the yeast saccharomyces cerevisiae. *Biochimica Et Biophysica Acta, 1773*(8), 1311-1340.

Chen, X. Q., Du, X., Liu, J., Balasubramanian, M. K., & Balasundaram, D. (2004). Identification of genes encoding putative nucleoporins and transport factors in the fission yeast schizosaccharomyces pombe: A deletion analysis. *Yeast, 21*(6), 495-509.

Chendrimada, T. P., Gregory, R. I., Kumaraswamy, E., Norman, J., Cooch, N., Nishikura, K., et al. (2005). TRBP recruits the dicer complex to Ago2 for microRNA processing and gene silencing. *Nature, 436*(7051), 740-744.

Chook, Y. M., and Blobel, G. (1999). Structure of the nuclear transport complex karyopherin-beta2-Ran x GppNHp. Nature, 399(6733), 230-237.

Chook, Y. M., & Suel, K. E. (2011). Nuclear import by karyopherin-betas: Recognition and inhibition. *Biochimica Et Biophysica Acta, 1813*(9), 1593-1606.

Chu, C. Y., & Rana, T. M. (2006). Translation repression in human cells by microRNA-induced gene silencing requires RCK/p54. *PLoS Biology, 4*(7), e210.

Chua, G., Lingner, C., Frazer, C., & Young, P. G. (2002). The sal3(+) gene encodes an importin-beta implicated in the nuclear import of Cdc25 in *Schizosaccharomyces pombe*. *Genetics, 162*(2), 689-703.

Cingolani, G., Bednenko, J., Gillespie, M. T., and Gerace, L. (2002). Molecular basis for the recognition of a nonclassical nuclear localization signal by importin beta. *Mol.Cell, 10*(6), 1345-1353.

Cingolani, G., Petosa, C., Weis, K., and Muller, C. W. (1999). Structure of importin-beta bound to the IBB domain of importin-alpha. *Nature, 399*(6733), 221-229.

Cogoni, C., & Macino, G. (1999). Gene silencing in neurospora crassa requires a protein homologous to RNA-dependent RNA polymerase. *Nature, 399*(6732), 166-169.

Colmenares, S. U., Buker, S. M., Buhler, M., Dlakic, M., & Moazed, D. (2007). Coupling of double-stranded RNA synthesis and siRNA generation in fission yeast RNAi. *Molecular Cell, 27*(3), 449-461.

Conti, E., Muller, C. W., and Stewart, M. (2006). Karyopherin flexibility in nucleocytoplasmic transport. *Curr.Opin.Struct.Biol., 16*(2), 237-244.

Cook, A., Bono, F., Jinek, M., and Conti, E. (2007). Structural biology of nucleocytoplasmic transport. *Annu.Rev.Biochem., 76* 647-671.

Cougot, N., Babajko, S., & Seraphin, B. (2004). Cytoplasmic foci are sites of mRNA decay in human cells. *The Journal of Cell Biology, 165*(1), 31-40.

Cox, D. N., Chao, A., Baker, J., Chang, L., Qiao, D., & Lin, H. (1998). A novel class of evolutionarily conserved genes defined by piwi are essential for stem cell self-renewal. *Genes & Development, 12*(23), 3715-3727.

Crombach, A., and Hogeweg, P. (2011). Is RNA-dependent RNA polymerase essential for transposon control? *BMC Syst.Biol., 5*, 104.

Cronshaw, J. M., Krutchinsky, A. N., Zhang, W., Chait, B. T., and Matunis, M. J. (2002). Proteomic analysis of the mammalian nuclear pore complex. *J.Cell Biol., 158*(5), 915-927.

Dalmay, T., Hamilton, A., Rudd, S., Angell, S., & Baulcombe, D. C. (2000). An RNA-dependent RNA polymerase gene in arabidopsis is required for posttranscriptional gene silencing mediated by a transgene but not by a virus. *Cell, 101*(5), 543-553.

Davis, L. I., and Blobel, G. (1986). Identification and characterization of a nuclear pore complex protein. *Cell, 45*(5), 699-709.

de Fougerolles, A., Vornlocher, H. P., Maraganore, J., & Lieberman, J. (2007). Interfering with disease: A progress report on siRNA-based therapeutics. *Nature Reviews.Drug Discovery, 6*(6), 443-453.

DeGrasse, J. A., DuBois, K. N., Devos, D., Siegel, T. N., Sali, A., Field, M. C., Rout, M. P., and Chait, B. T. (2009). Evidence for a shared nuclear pore complex architecture that is conserved from the last common eukaryotic ancestor. *Mol.Cell.Proteomics, 8*(9), 2119-2130.

Debeauchamp, J. L., Moses, A., Noffsinger, V. J., Ulrich, D. L., Job, G., Kosinski, A. M., et al. (2008). Chp1-Tas3 interaction is required to recruit RITS to fission yeast centromeres and for maintenance of centromeric heterochromatin. *Molecular and Cellular Biology, 28*(7), 2154-2166.

Decker, C. J., Teixeira, D., & Parker, R. (2007). Edc3p and a glutamine/asparagine-rich domain of Lsm4p function in processing body assembly in saccharomyces cerevisiae. *The Journal of Cell Biology, 179*(3), 437-449.

Denli, A. M., Tops, B. B., Plasterk, R. H., Ketting, R. F., & Hannon, G. J. (2004). Processing of primary microRNAs by the microprocessor complex. *Nature, 432*(7014), 231-235.

Djupedal, I., & Ekwall, K. (2009). Epigenetics: Heterochromatin meets RNAi. *Cell Research, 19*(3), 282-295.

Djupedal, I., Kos-Braun, I. C., Mosher, R. A., Soderholm, N., Simmer, F., Hardcastle, T. J., et al. (2009). Analysis of small RNA in fission yeast; centromeric siRNAs are potentially generated through a structured RNA. *The EMBO Journal, 28*(24), 3832-3844.

Drinnenberg, I. A., Weinberg, D. E., Xie, K. T., Mower, J. P., Wolfe, K. H., Fink, G. R., et al. (2009). RNAi in budding yeast. *Science, 326*(5952), 544-550.

Dunn, J. J. (1976). RNase III cleavage of single-stranded RNA. effect of ionic strength on the fideltiy of cleavage. *The Journal of Biological Chemistry, 251*(12), 3807-3814.

Ebert, A., Lein, S., Schotta, G., & Reuter, G. (2006). Histone modification and the control of heterochromatic gene silencing in drosophila. *Chromosome Research, 14*(4), 377-392.

Elbashir, S. M., Harborth, J., Lendeckel, W., Yalcin, A., Weber, K., & Tuschl, T. (2001). Duplexes of 21-nucleotide RNAs mediate RNA interference in cultured mammalian cells. *Nature, 411*(6836), 494-498.

El-Shami, M., Pontier, D., Lahmy, S., Braun, L., Picart, C., Vega, D., et al. (2007). Reiterated WG/GW motifs form functionally and evolutionarily conserved ARGONAUTE-binding platforms in RNAi-related components. *Genes & Development, 21*(20), 2539-2544.

Ender, C., & Meister, G. (2010). Argonaute proteins at a glance. *Journal of Cell Science, 123*(11), 1819-1823.

Esteller, M. (2011). Non-coding RNAs in human disease. *Nature Reviews Genetics, 12*(12), 861-874.

Eulalio, A., Behm-Ansmant, I., & Izaurralde, E. (2007a). P bodies: At the crossroads of post-transcriptional pathways. *Nature Reviews Molecular Cell Biology, 8*(1), 9-22.

Eulalio, A., Behm-Ansmant, I., Schweizer, D., & Izaurralde, E. (2007b). P-body formation is a consequence, not the cause, of RNA-mediated gene silencing. *Molecular and Cellular Biology, 27*(11), 3970-3981.

Eulalio, A., Helms, S., Fritzsch, C., Fauser, M., & Izaurralde, E. (2009). A C-terminal silencing domain in GW182 is essential for miRNA function. *RNA, 15*(6), 1067-1077.

Eulalio, A., Huntzinger, E., & Izaurralde, E. (2008). GW182 interaction with argonaute is essential for miRNA-mediated translational repression and mRNA decay. *Nature Structural & Molecular Biology, 15*(4), 346-353.

Eulalio, A., Huntzinger, E., Nishihara, T., Rehwinkel, J., Fauser, M., & Izaurralde, E. (2009). Deadenylation is a widespread effect of miRNA regulation. *RNA, 15*(1), 21-32.

Eulalio, A., Rehwinkel, J., Stricker, M., Huntzinger, E., Yang, S. F., Doerks, T., et al. (2007). Target-specific requirements for enhancers of decapping in miRNA-mediated gene silencing. *Genes & Development, 21*(20), 2558-2570.

Eulalio, A., Tritschler, F., & Izaurralde, E. (2009). The GW182 protein family in animal cells: New insights into domains required for miRNA-mediated gene silencing. *RNA, 15*(8), 1433-1442.

Eystathioy, T., Chan, E. K., Tenenbaum, S. A., Keene, J. D., Griffith, K., & Fritzler, M. J. (2002). A phosphorylated cytoplasmic autoantigen, GW182, associates with a unique population of human mRNAs within novel cytoplasmic speckles. *Molecular Biology of the Cell, 13*(4), 1338-1351.

Fabian, M. R., Mathonnet, G., Sundermeier, T., Mathys, H., Zipprich, J. T., Svitkin, Y. V., et al. (2009). Mammalian miRNA RISC recruits CAF1 and PABP to affect PABP-dependent deadenylation. *Molecular Cell, 35*(6), 868-880.

Fedorov, Y., Anderson, E. M., Birmingham, A., Reynolds, A., Karpilow, J., Robinson, K., et al. (2006). Off-target effects by siRNA can induce toxic phenotype. *RNA, 12*(7), 1188-1196.

Filipowicz, W., Jaskiewicz, L., Kolb, F. A., & Pillai, R. S. (2005). Post-transcriptional gene silencing by siRNAs and miRNAs. *Current Opinion in Structural Biology, 15*(3), 331-341.

Fire, A., Xu, S., Montgomery, M. K., Kostas, S. A., Driver, S. E., & Mello, C. C. (1998). Potent and specific genetic interference by double-stranded RNA in caenorhabditis elegans. *Nature, 391*(6669), 806-811.

Fong, C. S., Sato, M., & Toda, T. (2010). Fission yeast Pcp1 links polo kinase-mediated mitotic entry to gamma-tubulin-dependent spindle formation. *The EMBO Journal, 29*(1), 120-130.

Forsburg, S. L., & Rhind, N. (2006). Basic methods for fission yeast. *Yeast, 23*(3), 173-183.

Forstemann, K., Tomari, Y., Du, T., Vagin, V. V., Denli, A. M., Bratu, D. P., et al. (2005). Normal microRNA maturation and germ-line stem cell maintenance requires loquacious, a double-stranded RNA-binding domain protein. *PLoS Biology, 3*(7), e236.

Fried, H., & Kutay, U. (2003). Nucleocytoplasmic transport: Taking an inventory. *Cellular and Molecular Life Sciences, 60*(8), 1659-1688.

Friedman, R. C., Farh, K. K., Burge, C. B., & Bartel, D. P. (2009). Most mammalian mRNAs are conserved targets of microRNAs. *Genome Research, 19*(1), 92-105.

Fuchs, U., Damm-Welk, C., & Borkhardt, A. (2004). Silencing of disease-related genes by small interfering RNAs. *Current Molecular Medicine, 4*(5), 507-517.

Ge, D., Lamontagne, B., & Elela, S. A. (2005). RNase III-mediated silencing of a glucose-dependent repressor in yeast. *Current Biology, 15*(2), 140-145.

Geymonat, M., Spanos, A., Wells, G. P., Smerdon, S. J., & Sedgwick, S. G. (2004). Clb6/Cdc28 and Cdc14 regulate phosphorylation status and cellular localization of Swi6. *Molecular and Cellular Biology, 24*(6), 2277-2285.

Ghildiyal, M., & Zamore, P. D. (2009). Small silencing RNAs: An expanding universe. *Nature Reviews Genetics, 10*(2), 94-108.

Giraldez, A. J., Mishima, Y., Rihel, J., Grocock, R. J., Van Dongen, S., Inoue, K., et al. (2006). Zebrafish MiR-430 promotes deadenylation and clearance of maternal mRNAs. *Science, 312*(5770), 75-79.

Goldfarb, D. S., Corbett, A. H., Mason, D. A., Harreman, M. T., and Adam, S. A. (2004). Importin alpha: a multipurpose nuclear-transport receptor. *Trends Cell Biol., 14*(9), 505-514.

Gregory, R. I., Yan, K. P., Amuthan, G., Chendrimada, T., Doratotaj, B., Cooch, N., et al. (2004). The microprocessor complex mediates the genesis of microRNAs. *Nature, 432*(7014), 235-240.

Grewal, S. I. (2010). RNAi-dependent formation of heterochromatin and its diverse functions. *Current Opinion in Genetics & Development, 20*(2), 134-141.

Grewal, S. I., & Jia, S. (2007). Heterochromatin revisited. *Nature Reviews Genetics, 8*(1), 35-46.

Grewal, S. I., & Moazed, D. (2003). Heterochromatin and epigenetic control of gene expression. *Science, 301*(5634), 798-802.

Groves, M. R., Hanlon, N., Turowski, P., Hemmings, B. A., and Barford, D. (1999). The structure of the protein phosphatase 2A PR65/A subunit reveals the conformation of its 15 tandemly repeated HEAT motifs. *Cell, 96*(1), 99-110.

Guang, S., Bochner, A. F., Pavelec, D. M., Burkhart, K. B., Harding, S., Lachowiec, J., et al. (2008). An argonaute transports siRNAs from the cytoplasm to the nucleus. *Science, 321*(5888), 537-541.

Haase, A. D., Jaskiewicz, L., Zhang, H., Laine, S., Sack, R., Gatignol, A., et al. (2005). TRBP, a regulator of cellular PKR and HIV-1 virus expression, interacts with dicer and functions in RNA silencing. *EMBO Reports, 6*(10), 961-967.

Hagan, I., & Yanagida, M. (1990). Novel potential mitotic motor protein encoded by the fission yeast *cut7+* gene. *Nature, 347*(6293), 563-566.

Hagan, I., & Yanagida, M. (1992). Kinesin-related cut7 protein associates with mitotic and meiotic spindles in fission yeast. *Nature, 356*(6364), 74-76.

Halic, M., & Moazed, D. (2010). Dicer-independent primal RNAs trigger RNAi and heterochromatin formation. *Cell, 140*(4), 504-516.

Hall, I. M., Shankaranarayana, G. D., Noma, K., Ayoub, N., Cohen, A., & Grewal, S. I. (2002). Establishment and maintenance of a heterochromatin domain. *Science, 297*(5590), 2232-2237.

Hammond, S. M., Bernstein, E., Beach, D., & Hannon, G. J. (2000). An RNA-directed nuclease mediates post-transcriptional gene silencing in drosophila cells. *Nature, 404*(6775), 293-296.

Han, J., Lee, Y., Yeom, K. H., Kim, Y. K., Jin, H., & Kim, V. N. (2004). The drosha-DGCR8 complex in primary microRNA processing. *Genes & Development, 18*(24), 3016-3027.

Han, J., Lee, Y., Yeom, K. H., Nam, J. W., Heo, I., Rhee, J. K., et al. (2006). Molecular basis for the recognition of primary microRNAs by the drosha-DGCR8 complex. *Cell, 125*(5), 887-901.

Hannon, G. J. (2002). RNA interference. *Nature, 418*(6894), 244-251.

Heo, I., & Kim, V. N. (2009). Regulating the regulators: Posttranslational modifications of RNA silencing factors. *Cell, 139*(1), 28-31.

Hock, J., & Meister, G. (2008). The argonaute protein family. *Genome Biology, 9*(2), 210.

Hoelz, A., Debler, E. W., and Blobel, G. (2011). The structure of the nuclear pore complex. *Annu.Rev.Biochem., 80*, 613-643.

Hong, E. J., Villen, J., Gerace, E. L., Gygi, S. P., & Moazed, D. (2005). A cullin E3 ubiquitin ligase complex associates with Rik1 and the Clr4 histone H3-K9 methyltransferase and is required for RNAi-mediated heterochromatin formation. *RNA Biology, 2*(3), 106-111.

Hsia, K. C., Stavropoulos, P., Blobel, G., and Hoelz, A. (2007). Architecture of a coat for the nuclear pore membrane. *Cell, 131*(7), 1313-1326.

Huntzinger, E., Braun, J. E., Heimstadt, S., Zekri, L., & Izaurralde, E. (2010). Two PABPC1-binding sites in GW182 proteins promote miRNA-mediated gene silencing. *The EMBO Journal, 29*(24), 4146-4160.

Huntzinger, E., & Izaurralde, E. (2011). Gene silencing by microRNAs: Contributions of translational repression and mRNA decay. *Nature Reviews Genetics, 12*(2), 99-110.

Hutvagner, G., McLachlan, J., Pasquinelli, A. E., Balint, E., Tuschl, T., & Zamore, P. D. (2001). A cellular function for the RNA-interference enzyme dicer in the maturation of the let-7 small temporal RNA. *Science, 293*(5531), 834-838.

Hutvagner, G., & Zamore, P. D. (2002). A microRNA in a multiple-turnover RNAi enzyme complex. *Science, 297*(5589), 2056-2060.

Irvine, D. V., Zaratiegui, M., Tolia, N. H., Goto, D. B., Chitwood, D. H., Vaughn, M. W., et al. (2006). Argonaute slicing is required for heterochromatic silencing and spreading. *Science, 313*(5790), 1134-1137.

Ivanov, P. A., Chudinova, E. M., & Nadezhdina, E. S. (2003). Disruption of microtubules inhibits cytoplasmic ribonucleoprotein stress granule formation. *Experimental Cell Research, 290*(2), 227-233.

Jackson, A. L., Burchard, J., Schelter, J., Chau, B. N., Cleary, M., Lim, L., et al. (2006). Widespread siRNA "off-target" transcript silencing mediated by seed region sequence complementarity. *RNA, 12*(7), 1179-1187.

Jakel, S., Albig, W., Kutay, U., Bischoff, F. R., Schwamborn, K., Doenecke, D., and Gorlich, D. (1999). The importin beta/importin 7 heterodimer is a functional nuclear import receptor for histone H1. *EMBO J., 18*(9), 2411-2423.

Jakymiw, A., Ikeda, K., Fritzler, M. J., Reeves, W. H., Satoh, M., & Chan, E. K. (2006). Autoimmune targeting of key components of RNA interference. *Arthritis Research & Therapy, 8*(4), R87.

Jakymiw, A., Lian, S., Eystathioy, T., Li, S., Satoh, M., Hamel, J. C., et al. (2005). Disruption of GW bodies impairs mammalian RNA interference. *Nature Cell Biology, 7*(12), 1267-1274.

Jakymiw, A., Pauley, K. M., Li, S., Ikeda, K., Lian, S., Eystathioy, T., et al. (2007). The role of GW/P-bodies in RNA processing and silencing. *Journal of Cell Science, 120*(8), 1317-1323.

Janowski, B. A., Huffman, K. E., Schwartz, J. C., Ram, R., Nordsell, R., Shames, D. S., et al. (2006). Involvement of AGO1 and AGO2 in mammalian transcriptional silencing. *Nature Structural & Molecular Biology, 13*(9), 787-792.

Jaronczyk, K., Carmichael, J. B., & Hobman, T. C. (2005). Exploring the functions of RNA interference pathway proteins: Some functions are more RISCy than others? *The Biochemical Journal, 387*(3), 561-571.

Jenuwein, T. (2001). Re-SET-ting heterochromatin by histone methyltransferases. *Trends in Cell Biology, 11*(6), 266-273.

Jenuwein, T., & Allis, C. D. (2001). Translating the histone code. *Science, 293*(5532), 1074-1080.

Jiang, F., Ye, X., Liu, X., Fincher, L., McKearin, D., & Liu, Q. (2005). Dicer-1 and R3D1-L catalyze microRNA maturation in drosophila. *Genes & Development, 19*(14), 1674-1679.

Jinek, M., & Doudna, J. A. (2009). A three-dimensional view of the molecular machinery of RNA interference. *Nature, 457*(7228), 405-412.

Johnston, M., & Hutvagner, G. (2011). Posttranslational modification of argonautes and their role in small RNA-mediated gene regulation. *Silence, 2*, 5.

Kaffman, A., Rank, N. M., O'Neill, E. M., Huang, L. S., & O'Shea, E. K. (1998a). The receptor Msn5 exports the phosphorylated transcription factor Pho4 out of the nucleus. *Nature, 396*(6710), 482-486.

Kaffman, A., Rank, N. M., & O'Shea, E. K. (1998b). Phosphorylation regulates association of the transcription factor Pho4 with its import receptor Pse1/Kap121. *Genes & Development, 12*(17), 2673-2683.

Kalderon, D., Roberts, B. L., Richardson, W. D., & Smith, A. E. (1984). A short amino acid sequence able to specify nuclear location. *Cell, 39*(3 Pt 2), 499-509.

Kapitein, L. C., Peterman, E. J., Kwok, B. H., Kim, J. H., Kapoor, T. M., & Schmidt, C. F. (2005). The bipolar mitotic kinesin Eg5 moves on both microtubules that it crosslinks. *Nature, 435*(7038), 114-118.

Kappel, C., Zachariae, U., Dolker, N., and Grubmuller, H. (2010). An unusual hydrophobic core confers extreme flexibility to HEAT repeat proteins. *Biophys.J., 99*(5), 1596-1603.

Kawamata, T., & Tomari, Y. (2010). Making RISC. *Trends in Biochemical Sciences, 35*(7), 368-376.

Ketting, R. F., Fischer, S. E., Bernstein, E., Sijen, T., Hannon, G. J., & Plasterk, R. H. (2001). Dicer functions in RNA interference and in synthesis of small RNA involved in developmental timing in *C. elegans*. *Genes & Development, 15*(20), 2654-2659.

Kim, D. H., Saetrom, P., Snove, O.,Jr, & Rossi, J. J. (2008). MicroRNA-directed transcriptional gene silencing in mammalian cells. *Proceedings of the National Academy of Sciences of the United States of America, 105*(42), 16230-16235.

Kim, D. H., Villeneuve, L. M., Morris, K. V., & Rossi, J. J. (2006). Argonaute-1 directs siRNA-mediated transcriptional gene silencing in human cells. *Nature Structural & Molecular Biology, 13*(9), 793-797.

Kim, J., Krichevsky, A., Grad, Y., Hayes, G. D., Kosik, K. S., Church, G. M., et al. (2004). Identification of many microRNAs that copurify with polyribosomes in mammalian neurons. *Proceedings of the National Academy of Sciences of the United States of America, 101*(1), 360-365.

Kim, V. N., Han, J., & Siomi, M. C. (2009). Biogenesis of small RNAs in animals. *Nature Reviews.Molecular Cell Biology, 10*(2), 126-139.

Kim, Y. K., Heo, I., & Kim, V. N. (2010). Modifications of small RNAs and their associated proteins. *Cell, 143*(5), 703-709.

Kirino, Y., Vourekas, A., Sayed, N., de Lima Alves, F., Thomson, T., Lasko, P., et al. (2010). Arginine methylation of aubergine mediates tudor binding and germ plasm localization. *RNA, 16*(1), 70-78.

Kotaja, N., Lin, H., Parvinen, M., & Sassone-Corsi, P. (2006). Interplay of PIWI/Argonaute protein MIWI and kinesin KIF17b in chromatoid bodies of male germ cells. *Journal of Cell Science, 119*(13), 2819-2825.

Kufel, J., Dichtl, B., & Tollervey, D. (1999). Yeast Rnt1p is required for cleavage of the pre-ribosomal RNA in the 3' ETS but not the 5' ETS. *RNA, 5*(7), 909-917.

Lamontagne, B., Larose, S., Boulanger, J., & Elela, S. A. (2001). The RNase III family: A conserved structure and expanding functions in eukaryotic dsRNA metabolism. *Current Issues in Molecular Biology, 3*(4), 71-78.

Lee, S. R., Talsky, K. B., & Collins, K. (2009). A single RNA-dependent RNA polymerase assembles with mutually exclusive nucleotidyl transferase subunits to direct different pathways of small RNA biogenesis. *RNA, 15*(7), 1363-1374.

Lee, Y., Ahn, C., Han, J., Choi, H., Kim, J., Yim, J., et al. (2003). The nuclear RNase III drosha initiates microRNA processing. *Nature, 425*(6956), 415-419.

Lee, Y., Hur, I., Park, S. Y., Kim, Y. K., Suh, M. R., & Kim, V. N. (2006). The role of PACT in the RNA silencing pathway. *The EMBO Journal, 25*(3), 522-532.

Lee, S. J., Sekimoto, T., Yamashita, E., Nagoshi, E., Nakagawa, A., Imamoto, N., Yoshimura, M., Sakai, H., Chong, K. T., Tsukihara, T., and Yoneda, Y. (2003). The structure of importin-beta bound to SREBP-2: nuclear import of a transcription factor. *Science, 302*(5650), 1571-1575.

Lehmann, E., Brueckner, F., & Cramer, P. (2007). Molecular basis of RNA-dependent RNA polymerase II activity. *Nature, 450*(7168), 445-449.

Lejeune, E., & Allshire, R. C. (2011). Common ground: Small RNA programming and chromatin modifications. *Current Opinion in Cell Biology, 23*(3), 258-265.

Lejeune, E., Bayne, E. H., & Allshire, R. C. (2010). On the connection between RNAi and heterochromatin at centromeres. *Cold Spring Harbor Symposia on Quantitative Biology, 75*, 275-283.

Leung, A. K., Calabrese, J. M., & Sharp, P. A. (2006). Quantitative analysis of argonaute protein reveals microRNA-dependent localization to stress granules. *Proceedings of the National Academy of Sciences of the United States of America, 103*(48), 18125-18130.

Lewis, B. P., Shih, I. H., Jones-Rhoades, M. W., Bartel, D. P., & Burge, C. B. (2003). Prediction of mammalian microRNA targets. *Cell, 115*(7), 787-798.

Li, E. (2002). Chromatin modification and epigenetic reprogramming in mammalian development. *Nature Reviews Genetics, 3*(9), 662-673.

Li, L., Gu, W., Liang, C., Liu, Q., Mello, C. C., & Liu, Y. (2012). The translin-TRAX complex (C3PO) is a ribonuclease in tRNA processing. *Nature Structural & Molecular Biology, 19*(8), 824-830.

Li, Y., Lin, L., & Jin, P. (2008). The microRNA pathway and fragile X mental retardation protein. *Biochimica Et Biophysica Acta, 1779*(11), 702-705.

Lian, S., Jakymiw, A., Eystathioy, T., Hamel, J. C., Fritzler, M. J., & Chan, E. K. (2006). GW bodies, microRNAs and the cell cycle. *Cell Cycle, 5*(3), 242-245.

Lim, M. A., Kikani, C. K., Wick, M. J., & Dong, L. Q. (2003). Nuclear translocation of 3'-phosphoinositide-dependent protein kinase 1 (PDK-1): A potential regulatory mechanism for PDK-1 function. *Proceedings of the National Academy of Sciences of the United States of America, 100*(24), 14006-14011.

Lin, X., Ruan, X., Anderson, M. G., McDowell, J. A., Kroeger, P. E., Fesik, S. W., et al. (2005). siRNA-mediated off-target gene silencing triggered by a 7 nt complementation. *Nucleic Acids Research, 33*(14), 4527-4535.

Lingel, A., Simon, B., Izaurralde, E., & Sattler, M. (2004). Nucleic acid 3'-end recognition by the Argonaute2 PAZ domain. *Nature Structural & Molecular Biology,* 11(6), 576-577.

Lipardi, C., and Paterson, B. M. (2011). Retraction for Lipardi and Paterson, "Identification of an RNA-dependent RNA polymerase in Drosophila involved in RNAi and transposon suppression. *Proc.Natl.Acad.Sci.,* 108(36), 15010.

Lipardi, C., and Paterson, B. M. (2010). Identification of an RNA-dependent RNA polymerase in Drosophila establishes a common theme in RNA silencing. *Fly*, 4(1), 30-35.

Lipardi, C., and Paterson, B. M. (2009). Identification of an RNA-dependent RNA polymerase in Drosophila involved in RNAi and transposon suppression. *Proc.Natl.Acad.Sci., 106*(37), 15645-15650.

Lipardi, C., Wei, Q., & Paterson, B. M. (2001). RNAi as random degradative PCR: SiRNA primers convert mRNA into dsRNAs that are degraded to generate new siRNAs. *Cell, 107*(3), 297-307.

Liu, J., Carmell, M. A., Rivas, F. V., Marsden, C. G., Thomson, J. M., Song, J. J., et al. (2004). Argonaute2 is the catalytic engine of mammalian RNAi. *Science, 305*(5689), 1437-1441.

Liu, J., Rivas, F. V., Wohlschlegel, J., Yates, J. R.,3rd, Parker, R., & Hannon, G. J. (2005a). A role for the P-body component GW182 in microRNA function. *Nature Cell Biology, 7*(12), 1261-1266.

Liu, J., Valencia-Sanchez, M. A., Hannon, G. J., & Parker, R. (2005b). MicroRNA-dependent localization of targeted mRNAs to mammalian P-bodies. *Nature Cell Biology, 7*(7), 719-723.

Liu, Q., Rand, T. A., Kalidas, S., Du, F., Kim, H. E., Smith, D. P., et al. (2003). R2D2, a bridge between the initiation and effector steps of the drosophila RNAi pathway. *Science, 301*(5641), 1921-1925.

Liu, Y., Ye, X., Jiang, F., Liang, C., Chen, D., Peng, J., et al. (2009). C3PO, an endoribonuclease that promotes RNAi by facilitating RISC activation. *Science, 325*(5941), 750-753.

Livak, K. J., & Schmittgen, T. D. (2001). Analysis of relative gene expression data using real-time quantitative PCR and the 2(-delta delta C(T)) method. *Methods, 25*(4), 402-408.

Loschi, M., Leishman, C. C., Berardone, N., & Boccaccio, G. L. (2009). Dynein and kinesin regulate stress-granule and P-body dynamics. *Journal of Cell Science, 122*(21), 3973-3982.

Lusk, C. P., Makhnevych, T., & Wozniak, R. W. (2004). New ways to skin a kap: Mechanisms for controlling nuclear transport. *Biochemistry and Cell Biology, 82*(6), 618-625.

MacRae, I. J., & Doudna, J. A. (2007). Ribonuclease revisited: Structural insights into ribonuclease III family enzymes. *Current Opinion in Structural Biology, 17*(1), 138-145.

MacRae, I. J., Ma, E., Zhou, M., Robinson, C. V., & Doudna, J. A. (2008). In vitro reconstitution of the human RISC-loading complex. *Proceedings of the National Academy of Sciences of the United States of America, 105*(2), 512-517.

Maida, Y., Yasukawa, M., Furuuchi, M., Lassmann, T., Possemato, R., Okamoto, N., et al. (2009). An RNA-dependent RNA polymerase formed by TERT and the RMRP RNA. *Nature, 461*(7261), 230-235.

Mallik, R., & Gross, S. P. (2004). Molecular motors: Strategies to get along. *Current Biology, 14*(22), R971-82.

Maniataki, E., & Mourelatos, Z. (2005). A human, ATP-independent, RISC assembly machine fueled by pre-miRNA. *Genes & Development, 19*(24), 2979-2990.

Maroney, P. A., Yu, Y., Fisher, J., & Nilsen, T. W. (2006). Evidence that microRNAs are associated with translating messenger RNAs in human cells. *Nature Structural & Molecular Biology, 13*(12), 1102-1107.

Marques, J. T., & Williams, B. R. (2005). Activation of the mammalian immune system by siRNAs. *Nature Biotechnology, 23*(11), 1399-1405.

Martens, H., Novotny, J., Oberstrass, J., Steck, T. L., Postlethwait, P., & Nellen, W. (2002). RNAi in dictyostelium: The role of RNA-directed RNA polymerases and double-stranded RNase. *Molecular Biology of the Cell, 13*(2), 445-453.

Martinez, J., Patkaniowska, A., Urlaub, H., Luhrmann, R., & Tuschl, T. (2002). Single-stranded antisense siRNAs guide target RNA cleavage in RNAi. *Cell, 110*(5), 563-574.

Martinez, J., & Tuschl, T. (2004). RISC is a 5' phosphomonoester-producing RNA endonuclease. *Genes & Development, 18*(9), 975-980.

Mason, D. A., Stage, D. E., and Goldfarb, D. S. (2009). Evolution of the metazoan-specific importin alpha gene family. *J.Mol.Evol., 68*(4), 351-365.

Mathonnet, G., Fabian, M. R., Svitkin, Y. V., Parsyan, A., Huck, L., Murata, T., et al. (2007). MicroRNA inhibition of translation initiation in vitro by targeting the cap-binding complex eIF4F. *Science, 317*(5845), 1764-1767.

Matzke, M. A., Primig, M., Trnovsky, J., and Matzke, A. J. (1989). Reversible methylation and inactivation of marker genes in sequentially transformed tobacco plants. *EMBO J.*, 8(3), 643-649.

Meister, G., Landthaler, M., Patkaniowska, A., Dorsett, Y., Teng, G., & Tuschl, T. (2004). Human Argonaute2 mediates RNA cleavage targeted by miRNAs and siRNAs. *Molecular Cell, 15*(2), 185-197.

Meister, G., Landthaler, M., Peters, L., Chen, P. Y., Urlaub, H., Luhrmann, R., et al. (2005). Identification of novel argonaute-associated proteins. *Current Biology, 15*(23), 2149-2155.

Meister, G., & Tuschl, T. (2004). Mechanisms of gene silencing by double-stranded RNA. *Nature, 431*(7006), 343-349.

Mello, C. C., & Conte, D.,Jr. (2004). Revealing the world of RNA interference. *Nature, 431*(7006), 338-342.

Miki, H., Setou, M., Kaneshiro, K., & Hirokawa, N. (2001). All kinesin superfamily protein, KIF, genes in mouse and human. *Proceedings of the National Academy of Sciences of the United States of America, 98*(13), 7004-7011.

Moazed, D. (2009). Small RNAs in transcriptional gene silencing and genome defence. *Nature, 457*(7228), 413-420.

Moazed, D., Buhler, M., Buker, S. M., Colmenares, S. U., Gerace, E. L., Gerber, S. A., et al. (2006). Studies on the mechanism of RNAi-dependent heterochromatin assembly. *Cold Spring Harbor Symposia on Quantitative Biology, 71*, 461-471.

Mosammaparast, N., and Pemberton, L. F. (2004). Karyopherins: from nuclear-transport mediators to nuclear-function regulators. *Trends Cell Biol., 14*(10), 547-556.

Mosammaparast, N., Guo, Y., Shabanowitz, J., Hunt, D. F., and Pemberton, L. F. (2002). Pathways mediating the nuclear import of histones H3 and H4 in yeast. *J.Biol.Chem., 277*(1), 862-868.

Mosammaparast, N., Jackson, K. R., Guo, Y., Brame, C. J., Shabanowitz, J., Hunt, D. F., et al. (2001). Nuclear import of histone H2A and H2B is mediated by a network of karyopherins. *The Journal of Cell Biology, 153*(2), 251-262.

Mosammaparast, N., & Pemberton, L. F. (2004). Karyopherins: From nuclear-transport mediators to nuclear-function regulators. *Trends in Cell Biology, 14*(10), 547-556.

Moser, J. J., & Fritzler, M. J. (2010). Cytoplasmic ribonucleoprotein (RNP) bodies and their relationship to GW/P bodies. *The International Journal of Biochemistry & Cell Biology, 42*(6), 828-843.

Motamedi, M. R., Verdel, A., Colmenares, S. U., Gerber, S. A., Gygi, S. P., & Moazed, D. (2004). Two RNAi complexes, RITS and RDRC, physically interact and localize to noncoding centromeric RNAs. *Cell, 119*(6), 789-802.

Mourrain, P., Beclin, C., Elmayan, T., Feuerbach, F., Godon, C., Morel, J. B., et al. (2000). Arabidopsis SGS2 and SGS3 genes are required for posttranscriptional gene silencing and natural virus resistance. *Cell, 101*(5), 533-542.

Muhlhausser, P., Muller, E. C., Otto, A., & Kutay, U. (2001). Multiple pathways contribute to nuclear import of core histones. *EMBO Reports, 2*(8), 690-696.

Nadezhdina, E. S., Lomakin, A. J., Shpilman, A. A., Chudinova, E. M., & Ivanov, P. A. (2010). Microtubules govern stress granule mobility and dynamics. *Biochimica Et Biophysica Acta, 1803*(3), 361-371.

Nagel, R., & Ares, M.,Jr. (2000). Substrate recognition by a eukaryotic RNase III: The double-stranded RNA-binding domain of Rnt1p selectively binds RNA containing a 5'-AGNN-3' tetraloop. *RNA, 6*(8), 1142-1156.

Nardozzi, J. D., Lott, K., and Cingolani, G. (2010). Phosphorylation meets nuclear import: a review. *Cell.Commun.Signal., 8* 32.

Noma, K., Sugiyama, T., Cam, H., Verdel, A., Zofall, M., Jia, S., et al. (2004). RITS acts in cis to promote RNA interference-mediated transcriptional and post-transcriptional silencing. *Nature Genetics, 36*(11), 1174-1180.

Nottrott, S., Simard, M. J., & Richter, J. D. (2006). Human let-7a miRNA blocks protein production on actively translating polyribosomes. *Nature Structural & Molecular Biology, 13*(12), 1108-1114.

Ohn, T., Kedersha, N., Hickman, T., Tisdale, S., & Anderson, P. (2008). A functional RNAi screen links O-GlcNAc modification of ribosomal proteins to stress granule and processing body assembly. *Nature Cell Biology, 10*(10), 1224-1231.

Okamura, K., & Lai, E. C. (2008). Endogenous small interfering RNAs in animals. *Nature Reviews.Molecular Cell Biology, 9*(9), 673-678.

O'Reilly, A. J., Dacks, J. B., & Field, M. C. (2011). Evolution of the karyopherin-beta family of nucleocytoplasmic transport factors; ancient origins and continued specialization. *PloS One, 6*(4), e19308.

Paddison, P. J., Caudy, A. A., Bernstein, E., Hannon, G. J., & Conklin, D. S. (2002). Short hairpin RNAs (shRNAs) induce sequence-specific silencing in mammalian cells. *Genes & Development, 16*(8), 948-958.

Pare, J. M., Lopez-Orozco, J., & Hobman, T. C. (2011). MicroRNA-binding is required for recruitment of human argonaute 2 to stress granules and P-bodies. *Biochemical and Biophysical Research Communications, 414*(1), 259-264.

Pare, J. M., Tahbaz, N., Lopez-Orozco, J., LaPointe, P., Lasko, P., & Hobman, T. C. (2009). Hsp90 regulates the function of argonaute 2 and its recruitment to stress granules and P-bodies. *Molecular Biology of the Cell, 20*(14), 3273-3284.

Park, J., Freitag, S. I., Young, P. G., & Hobman, T. C. (2012). The karyopherin Sal3 is required for nuclear import of the core RNA interference pathway protein Rdp1. *Traffic, 13*(4):520-531.

Parker, J. S., Roe, S. M., & Barford, D. (2005). Structural insights into mRNA recognition from a PIWI domain-siRNA guide complex. *Nature, 434*(7033), 663-666.

Parker, R., & Sheth, U. (2007). P bodies and the control of mRNA translation and degradation. *Molecular Cell, 25*(5), 635-646.

Paroo, Z., Ye, X., Chen, S., & Liu, Q. (2009). Phosphorylation of the human microRNA-generating complex mediates MAPK/Erk signaling. *Cell, 139*(1), 112-122.

Parry, D. H., Xu, J., & Ruvkun, G. (2007). A whole-genome RNAi screen for C. elegans miRNA pathway genes. *Current Biology, 17*(23), 2013-2022.

Partridge, J. F., DeBeauchamp, J. L., Kosinski, A. M., Ulrich, D. L., Hadler, M. J., & Noffsinger, V. J. (2007). Functional separation of the requirements for establishment and maintenance of centromeric heterochromatin. *Molecular Cell, 26*(4), 593-602.

Partridge, J. F., Scott, K. S., Bannister, A. J., Kouzarides, T., & Allshire, R. C. (2002). Cis-acting DNA from fission yeast centromeres mediates histone H3 methylation and recruitment of silencing factors and cohesin to an ectopic site. *Current Biology, 12*(19), 1652-1660.

Pelczar, H., Woisard, A., Lemaitre, J. M., Chachou, M., & Andeol, Y. (2010). Evidence for an RNA polymerization activity in axolotl and xenopus egg extracts. *PloS One, 5*(12), e14411.

Peng, Y., & Weisman, L. S. (2008). The cyclin-dependent kinase Cdk1 directly regulates vacuole inheritance. *Developmental Cell, 15*(3), 478-485.

Peters, A. H., O'Carroll, D., Scherthan, H., Mechtler, K., Sauer, S., Schofer, C., et al. (2001). Loss of the Suv39h histone methyltransferases impairs mammalian heterochromatin and genome stability. *Cell, 107*(3), 323-337.

Peters, L., & Meister, G. (2007). Argonaute proteins: Mediators of RNA silencing. *Molecular Cell, 26*(5), 611-623.

Petersen, C. P., Bordeleau, M. E., Pelletier, J., & Sharp, P. A. (2006). Short RNAs repress translation after initiation in mammalian cells. *Molecular Cell, 21*(4), 533-542.

Pidoux, A., Mellone, B., & Allshire, R. (2004). Analysis of chromatin in fission yeast. *Methods, 33*(3), 252-259.

Pidoux, A. L., & Allshire, R. C. (2004). Kinetochore and heterochromatin domains of the fission yeast centromere. *Chromosome Research : An International Journal on the Molecular, Supramolecular and Evolutionary Aspects of Chromosome Biology, 12*(6), 521-534.

Pidoux, A. L., LeDizet, M., & Cande, W. Z. (1996). Fission yeast pkl1 is a kinesin-related protein involved in mitotic spindle function. *Molecular Biology of the Cell, 7*(10), 1639-1655.

Pidoux, A. L., Uzawa, S., Perry, P. E., Cande, W. Z., & Allshire, R. C. (2000). Live analysis of lagging chromosomes during anaphase and their effect on spindle elongation rate in fission yeast. *Journal of Cell Science, 113 (23)*, 4177-4191.

Pillai, R. S., Bhattacharyya, S. N., Artus, C. G., Zoller, T., Cougot, N., Basyuk, E., et al. (2005). Inhibition of translational initiation by let-7 MicroRNA in human cells. *Science, 309*(5740), 1573-1576.

Pillai, R. S., Bhattacharyya, S. N., & Filipowicz, W. (2007). Repression of protein synthesis by miRNAs: How many mechanisms? *Trends in Cell Biology, 17*(3), 118-126.

Preall, J. B., & Sontheimer, E. J. (2005). RNAi: RISC gets loaded. *Cell, 123*(4), 543-545.

Qi, H. H., Ongusaha, P. P., Myllyharju, J., Cheng, D., Pakkanen, O., Shi, Y., et al. (2008). Prolyl 4-hydroxylation regulates argonaute 2 stability. *Nature, 455*(7211), 421-424.

Qi, J., & Mu, D. (2012). MicroRNAs and lung cancers: From pathogenesis to clinical implications. *Frontiers of Medicine, 6*(2), 134-155.

Reichelt, R., Holzenburg, A., Buhle, E. L.,Jr, Jarnik, M., Engel, A., and Aebi, U. (1990). Correlation between structure and mass distribution of the nuclear pore complex and of distinct pore complex components. *J.Cell Biol., 110*(4), 883-894.

Regnier, P., & Grunberg-Manago, M. (1989). Cleavage by RNase III in the transcripts of the met Y-nus-A-infB operon of escherichia coli releases the tRNA and initiates the decay of the downstream mRNA. *Journal of Molecular Biology, 210*(2), 293-302.

Rehwinkel, J., Behm-Ansmant, I., Gatfield, D., & Izaurralde, E. (2005). A crucial role for GW182 and the DCP1:DCP2 decapping complex in miRNA-mediated gene silencing. *RNA, 11*(11), 1640-1647.

Ribbeck, K., Lipowsky, G., Kent, H. M., Stewart, M., and Gorlich, D. (1998). NTF2 mediates nuclear import of Ran. *EMBO J., 17*(22), 6587-6598.

Reuter, M., Chuma, S., Tanaka, T., Franz, T., Stark, A., & Pillai, R. S. (2009). Loss of the mili-interacting tudor domain-containing protein-1 activates transposons and alters the mili-associated small RNA profile. *Nature Structural & Molecular Biology, 16*(6), 639-646.

Ringrose, L., & Paro, R. (2004). Epigenetic regulation of cellular memory by the polycomb and trithorax group proteins. *Annual Review of Genetics, 38*, 413-443.

Rivas, F. V., Tolia, N. H., Song, J. J., Aragon, J. P., Liu, J., Hannon, G. J., et al. (2005). Purified Argonaute2 and an siRNA form recombinant human RISC. *Nature Structural & Molecular Biology, 12*(4), 340-349.

Robertson, H. D., Webster, R. E., & Zinder, N. D. (1968). Purification and properties of ribonuclease III from escherichia coli. *The Journal of Biological Chemistry, 243*(1), 82-91.

Rodriguez, A. J., Seipel, S. A., Hamill, D. R., Romancino, D. P., DI Carlo, M., Suprenant, K. A., et al. (2005). Seawi--a sea urchin piwi/argonaute family member is a component of MT-RNP complexes. *RNA, 11*(5), 646-656.

Rout, M. P., Aitchison, J. D., Magnasco, M. O., and Chait, B. T. (2003). Virtual gating and nuclear transport: the hole picture. *Trends Cell Biol., 13*(12), 622-628.

Rout, M. P., Aitchison, J. D., Suprapto, A., Hjertaas, K., Zhao, Y., and Chait, B. T. (2000). The yeast nuclear pore complex: composition, architecture, and transport mechanism. *J.Cell Biol., 148*(4), 635-651.

Rout, M. P., and Aitchison, J. D. (2001). The nuclear pore complex as a transport machine. *J.Biol.Chem., 276*(20), 16593-16596.

Rout, M. P., Blobel, G., and Aitchison, J. D. (1997). A distinct nuclear import pathway used by ribosomal proteins. *Cell, 89*(5), 715-725.

Rudel, S., & Meister, G. (2008). Phosphorylation of argonaute proteins: Regulating gene regulators. *The Biochemical Journal, 413*(3), e7-9.

Rudel, S., Wang, Y., Lenobel, R., Korner, R., Hsiao, H. H., Urlaub, H., et al. (2011). Phosphorylation of human argonaute proteins affects small RNA binding. *Nucleic Acids Research, 39*(6), 2330-2343.

Rybak, A., Fuchs, H., Hadian, K., Smirnova, L., Wulczyn, E. A., Michel, G., et al. (2009). The let-7 target gene mouse lin-41 is a stem cell specific E3 ubiquitin ligase for the miRNA pathway protein Ago2. *Nature Cell Biology, 11*(12), 1411-1420.

Sabatinos, S. A., & Forsburg, S. L. (2010). Molecular genetics of schizosaccharomyces pombe. *Methods in Enzymology, 470*, 759-795.

Sadaie, M., Iida, T., Urano, T., & Nakayama, J. (2004). A chromodomain protein, Chp1, is required for the establishment of heterochromatin in fission yeast. *The EMBO Journal, 23*(19), 3825-3835.

Saetrom, P., Heale, B. S., Snove, O.,Jr, Aagaard, L., Alluin, J., & Rossi, J. J. (2007). Distance constraints between microRNA target sites dictate efficacy and cooperativity. *Nucleic Acids Research, 35*(7), 2333-2342.

Saito, K., Ishizuka, A., Siomi, H., & Siomi, M. C. (2005). Processing of pre-microRNAs by the dicer-1-loquacious complex in drosophila cells. *PLoS Biology, 3*(7), e235.

Sasaki, T., & Shimizu, N. (2007). Evolutionary conservation of a unique amino acid sequence in human DICER protein essential for binding to argonaute family proteins. *Gene, 396*(2), 312-320.

Schalch, T., Job, G., Noffsinger, V. J., Shanker, S., Kuscu, C., Joshua-Tor, L., et al. (2009). High-affinity binding of Chp1 chromodomain to K9 methylated histone H3 is required to establish centromeric heterochromatin. *Molecular Cell, 34*(1), 36-46.

Schiebel, W., Haas, B., Marinkovic, S., Klanner, A., & Sanger, H. L. (1993). RNA-directed RNA polymerase from tomato leaves. I. purification and physical properties. *The Journal of Biological Chemistry, 268*(16), 11851-11857.

Schirle, N. T., & MacRae, I. J. (2012). The crystal structure of human Argonaute2. *Science, 336*(6084), 1037-1040.

Schoch, C. L., Aist, J. R., Yoder, O. C., & Gillian Turgeon, B. (2003). A complete inventory of fungal kinesins in representative filamentous ascomycetes. *Fungal Genetics and Biology, 39*(1), 1-15.

Sen, G. L., & Blau, H. M. (2005). Argonaute 2/RISC resides in sites of mammalian mRNA decay known as cytoplasmic bodies. *Nature Cell Biology, 7*(6), 633-636.

Shabalina, S. A., & Koonin, E. V. (2008). Origins and evolution of eukaryotic RNA interference. *Trends in Ecology & Evolution, 23*(10), 578-587.

Sheth, U., & Parker, R. (2003). Decapping and decay of messenger RNA occur in cytoplasmic processing bodies. *Science, 300*(5620), 805-808.

Shimada, A., Dohke, K., Sadaie, M., Shinmyozu, K., Nakayama, J., Urano, T., et al. (2009). Phosphorylation of Swi6/HP1 regulates transcriptional gene silencing at heterochromatin. *Genes & Development, 23*(1), 18-23.

Shiu, P. K., Raju, N. B., Zickler, D., & Metzenberg, R. L. (2001). Meiotic silencing by unpaired DNA. *Cell, 107*(7), 905-916.

Sigova, A., Rhind, N., & Zamore, P. D. (2004). A single argonaute protein mediates both transcriptional and posttranscriptional silencing in *Schizosaccharomyces pombe*. *Genes & Development, 18*(19), 2359-2367.

Sijen, T., Fleenor, J., Simmer, F., Thijssen, K. L., Parrish, S., Timmons, L., et al. (2001). On the role of RNA amplification in dsRNA-triggered gene silencing. *Cell, 107*(4), 465-476.

Simmer, F., Buscaino, A., Kos-Braun, I. C., Kagansky, A., Boukaba, A., Urano, T., et al. (2010). Hairpin RNA induces secondary small interfering RNA synthesis and silencing in *trans* in fission yeast. *EMBO Reports, 11*(2), 112-118.

Siomi, H., & Siomi, M. C. (2009). On the road to reading the RNA-interference code. *Nature, 457*(7228), 396-404.

Sledz, C. A., Holko, M., de Veer, M. J., Silverman, R. H., & Williams, B. R. (2003). Activation of the interferon system by short-interfering RNAs. *Nature Cell Biology, 5*(9), 834-839.

Smardon, A., Spoerke, J. M., Stacey, S. C., Klein, M. E., Mackin, N., & Maine, E. M. (2000). EGO-1 is related to RNA-directed RNA polymerase and functions in germ-line development and RNA interference in C. elegans. *Current Biology, 10*(4), 169-178.

Smillie, D. A., Llinas, A. J., Ryan, J. T., Kemp, G. D., & Sommerville, J. (2004). Nuclear import and activity of histone deacetylase in xenopus oocytes is regulated by phosphorylation. *Journal of Cell Science, 117*(9), 1857-1866.

Song, J. J., Liu, J., Tolia, N. H., Schneiderman, J., Smith, S. K., Martienssen, R. A., et al. (2003). The crystal structure of the Argonaute2 PAZ domain reveals an RNA binding motif in RNAi effector complexes. *Nature Structural Biology, 10*(12), 1026-1032.

Stoica, C., Carmichael, J. B., Parker, H., Pare, J., & Hobman, T. C. (2006). Interactions between the RNA interference effector protein Ago1 and 14-3-3 proteins: Consequences for cell cycle progression. *The Journal of Biological Chemistry, 281*(49), 37646-37651.

Stoica, C., Park, J., Pare, J. M., Willows, S., & Hobman, T. C. (2010). The kinesin motor protein Cut7 regulates biogenesis and function of Ago1-complexes. *Traffic, 11*(1), 25-36.

Sugiura, R., Satoh, R., Ishiwata, S., Umeda, N., & Kita, A. (2011). Role of RNA-binding proteins in MAPK signal transduction pathway. *Journal of Signal Transduction, 2011*, 109746.

Sugiyama, T., Cam, H., Verdel, A., Moazed, D., & Grewal, S. I. (2005). RNA-dependent RNA polymerase is an essential component of a self-enforcing loop coupling heterochromatin assembly to siRNA production. *Proceedings of the National Academy of Sciences of the United States of America, 102*(1), 152-157.

Surjit, M., Kumar, R., Mishra, R. N., Reddy, M. K., Chow, V. T., & Lal, S. K. (2005). The severe acute respiratory syndrome coronavirus nucleocapsid protein is phosphorylated and localizes in the cytoplasm by 14-3-3-mediated translocation. *Journal of Virology, 79*(17), 11476-11486.

Sweet, T. J., Boyer, B., Hu, W., Baker, K. E., & Coller, J. (2007). Microtubule disruption stimulates P-body formation. *RNA, 13*(4), 493-502.

Tabara, H., Yigit, E., Siomi, H., & Mello, C. C. (2002). The dsRNA binding protein RDE-4 interacts with RDE-1, DCR-1, and a DExH-box helicase to direct RNAi in *C. elegans*. *Cell, 109*(7), 861-871.

Tahbaz, N., Carmichael, J. B., & Hobman, T. C. (2001). GERp95 belongs to a family of signal-transducing proteins and requires Hsp90 activity for stability and golgi localization. *The Journal of Biological Chemistry, 276*(46), 43294-43299.

Tahbaz, N., Kolb, F. A., Zhang, H., Jaronczyk, K., Filipowicz, W., & Hobman, T. C. (2004). Characterization of the interactions between mammalian PAZ PIWI domain proteins and dicer. *EMBO Reports, 5*(2), 189-194.

Tang, X., Zhang, Y., Tucker, L., & Ramratnam, B. (2010). Phosphorylation of the RNase III enzyme drosha at Serine300 or Serine302 is required for its nuclear localization. *Nucleic Acids Research, 38*(19), 6610-6619.

Taubert, H., Greither, T., Kaushal, D., Wurl, P., Bache, M., Bartel, F., et al. (2007). Expression of the stem cell self-renewal gene hiwi and risk of tumour-related death in patients with soft-tissue sarcoma. *Oncogene, 26*(7), 1098-1100.

Terry, L. J., Shows, E. B., & Wente, S. R. (2007). Crossing the nuclear envelope: Hierarchical regulation of nucleocytoplasmic transport. *Science, 318*(5855), 1412-1416.

Thermann, R., & Hentze, M. W. (2007). Drosophila miR2 induces pseudo-polysomes and inhibits translation initiation. *Nature, 447*(7146), 875-878.

Thomson, T., & Lin, H. (2009). The biogenesis and function of PIWI proteins and piRNAs: Progress and prospect. *Annual Review of Cell and Developmental Biology, 25*, 355-376.

Till, S., Lejeune, E., Thermann, R., Bortfeld, M., Hothorn, M., Enderle, D., et al. (2007). A conserved motif in argonaute-interacting proteins mediates functional interactions through the argonaute PIWI domain. *Nature Structural & Molecular Biology, 14*(10), 897-903.

Tolia, N. H., & Joshua-Tor, L. (2007). Slicer and the argonautes. *Nature Chemical Biology, 3*(1), 36-43.

Tomari, Y., Du, T., Haley, B., Schwarz, D. S., Bennett, R., Cook, H. A., et al. (2004a). RISC assembly defects in the drosophila RNAi mutant armitage. *Cell, 116*(6), 831-841.

Tomari, Y., Matranga, C., Haley, B., Martinez, N., & Zamore, P. D. (2004b). A protein sensor for siRNA asymmetry. *Science, 306*(5700), 1377-1380.

Tomari, Y., & Zamore, P. D. (2005). Perspective: Machines for RNAi. *Genes & Development, 19*(5), 517-529.

Tran, E. J., Bolger, T. A., and Wente, S. R. (2007). SnapShot: nuclear transport. *Cell, 131*(2), 420.

Vagin, V. V., Hannon, G. J., & Aravin, A. A. (2009). Arginine methylation as a molecular signature of the piwi small RNA pathway. *Cell Cycle, 8*(24), 4003-4004.

van Dijk, E., Cougot, N., Meyer, S., Babajko, S., Wahle, E., & Seraphin, B. (2002). Human Dcp2: A catalytically active mRNA decapping enzyme located in specific cytoplasmic structures. *The EMBO Journal, 21*(24), 6915-6924.

Verdel, A., Jia, S., Gerber, S., Sugiyama, T., Gygi, S., Grewal, S. I., et al. (2004). RNAi-mediated targeting of heterochromatin by the RITS complex. *Science, 303*(5658), 672-676.

Verdel, A., Vavasseur, A., Le Gorrec, M., & Touat-Todeschini, L. (2009). Common themes in siRNA-mediated epigenetic silencing pathways. *The International Journal of Developmental Biology, 53*(2-3), 245-257.

Volpe, T., Schramke, V., Hamilton, G. L., White, S. A., Teng, G., Martienssen, R. A., et al. (2003). RNA interference is required for normal centromere function in fission yeast. *Chromosome Research, 11*(2), 137-146.

Volpe, T. A., Kidner, C., Hall, I. M., Teng, G., Grewal, S. I., & Martienssen, R. A. (2002). Regulation of heterochromatic silencing and histone H3 lysine-9 methylation by RNAi. *Science, 297*(5588), 1833-1837.

Wakiyama, M., Takimoto, K., Ohara, O., & Yokoyama, S. (2007). Let-7 microRNA-mediated mRNA deadenylation and translational repression in a mammalian cell-free system. *Genes & Development, 21*(15), 1857-1862.

Wang, Y., Juranek, S., Li, H., Sheng, G., Tuschl, T., & Patel, D. J. (2008). Structure of an argonaute silencing complex with a seed-containing guide DNA and target RNA duplex. *Nature, 456*(7224), 921-926.

Wang, Y., Juranek, S., Li, H., Sheng, G., Wardle, G. S., Tuschl, T., et al. (2009). Nucleation, propagation and cleavage of target RNAs in *ago* silencing complexes. *Nature, 461*(7265), 754-761.

Weinmann, L., Hock, J., Ivacevic, T., Ohrt, T., Mutze, J., Schwille, P., et al. (2009). Importin 8 is a gene silencing factor that targets argonaute proteins to distinct mRNAs. *Cell, 136*(3), 496-507.

Weis, K. (2003). Regulating access to the genome: Nucleocytoplasmic transport throughout the cell cycle. *Cell, 112*(4), 441-451.

Wente, S. R., and Rout, M. P. (2010). The nuclear pore complex and nuclear transport. *Cold Spring Harb Perspect.Biol., 2*(10), a000562.

West, R. R., Malmstrom, T., Troxell, C. L., & McIntosh, J. R. (2001). Two related kinesins, klp5+ and klp6+, foster microtubule disassembly and are required for meiosis in fission yeast. *Molecular Biology of the Cell, 12*(12), 3919-3932.

Westphal, H., & Crouch, R. J. (1975). Cleavage of adenovirus messenger RNA and of 28S and 18S ribosomal RNA by RNase III. *Proceedings of the National Academy of Sciences of the United States of America, 72*(8), 3077-3081.

Wood, V., Gwilliam, R., Rajandream, M. A., Lyne, M., Lyne, R., Stewart, A., et al. (2002). The genome sequence of schizosaccharomyces pombe. *Nature, 415*(6874), 871-880.

Wozniak, R. W., Rout, M. P., and Aitchison, J. D. (1998). Karyopherins and kissing cousins. *Trends Cell Biol., 8*(5), 184-188.

Wu, H., Xu, H., Miraglia, L. J., & Crooke, S. T. (2000). Human RNase III is a 160-kDa protein involved in preribosomal RNA processing. *The Journal of Biological Chemistry, 275*(47), 36957-36965.

Wu, L., & Belasco, J. G. (2005). Micro-RNA regulation of the mammalian lin-28 gene during neuronal differentiation of embryonal carcinoma cells. *Molecular and Cellular Biology, 25*(21), 9198-9208.

Wu, L., Fan, J., & Belasco, J. G. (2006). MicroRNAs direct rapid deadenylation of mRNA. *Proceedings of the National Academy of Sciences of the United States of America, 103*(11), 4034-4039.

Xie, Z., Johansen, L. K., Gustafson, A. M., Kasschau, K. D., Lellis, A. D., Zilberman, D., et al. (2004). Genetic and functional diversification of small RNA pathways in plants. *PLoS Biology, 2*(5), E104.

Yamada, T., Fischle, W., Sugiyama, T., Allis, C. D., & Grewal, S. I. (2005). The nucleation and maintenance of heterochromatin by a histone deacetylase in fission yeast. *Molecular Cell, 20*(2), 173-185.

Yamamoto, A., West, R. R., McIntosh, J. R., & Hiraoka, Y. (1999). A cytoplasmic dynein heavy chain is required for oscillatory nuclear movement of meiotic prophase and efficient meiotic recombination in fission yeast. *The Journal of Cell Biology, 145*(6), 1233-1249.

Ye, X., Huang, N., Liu, Y., Paroo, Z., Huerta, C., Li, P., et al. (2011). Structure of C3PO and mechanism of human RISC activation. *Nature Structural & Molecular Biology, 18*(6), 650-657.

Yigit, E., Batista, P. J., Bei, Y., Pang, K. M., Chen, C. C., Tolia, N. H., et al. (2006). Analysis of the C. elegans argonaute family reveals that distinct argonautes act sequentially during RNAi. *Cell, 127*(4), 747-757.

Yuan, Y. R., Pei, Y., Ma, J. B., Kuryavyi, V., Zhadina, M., Meister, G., et al. (2005). Crystal structure of A. aeolicus argonaute, a site-specific DNA-guided endoribonuclease, provides insights into RISC-mediated mRNA cleavage. *Molecular Cell, 19*(3), 405-419.

Zaratiegui, M., Irvine, D. V., & Martienssen, R. A. (2007). Noncoding RNAs and gene silencing. *Cell, 128*(4), 763-776.

Zekri, L., Huntzinger, E., Heimstadt, S., & Izaurralde, E. (2009). The silencing domain of GW182 interacts with PABPC1 to promote translational repression and degradation of microRNA targets and is required for target release. *Molecular and Cellular Biology, 29*(23), 6220-6231.

Zeng, Y., Sankala, H., Zhang, X., & Graves, P. R. (2008). Phosphorylation of argonaute 2 at serine-387 facilitates its localization to processing bodies. *The Biochemical Journal, 413*(3), 429-436.

Zhang, H., Kolb, F. A., Jaskiewicz, L., Westhof, E., & Filipowicz, W. (2004). Single processing center models for human dicer and bacterial RNase III. *Cell, 118*(1), 57-68.

Zhang, K., Mosch, K., Fischle, W., & Grewal, S. I. (2008). Roles of the Clr4 methyltransferase complex in nucleation, spreading and maintenance of heterochromatin. *Nature Structural & Molecular Biology, 15*(4), 381-388.

Zhang, T., Lei, J., Yang, H., Xu, K., Wang, R., & Zhang, Z. (2011). An improved method for whole protein extraction from yeast saccharomyces cerevisiae. *Yeast, 28*(11), 795-798.

Zofall, M., & Grewal, S. I. (2006). RNAi-mediated heterochromatin assembly in fission yeast. *Cold Spring Harbor Symposia on Quantitative Biology, 71*, 487-496.

APPENDIX:

Ago1 in fission yeast is thought to perform multiple functions in different cellular compartments. I hypothesized that Ago1 is subjected to extensive regulation through interaction with other proteins and/or by post-translational modifications. With respect to the latter, the activities of many eukaryotic proteins are regulated by phosphorylation, and emerging data suggest that components of the RNAi apparatus are as well (refer to Section 1.4.3 and Figure 1.8). Given that RNAi plays a critical role in regulating gene expression on a global level, surprisingly little is known about how kinases and phosphatases regulate this process. Moreover, all studies to date have mostly focused on metazoan systems.

There are multiple reasons to think that phosphorylation of Argonaute proteins is a conserved process. In virtually all cases, there is a positionally conserved tyrosine residue (i.e., Y529 in hAgo2) at the extreme N-termini of the PIWI domains of Argonaute proteins from mammals, plants, and yeasts (Johnston and Hutvagner 2011; Rudel et al. 2011). A previous study also showed that 14-3-3 proteins, which bind to phospho-amino acid residues, interact with both human and fission yeast Argonaute proteins (Stoica et al. 2006). Accordingly, I hypothesized that the Argonaute protein in *S. pombe* is phosphorylated and that this is important for its localization and function.

First, to study the physiological function of Ago1 phosphorylation, I generated yeast strains expressing GFP-tagged wild-type and Ago1 mutants that mimic non-phosphorylated and constitutively phosphorylated forms of the protein. Specifically, a tyrosine residue (Y513) within the predicted 5'-phosphate binding pocket region, which corresponds to Y529 in hAgo2 (Johnston and Hutvagner

2011; Rudel et al. 2011), was changed to phenylalanine or glutamate. Mutations of Y487F and Y487E were used as negative controls. Preliminary results show that localization of both Y513F and Y513E Ago1 mutants to P-bodies was decreased compared to wild-type Ago1 (Figure A1). I also examined targeting of GFP-Ago1 in yeast treated with the kinase inhibitor, staurosporine. My preliminary results indicate that the number of Ago1-positive PBs was significantly decreased after treatment with staurosporine. Moreover, large Ago1-containing aggregates were observed in the staurosporine-treated cells (Figure A2). Quantification of the data showed control cells contain an average number of 7.3 Ago1-positive PBs, whereas the staurosporine-treated cells possess, on average, only 3.4 Ago1-positive PBs per cell.

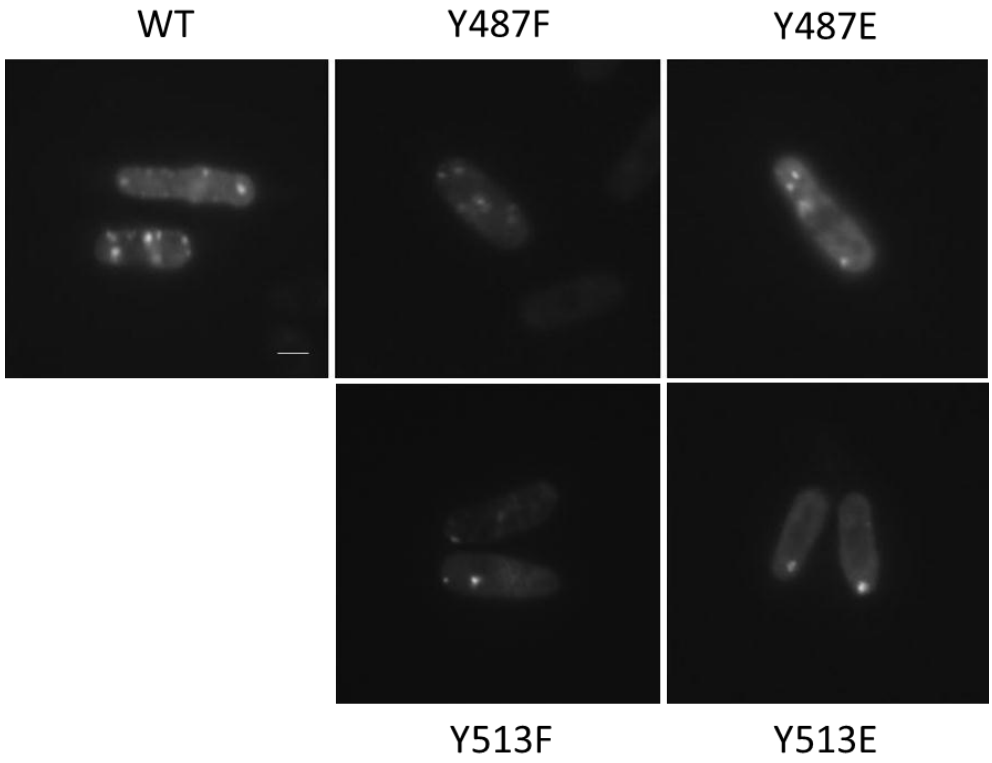

Figure A1. Mutations in the predicted 5'-siRNA binding pocket region of Ago1 disrupts targeting to P-bodies. Yeast strains expressing GFP-tagged wild-type Ago1 (WT) or mutant Ago1 proteins (Y513F and Y513E) were fixed and viewed by fluorescence microscopy. Mutations of Y487F and Y487E were used as negative controls. Bars = 3 μm.

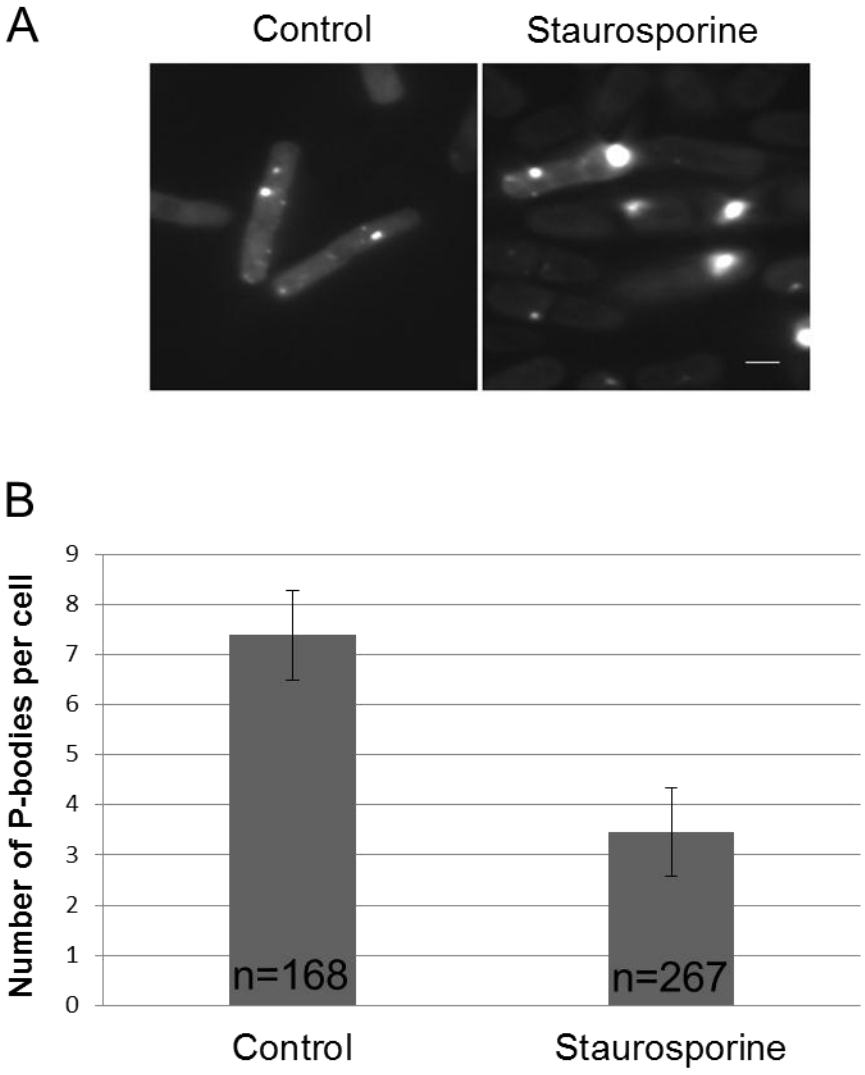

Figure A2. The number of Ago1-positive PBs is decreased by staurosporine treatment. A. Fluorescent microscopic images of wild-type yeast expressing GFP-tagged Ago1 with and without staurosporine (2 µM) for 16 hours. Bars = 3 µm. **B.** Quantification of Ago1-positive PB numbers. n = number of cells counted with Ago1-positive PBs. Standard error bars are shown.